University of Alberta

Molecular Mechanisms Involved in the Interaction between Protein Phosphatase-1 and Inhibitor-2

©

By

Patrick William Douglas Turc

A thesis submitted to the Faculty of Graduate Studies and Research in partial fulfillment
of the requirements for the degree of Master of Science

Department of Biochemistry

Edmonton, Alberta

Spring 2004

Canadä

Abstract

Protein phosphatase-1 (PP-1), an important eukaryotic Ser/Thr phosphatase, is controlled *in vivo* by regulatory subunits, one of which is a protein called inhibitor-2 (I-2). PP-1 and I-2 form a 1:1 complex, both *in vivo* and *in vitro,* which is thought to be inactive.

The present study presents evidence that the PP-1:I-2 complex possesses residual phosphatase activity. This discovery led to an investigation of the $\beta12$-$\beta13$ loop region of PP-1, especially residue F276, and of residue Y134 located in a separate region near the catalytic site of PP-1. This study shows these residues to be involved in mediating substrate accessibility to the PP-1 active site.

The RVxF binding pocket of PP-1, particularily residues F257 and C291, is known to interact with a glycogen binding subunit, G_M. This study shows these residues to be involved in the inhibition of PP-1 by I-2 and also suggests that I-2 interacts differently with PP-1 than with the G_M subunit.

"Throughout all the ages, only one thing has been able to explain perfectly the human race, the many material dimensions that exist, all life, and the entire universe: BUDDHA LAW"

Li Hongzhi

June 2, 1992

To all those trying to understand life, and their place in it.

Acknowledgments

I would like to start off by thanking everyone involved in my studies, from friends and family to co-workers and fellow students. You have all enriched my life and helped me to achieve my goals. A special thank you goes out to my fellow graduate students, Mikolaj Raszek, Kathleen Perreault, and Andrea Fong whose friendships will be strong memories for many years to come.

I would like to thank my supervisor Dr. Charles Holmes for his guidance and support throughout my studies. I would also like to thank Marcia Craig for her feedback and suggestions. I would especially like to thank Marcia for her thorough work on editing this thesis.

Thank you to my Mom and Dad for their support in my studies and especially Dad's laptop which was instrumental in writing my thesis and presenting my Defense seminar.

A thank you also goes out to Kirsty Dunlop, that special someone who supported me through the most difficult times and was a source of great encouragement.

Lastly, I would like to thank Mr. Li Hongzhi for making Falun Dafa (Truth, Compassion, Forbearance) accessible to all people world wide. Completion of this thesis required great Forbearance.

Table of Contents

List of Tables

List of Figures

List of Abbreviations

Proteins

$[\gamma\text{-}^{32}P]ATP$	ATP containing ^{32}P at the γ position
^{32}P	radioactive phosphate
AKAP 149	A-kinase anchoring protein 149
AMP	adenosine mono phosphate
ATP	adenosine 5'-triphosphate
Bcl2	B-cell leukemia/lymphoma 2
BL21DE3	a high protein expression strain of *E. coli*
BSA	bovine serum albumin
Ca^{2+}	calcium cation
CaM	calmodulin
cAMP	cyclic AMP
cDNA	complementary DNA
CDK	cyclin dependent kinase
CK-2	casein kinase-2
CnA	calcineurin subunit A
CnB	calcineurin subunit B
DH5α	a high subcloning efficiency strain of *E. coli*
DNA	deoxyribonucleic acid
DSS	disuccinimidyl suberate
DTT	dithiothreitol
E. coli	Escherichia coli
EDTA	ethylenediaminetetraacetic acid
EGTA	ethylglycol-bis-(b-aminoethyl ether)-N, N, N', N'-tetraacetic acid
Fe^{2+}	iron cation
FPLC	fast protein liquid chromatography
G_M	glycogen-binding subunit of PP-1G from skeletal muscle

$G_{M[63-75]}$	a peptide of G_M containing only residues 63-75
GSK-3	glycogen synthase kinase-3
I-1	inhibitor-1, specific inhibitor of PP-1
I-2	inhibitor-2, specific inhibitor of PP-1
IC_{50}	inhibitor concentration which reduces enzymatic activity to 50% of its original activity
IPTG	isopropyl-b-D-thiogalactoside
K_i	dissociation constant
L5	50S ribosomal protein, binds PP-1
M_{110}	myosin-binding subunit of PP-1M
MCLR	microcystin containing Leu and Arg in the variable amino acid positions
Mg^{2+}	magnesium cation
MgOAc	magnesium acetate
Mn^{2+}	manganese cation
NIPP1	nuclear inhibitor of PP-1c
NMR	Nuclear Magnetic Resonance
NZCYM	a nutrient rich both for culturing bacterial cells
OA	okadaic acid
PKA	cAMP-dependent protein kinase
PMSF	phenylmethylsulfonyl fluoride
pNPP	para-nitrophenolphosphate
PP-1	protein phosphatase-1
PP-1c	catalytic subunit of PP-1
PP-1c:I-2	complex between PP-1c and I-2
PP-1G	complex of PP-1c and G_M subunit
PP-1M	complex of PP-1c and M_{110} subunit
PP-2A	protein phosphatase-2A
PP-2B	protein phosphatase-2B, calcineurin
PP-2C	protein phosphatase-2C
PP-4	protein phosphatase-4

PP-5	protein phosphatase-5
PP-6	protein phosphatase-6
PP-7	protein phosphatase-7
RVxF motif	amino acid sequence Arg-Val-(any amino acid)-Phe used by regulatory subunits to bind PP-1c through a common binding site
SDS	sodium dodecyl sulfate
SDS PAGE	polyacrylamide gel electrophoresis with SDS
TCA	trichloroacetic acid
wtPP-1c	wild type PP-1c
α	alpha
β	beta
γ	gamma

Standard Amino Acids

Name	3-Letter Code	1-Letter Code
Nonpolar		
Glycine	Gly	G
Alanine	Ala	A
Valine	Val	V
Leucine	Leu	L
Isoleucine	Ile	I
Methionine	Met	M
Proline	Pro	P
Phenylalanine	Phe	F
Tryptophan	Trp	W
Uncharged Polar		
Serine	Ser	S

Threonine	Thr	T
Tyrosine	Tyr	Y
Asparagine	Asn	N
Glutamine	Gln	Q
Cysteine	Cys	C

Charged

Lysine	Lys	K
Arginine	Arg	R
Histidine	His	H
Aspartic Acid	Asp	D
Glutamic Acid	Glu	E

Special Amino Acids

pSer	phosphoserine
pThr	phosphothreonine
pTyr	phosphotyrosine
Masp	D-erythro-β-methyl aspartic acid
Mdha	N-methyldehydroalanine

Units and Constants

Å	Ångstroms (10^{-10} meters)
cpm	counts per minute
g	acceleration due to gravity
hr	hours

II	integrated intensity
kDa	kiloDaltons
L	litres
mg	milligrams (10^{-3} grams)
min	minutes
ml	milliliters (10^{-3} liters)
mM	millimolar (10^{-3} molar)
nm	nanometers (10^{-9} meters)
nM	nanomolar (10^{-9} molar)
°C	degrees Celsius
OD_{600}	optical density at 600nm
pH	-log of the concentration of H^+ in solution
sec	seconds
U	units
v/v	volume per volume
w/v	weight per volume
μCi	micro Curies (10^{-6} Curies)
μg	micro grams (10^{-6} grams)
μl	micro liters (10^{-6} liters)
μM	micromolar (10^{-6} molar)
μmol	micro moles (10^{-6} moles)
μU	micro units (10^{-6} units)
nmol	nanomoles (10^{-9} units)

Chapter 1: Introduction

1.1 Regulation of Metabolism by Reversible Protein Phosphorylation

Many metabolic functions in the eukaryotic cell such as learning and memory [1], glycogen metabolism [2], cell cycle control [3], apoptosis [4], B cell signal transduction [5], and proper heart function [6] are regulated by reversible phosphorylation of serine, threonine, and tyrosine residues on enzymes and other proteins. Protein kinases phosphorylate proteins while protein phosphatases dephosphorylate proteins. The addition or removal of phosphate is usually accompanied by conformational and hence functional changes in the protein (Figure 1).

Together with reversibility and potential for signal amplification, protein phosphorylation is an essential and important process for cell signaling and regulation of metabolism in the eukaryotic cell. A classic example of cell signaling is as follows. An extracellular stimulus leads to G-protein signaling, which activates adenylate cyclase and produces a second messenger (cAMP). The second messenger then either stimulates or inhibits the actions of various protein kinases and phosphatases. This alters the phosphorylation states of other proteins and enzymes, leading to metabolic changes in the cell (Figure 2).

1.2 Classification of Protein Phosphatases

There are two groups of phosphatases, those that catalyze the hydrolysis of phosphorylated serine/threonine residues (p-Ser/Thr) and those that catalyze the hydrolysis of phosphorylated tyrosine residues (p-Tyr). A subset of tyrosine phosphatases can catalyze the hydrolysis of p-Ser/Thr as well as p-Tyr residues. Ser/Thr phosphatases are metalloenzymes, with 2 divalent cations at the centre of the catalytic site that help to bind the phosphate group on the substrate. Tyr phosphatases do not require metal cations,
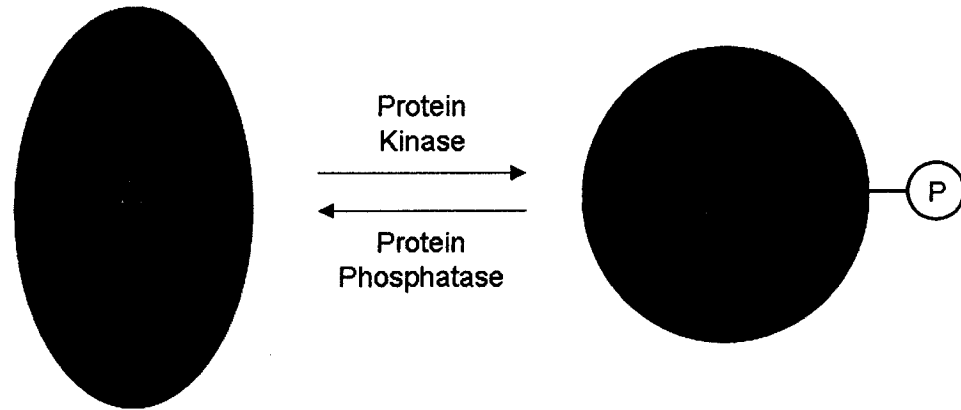
Figure 1: *Phosphorylation and Dephosphorylation.*

The function of protein kinases and phosphatases. The small "P" in the circle represents a phosphorylated amino acid residue. An example of the effects of protein phosphorylation and dephosphorylation is when proteins A and B are different conformations of the same enzyme, with phosphorylation and dephosphorylation leading to different levels of enzymatic activity.
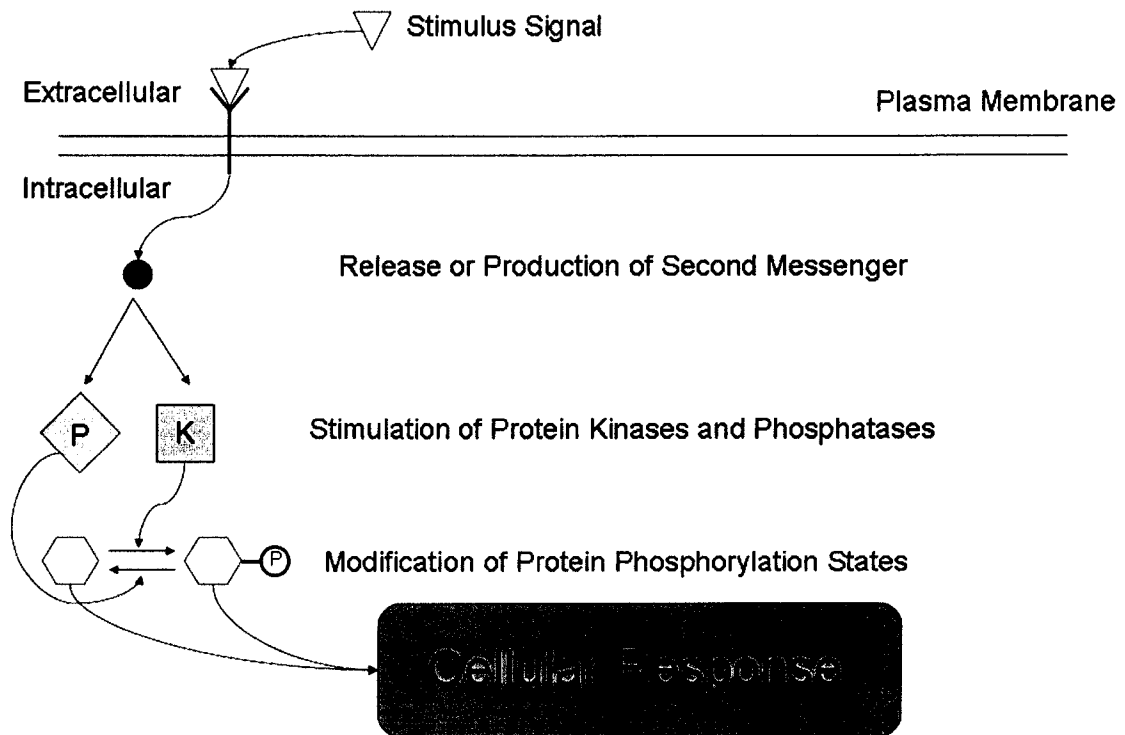
Figure 2: *Signal Transduction.*

The importance of reversible protein phosphorylation in cellular signal transduction. The large "P" is a phosphatase while the large "K" is a kinase. The small "P" in the circle represents a phosphorylated amino acid residue. The cellular response can be either an increase or decrease in the activity of a whole metabolic pathway. Different stimuli can alter the functions in the cell through the use of reversible phosphorylation to control a number of cellular functions.

instead a conserved cysteine residue in the active site catalyzes dephosphorylation reactions [7, 8].

In eukaryotic cells, more than 98% of all protein phosphorylation occurs on serine and threonine residues [9]. The Ser/Thr protein phosphatases are commonly classified into two groups, type 1 and type 2. Type 1 enzymes are classified by their ability to preferentially dephosphorylate the β subunit of glycogen phosphorylase kinase. Protein phosphatase-1 is sensitive to inhibition by nanomolar concentrations of two heat and acid stable proteins named inhibitor-1 (I-1) and inhibitor-2 (I-2). Type 2 protein phosphatases (protein phosphatase-2) preferentially dephosphorylate the α subunit of glycogen phosphorylase kinase and are insensitive to I-1 and I-2. Type-2 protein phosphatases can be further subdivided into three enzymes, 2A, 2B, and 2C (PP-2A, PP-2B, PP-2C) based on different requirements for divalent cations [10] (Table 1).

With the recent completion of the human genome project, four new Ser/Thr protein phosphatases have been classified based on sequence homology. These phosphatases, PP-4, 5, 6 and 7, have not been fully characterized and little is known about them. However, DNA and amino acid sequencing has shown that they are more structurally related to PP-1 and PP-2A than PP-2B and PP-2C [9].

1.3 Protein Phosphatase-1

Protein phosphatase-1 (PP-1) is an important member of the Ser/Thr phosphatase family. PP-1 is highly conserved in eukaryotes, with rabbit PP-1 showing 92% identity with *Drosophila* PP-1 and 80% identity with *Aspergillus* PP-1[10]. Overall, more than 80% identity has been retained between PP-1 from fungi and mammalian tissues [11].

Isoforms of Protein Phosphatase-1

The catalytic subunit of PP-1 (PP-1c) is widely expressed in mammalian tissues and regulates many biological processes including gene transcription, muscle contraction, glycogen metabolism and intracellular transport [12, 13]. Four isoforms of PP-1c: α, β,

Criteria	PP-1	PP-2A	PP-2B	PP-2C
Preference for α or β Subunit of Glycogen Phosphorylase Kinase	β	α	α	α
Inhibited by I-1 and I-2	Yes	No	No	No
Requirement for Divalent Cations	No	No	Yes Ca^{2+}	Yes Mg^{2+}

Table 1: *Classification of Ser/Thr Phosphatases.*

Classification of the major Ser/Thr protein phosphatases in eukaryotic cells.

γ1, and γ2, are expressed from three different genes. The sequences of the isoforms are identical except for the first thirty-four residues of the N terminal and last thirty-two residues of the C terminal tail (Figure 3).

The α, β, and γ1 isoforms are expressed in many tissues, but the γ2 isoform, which is translated from the same gene as γ1, is expressed only in testes. The present study has used the PP-1c$_{\gamma 1}$ isoform because it is the best understood of all the isoforms. In fact, the majority of PP-1c structural studies were carried out using the γ1 isoform. In addition, a practical benefit from working with the γ1 isoform is that it can be expressed and purified in large quantities from *Escherichia coli* [14]. For ease of terminology, PP-1c$_{\gamma 1}$ will henceforth be referred to as PP-1c.

Regulation of Protein Phosphatase-1 by Regulatory Subunits

Without some form of regulatory control, the ubiquitous activity of PP-1c would quickly destabilize the metabolism of the eukaryotic cell. In addition to regulatory control, efficient PP-1c activity requires targeting of the enzyme to its various substrates. One of the primary means by which PP-1c is regulated *in vivo* is by its association with regulatory subunits. These regulatory subunits associate and dissociate from PP-1c, either altering the enzyme's affinity for its substrates or localizing PP-1c to various cellular locations (Figure 4).

There are forty-five established or putative subunits with which PP-1c interacts [15]. Some subunits, such as the 50S ribosomal protein (L5), A-kinase anchoring protein 149 (AKAP 149), and B-cell leukemia/lymphoma 2 (Bcl2), act to localize PP-1c to different areas of the cell such as the endoplasmic reticulum, nuclear membrane, and mitochondrion respectively. Other subunits, such as the glycogen-binding subunit from skeletal muscle (G$_M$), myosin-binding subunit (M$_{110}$), and nuclear inhibitor of PP-1c (NIPP1), regulate the activity of PP-1c towards various substrates such as glycogen phosphorylase, myosin/actin, and the spliceosome respectively [15-18]. These many subunits allow PP-1c to be targeted and regulated in a precise and controlled manner.

```
                  10          20          30          40          50          60
PP1α    MSDSEKLNLD  SIIGRLLEVQ  GSRPGKNVQL  TENEIRGLCL  KSREIFLSQP  ILLELEAPLK
PP1β    MADGE-LNVD  SLITRLLEVR  GCRCGKIVQM  TEAEVRGLCI  KSREIFLSQP  ILLELEAPLK
PP1γ    MADLDKLNID  SIIQRLLEVR  GSKPGKNVQL  QENEIRGLCL  KSREIFLSQP  ILLELEAPLK


                  70          80          90          100         110         120
PP1α    ICGDIHGQYY  DLLRLFEYGG  FPPESNYLFL  GDYVDRGKQS  LETICLLLAY  KIKYPENFFL
PP1β    ICGDIHGQYY  DLLRLFEYGG  FPPESNYLFL  GDYVDRGKQS  LETICLLLAY  KIKYPENFFL
PP1γ    ICGDIHGQYY  DLLRLFEYGG  FPPESNYLFL  GDYVDRGKQS  LETICLLLAY  KIKYPENFFL


                  130         140         150         160         170         180
PP1α    LRGNHECASI  NRIYGFYDEC  KRRYNIKLWK  TFTDCFNCLP  IAAIVDEKIF  CCHGGLSPDL
PP1β    LRGNHECASI  NRIYGFYDEC  KRRFNIKLWK  TFTDCFNCLP  IAAIVDEKIF  CCHGGLSPDL
PP1γ    LRGNHECASI  NRIYGFYDEC  KRRYNIKLWK  TFTDCFNCLP  IAAIVDEKIF  CCHGGLSPDL


                  190         200         210         220         230         240
PP1α    QSMEQIRRIM  RPTDVPDQGL  LCDLLWSDPD  KDVQGWGEND  RGVSFTFGAE  VVAKFLHKHD
PP1β    QSMEQIRRIM  RPTDVPDTGL  LCDLLWSDPD  KDVQGWGEND  RGVSFTFGAD  VVSKFLNRHD
PP1γ    QSMEQIRRIM  RPTDVPDQGL  LCDLLWSDPD  KDVLGWGEND  RGVSFTFGAE  VVAKFLHKHD


                  250         260         270         280         290         300
PP1α    LDLICRAHQV  VEDGYEFFAK  RQLVTLFSAP  NYCGEFDNAG  AMMSVDETLM  CSFQILKPAD
PP1β    LDLICRAHQV  VEDGYEFFAK  RQLVTLFSAP  NYCGEFDNAG  GMMSVDETLM  CSFQILKPSE
PP1γ    LDLICRAHQV  VEDGYEFFAK  RQLVTLFSAP  NYCGEFDNAG  AMMSVDETLM  CSFQILKPAE


                  310         320
PP1α    KNKGKYGQFS  GLNPGGRPIT  PPRNSA--K-AKK
PP1β    K-KAKY-QYG  GLN-SGRPVT  PPRTANPPK--KR
PP1γ    K-K-K-----  -PNAT-RPVT  PPR-GMITKQAKK
```

Figure 3: *Isoforms of PP-1c.*

Amino acid sequences of the 3 major isoforms of PP-1c from human cells. The sequences enclosed in the boxes are the amino acid residues which vary significantly between isoforms of PP-1c. Not shown here is the testes specific form of PP-1γ, PP-1γ2. Note that amino acid sequences of the isoforms are identical except for N and C terminals. (Figure taken from [19]).
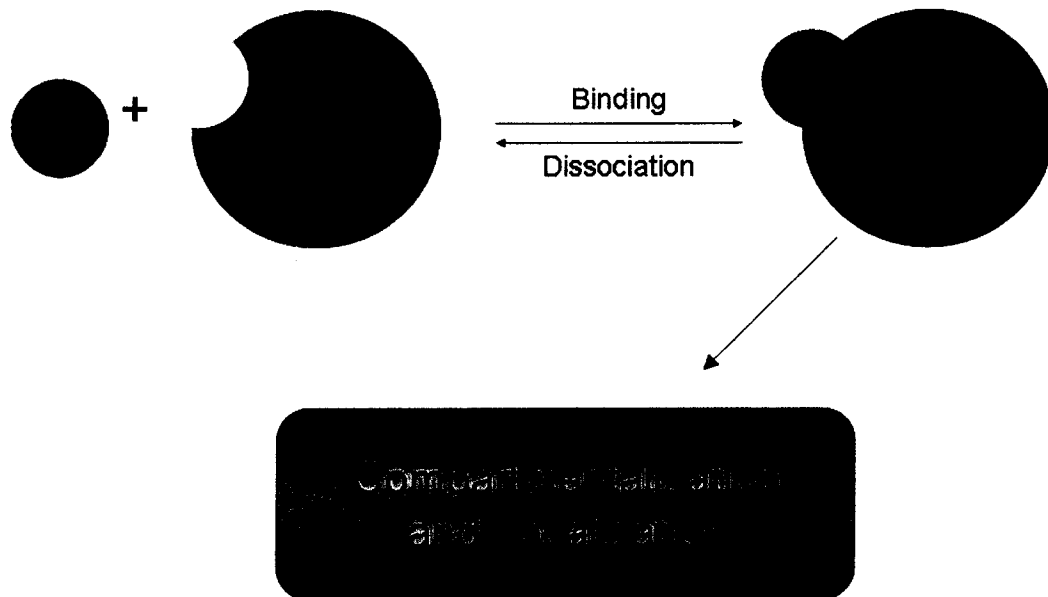
Figure 4: *Binding of Regulatory Subunits to PP-1c Assist in Compartmentalization and Localization of the Enzyme.*

Binding and dissociation of PP-1c regulatory subunits and their effects on PP-1c localization in the cell. Note that the diagram is not drawn to scale, and that regulatory subunits may be the same size, larger, or smaller than PP-1c. The G_M regulatory subunit, for example, targets PP-1c to the glycogen particle.

Regulation of Protein Phosphatase-1 by Phosphorylation

Phosphorylation of PP-1c is one of the mechanisms through which PP-1c is regulated *in vivo*. PP-1c is phosphorylated on Thr-311 in the C-terminal tail by cyclin dependant kinases (CDK) *in vitro* which leads to a decrease in phosphatase activity [20]. This phosphorylation also occurs *in vivo* and is regulated in a cell cycle dependant manner [21]. The mechanism for PP-1c inhibition by CDK phosphorylation is thought to involve the flexible C-terminal tail binding into the active site and blocking substrate access [22].

1.4 Protein Phosphatase-2B (Calcineurin)

PP-2B (calcineurin) and PP-1c have several important differences in structure, function, and regulation. First of all, calcineurin preferentially dephosphorylates the α-subunit of glycogen phosphorylase kinase while PP-1c preferentially dephosphorylates the β-subunit. In addition, PP-2B requires Ca^{2+} while PP-1c does not. Most importantly, calcineurin is poorly inhibited by natural toxins which intensely inhibit both PP-1c and PP-2A [22].

Unlike PP-1c, which consists of a single protein subunit, calcineurin is a heterodimer consisting of two subunits, an A subunit (60 kDa) and a B subunit (17 kDa) [11, 22, 23]. The calcineurin A subunit (CnA) contains the catalytic core which shares 40% identity with the catalytic core of PP-1c, as well as three regulatory domains (Figure 5). One of the regulatory domains associates with the B subunit of calcineurin (CnB) which functions to bind Ca^{2+} and is required for calcineurin phosphatase activity. The second regulatory domain associates with another subunit called calmodulin (CaM) which also binds Ca^{2+} and is required for calcineurin activity. In addition to the regulatory subunit binding sites, CnA also possesses an autoihibitory regulatory site, located in the C-terminal, which autoinhibits calcineurin activity in the absence of CaM binding. The mechanism for autoinhibition is thought to involve the flexible C-terminal tail of CnA folding into the catalytic site and blocking substrate access.
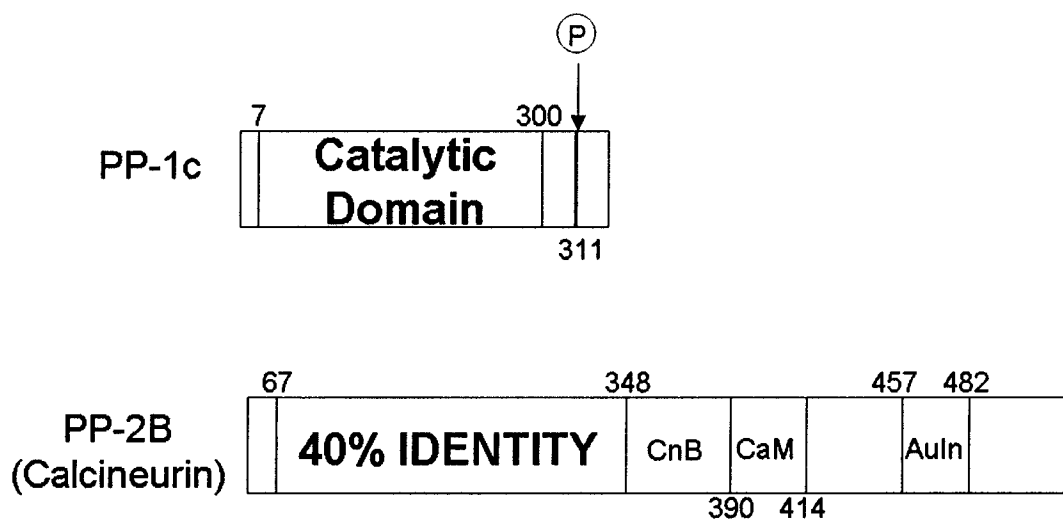
Figure 5: *Major Domains of Human PP-1c and Human PP-2B.*

Comparison of key regions between PP-1c and PP-2B. The catalytic domain of PP-1c is located between residues 7 and 300. Threonine-311, which is phosphorylated during autoinhibition, is also shown. The catalytic domain of PP-2B (calcineurin, which shares 40% identity with PP-1c) is situated between residues 67 and 348. The calcineurin B (CnB) binding domain is located between residues 348 and 390. The calmodulin (CaM) binding domain is found between residues 390 and 414. The autoihibitory domain (AuIn) of calcineurin is positioned between residues 457 and 482. (Figure taken from [24] and modified.)

1.5 Inhibitor Subunits and Exogenous Toxins of Protein Phosphatase-1

Inhibitor-1

Inhibitor-1 (I-1) is an 18.7 kDa endogenous inhibitor of PP-1c consisting of 166 amino acids [10, 11]. I-1 is stable towards detergents, organic solvents, and acids, as well as towards heat treatment. Circular dichroism shows I-1 to lack ordered structure and its asymmetry causes it to migrate anomalously during gel filtration. I-1 also migrates abnormally on sodium dodecyl sulfate polyacrylimide gels at an apparent molecular mass of 26 kDa due to its atypical binding of detergent. I-1 possesses two significant sequences which sets it apart from inhibitor-2 (Figure 6). Firstly, I-1 has a KIQF sequence located near its N-terminal, which attaches to PP-1c in the PP-1c regulatory subunit interaction site (called the RVxF binding pocket, explained below). Secondly, I-1 requires phosphorylation of Thr-35 by cAMP dependent protein kinase in order to exhibit its PP-1c inhibitory activity [22].

Inhibitor-2

The role of inhibitor-2 (I-2) in the cell is not well understood but it is believed to function primarily as a specific inhibitor of PP-1c activity. I-2 has been implicated in several reproductive and motility functions including the regulation of mitosis [25], chromosome segregation [26, 27], dephosphorylation at the actin cytoskeleton [28], and sperm motility [29].

Inhibitor-2 (I-2) is a 23 kDa endogenous inhibitor of PP-1c consisting of 204 residues [10, 11]. Like I-1, I-2 shows stability to detergents, organic solvents, and acids, as well as towards heat treatment. I-2 also has an asymmetric structure and thus runs anomalously on gel filtration. In addition, I-2 has an apparent molecular mass of 33 kDa on SDS PAGE due to its atypical binding of detergent. I-2 inhibition of PP-1c differs
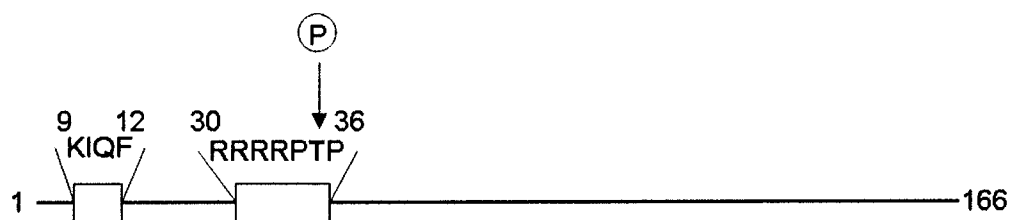
Figure 6: *Key Regions of I-1 Implicated in PP-1c Binding and Inhibition.*

The KIQF sequence of I-1, which binds the RVxF binding pocket on PP-1c, is between residues 9 and 12 on I-1. Residues 30-36 form a consensus sequence for cAMP-dependent protein kinase (PKA) phosphorylation. Phosphorylation of I-1 on threonine-35 is required for inhibition of PP-1c. (Figure taken from [19] and modified.)

from I-1 inhibition in that I-1 requires phosphorylation for its inhibitory activity whereas I-2 does not.

I-2 impedes the activity of PP-1c by binding to the phosphatase and blocking substrate access to the active site. This process is reversible by digestion of inhibitor using extremely low concentrations of trypsin which does not significantly digest the PP-1c [30].

Previous studies have shown that PP-1c and I-2 form a complex upon prolonged incubation (10 to 60 min). Incubation with I-2 is thought to induce a conformational change in PP-1c [31]. The stoichiometry of the complex is 1:1 as determined by densitometric analysis of a coomassie blue stained SDS PAGE gel [32].

The putative conformational change in PP-1c can be reversed to a limited degree (50% of original PP-1c activity) by incubation with both trypsin and Mn^{2+} [32]. Complete reactivation of the PP-1c:I-2 complex, however, requires phosphorylation on Thr-72 of I-2 by glycogen synthase kinase-3 (GSK-3) [30, 33].

Phosphorylation at Thr-72 reactivates the PP-1c:I-2 complex but does not release I-2 from PP-1c [32]. The phosphorylated I-2, still bound to PP-1c, is thought to be slowly autodephosphorylated by the phosphatase. Over time, the PP-1c:I-2 complex becomes inactive again [34]. This cycle may be repeated with renewed phosphorylation of Thr-72 of I-2 by GSK-3.

Natural Toxins

Several natural toxins bind tightly to and inhibit both PP-1c and PP-2A: okadaic acid, calyculins, and microcystins (Figure 7) [35]. Okadaic acid (OA), a C38 polyether fatty acid tumor promoter, is a potent inhibitor, which inhibits PP-2A two orders of magnitude more strongly than PP-1c. Okadaic acid is produced by dinoflagellates and becomes concentrated in the digestive tracts of shellfish which filter-feed on these organisms. Concentration of OA in shellfish is a major cause of diarrheic shellfish poisoning in humans. Calyculin A is an octamethyl polyhydroxylated C28 fatty acid linked to two γ-amino acids and esterified with phosphate. Calyculin A is isolated from marine sponges, and is a potent inhibitor of PP-1c and PP-2A [35].
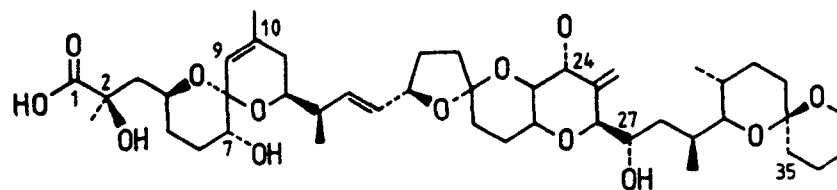
Okadaic acid
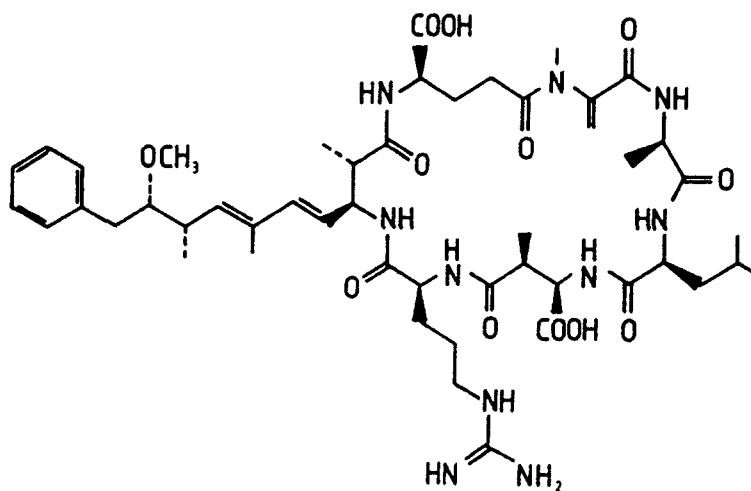
Microcystin-LR
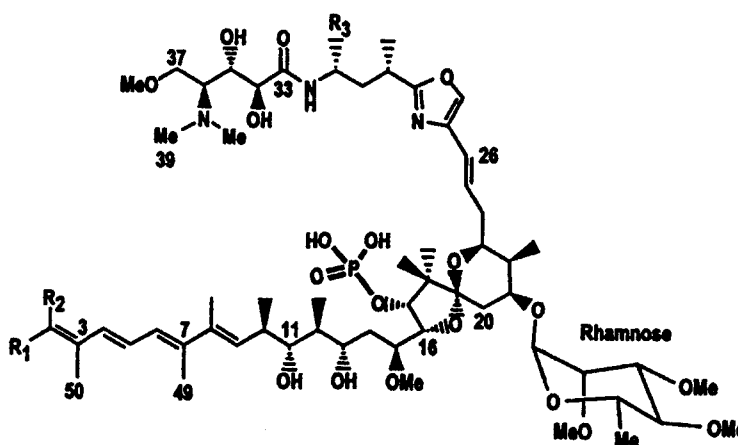
Clavosine A : R₁=H, R₂=CONH₂, R₃=Me
Clavosine B : R₁=CONH₂, R₂=H, R₃=Me
Calyculin A : R₁=H, R₂=CN, R₃=H, C21=OH

Figure 7: *Toxins of PP-1c.*

The chemical structures of several PP-1c toxins. (Figure taken from the following references [36, 37].)

Microcystins, a family of cyclic peptide hepatotoxins isolated from freshwater cyanobacteria, are potent inhibitors of PP-1 and PP-2A as are tumour promoters like okadaic acid. Microcystin is a powerful hepatotoxin and ingestion of contaminated water can lead to severe liver damage. Microcystin-LR (MCLR) is the most common form of the more than 60 microcystins discovered thus far [38]. All of the inhibitors listed above inhibit phosphatase activity with toxin concentrations in the low nanomolar range.

1.6 Structure and Interaction of Protein Phosphatase-1 with Inhibitors

Three Dimensional Structure of the Catalytic Subunit of Protein Phosphatase-1

PP-1c is a 37 kDa protein consisting of 323 amino acids in a single domain. In 1995, Egloff et al. elucidated the structure of recombinant PP-1c bound to tungstate, an analogue of phosphate [14]. The structure of PP-1c consists of a compact "kidney bean" shape composed of ten α-helices and three β-sheets with two divalent cations, Fe^{2+} and Mn^{2+}, contained in the catalytic domain. The binding of tungstate causes no significant change in the conformation of PP-1c (Figure 8). The key residues in the catalytic site are R96, I133, Y134, W206, R221, Y272, C273, E275, F276, and D277 (Figure 9).

Several key features of PP-1c have been discovered through analysis of the crystal structure of the PP-1c:microcystin-LR complex [24]. The active site of PP-1c is located at the branching point of a Y-shaped groove on the surface of the enzyme. The bottom of the Y-shaped groove contains a group of residues which have their hydrophobic side chains exposed to the surface and therefore is called the "hydrophobic groove". There are several acidic side chains on the right side of the Y-shaped groove, forming an "acidic groove". Finally, the C-terminal of the protein is located at the end of the left side of the Y-shaped groove and is called the "C-terminal groove" (Figure 10, Figure 11).
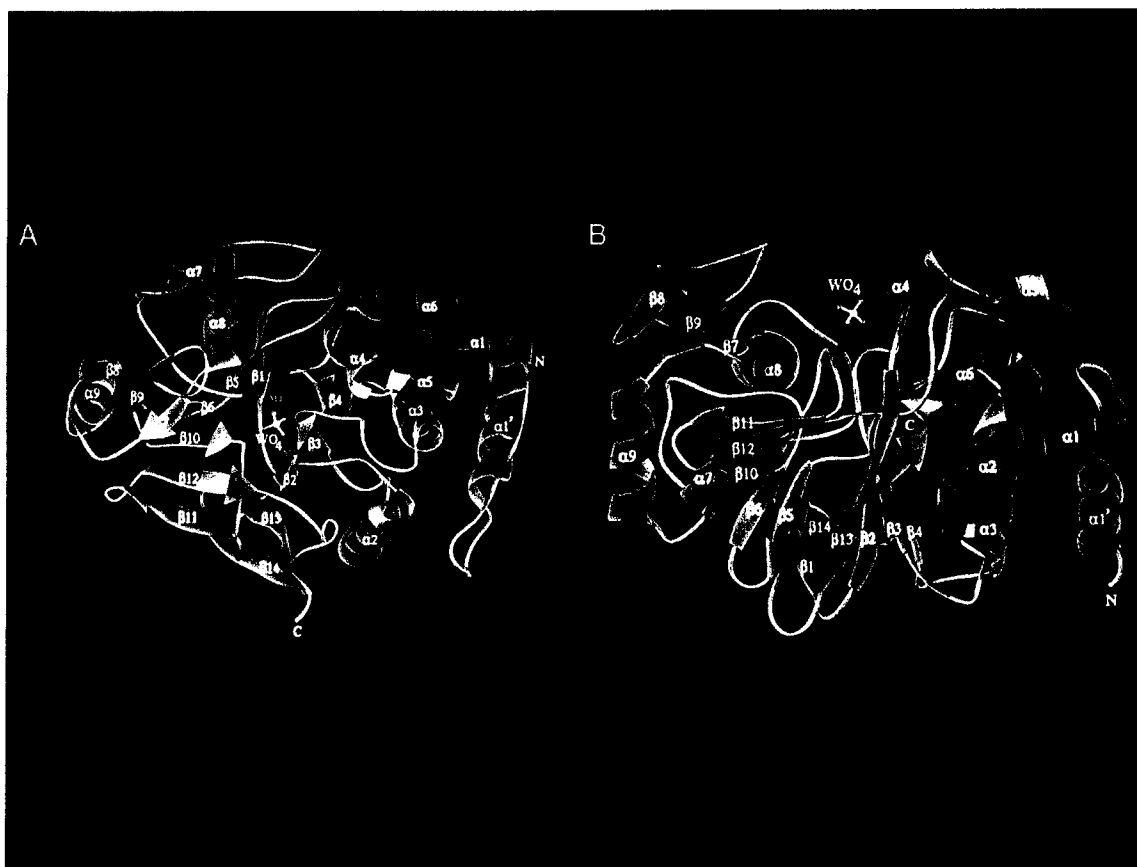
Figure 8: *Structure of PP-1c Bound to Tungstate.*

Two orthogonal views of a ribbon representation indicating the secondary structure elements of PP-1c and the catalytic site. The metal ions M1 (Fe^{2+}) and M2 (Mn^{2+}) are shown as *purple* spheres and the tungstate ion (WO_4) is indicated in *white*. (Figure taken from [14].)
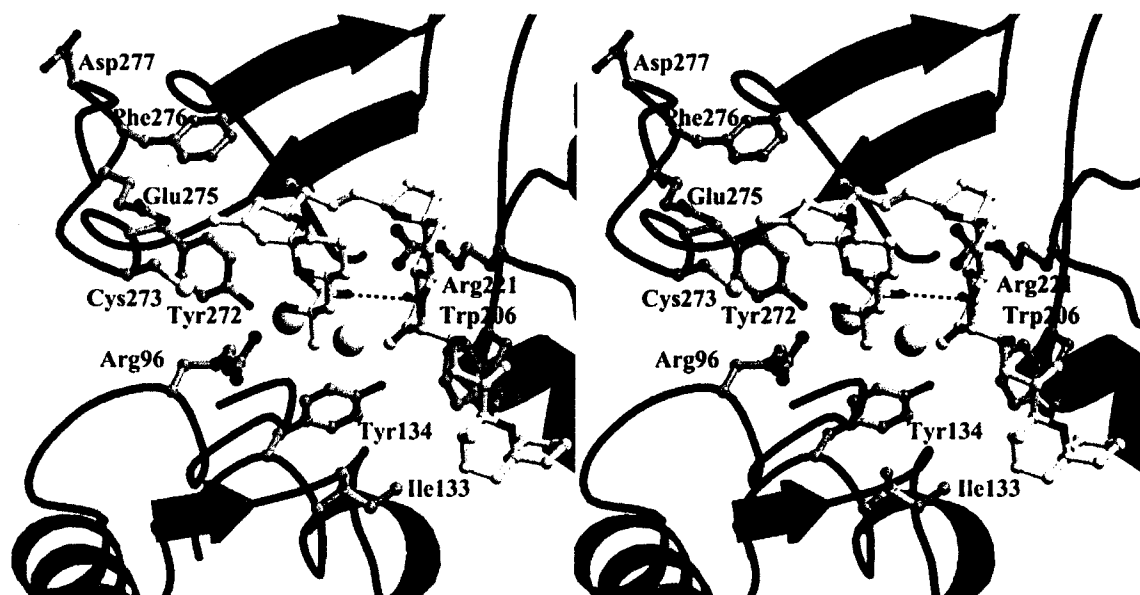
Figure 9: *Stereoview of the Catalytic Site of PP-1c Bound to Okadaic Acid.*

Stereo representation of the active site of the PP-1c:OA complex. Pertinent active site residues are labeled and are shown as a ball-and-stick representation with carbon atoms colored *gray*, oxygen atoms colored *red,* and nitrogen atoms colored *blue*. OA is shown as a ball-and-stick representation with carbon atoms colored *yellow* and oxygen atoms colored *red*. The intramolecular hydrogen bond in OA is shown as a *dashed line*. The active-site manganese atoms are shown as *yellow* spheres. (Figure taken from [39].)
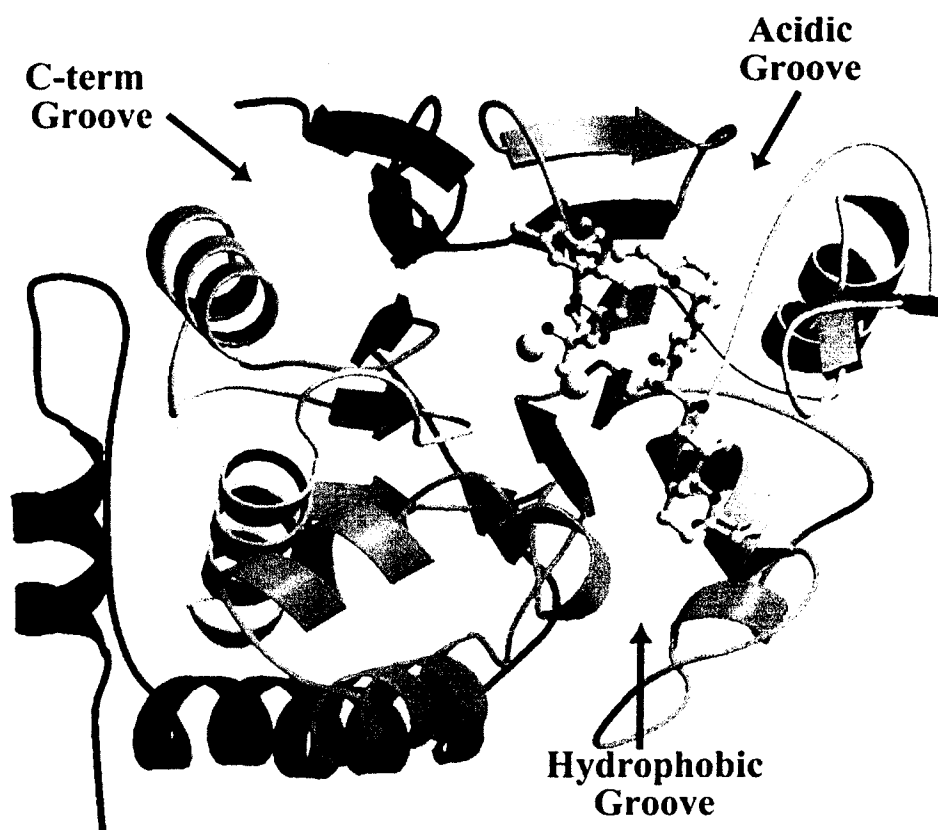
Figure 10: *Ribbon Structure of PP-1c Showing Grooves.*

Architecture of the PP-1c·OA complex with the protein shown as a ribbon representation, coloring is *blue* at the N terminus to *red* at the carboxyl terminus. OA is shown as ball-and-sticks with carbon atoms in *yellow* and oxygen atoms in *red*. The two manganese atoms in the active site are shown as *yellow* spheres. (Figure taken from [39].)
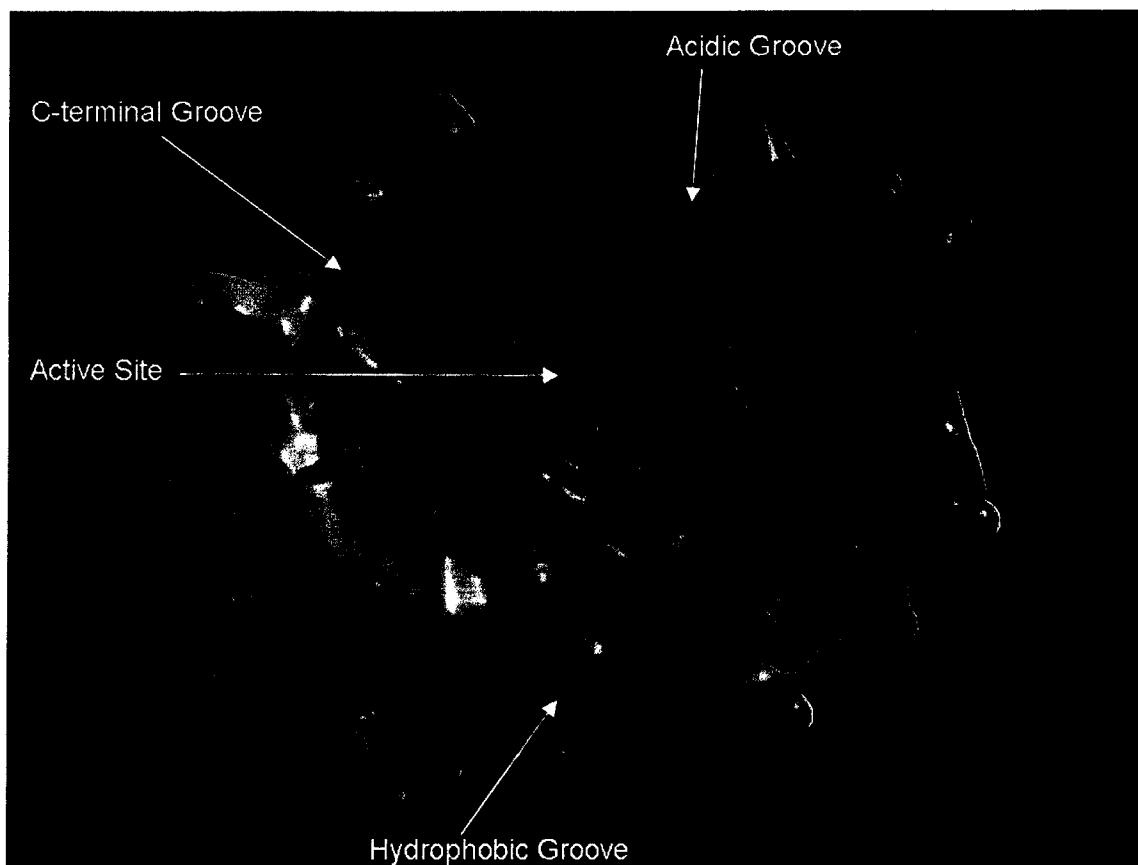
Figure 11: *Electrostatic Model of PP-1c Showing Grooves.*

The surface of PP-1c showing the catalytic site in the same orientation as in Figure 10. Areas coloured in *red* contain acidic, negative residues while areas coloured in *blue* contain basic, positive residues while *white* indicates a neutral charge. (Figure taken from [40].)

The β12-β13 Loop of Protein Phosphatase-1

Located in the C-terminal groove of PP-1c is a region called the β12-β13 loop. This loop sticks out of the protein at the edge of the catalytic binding site and is proposed to participate in catalysis since the phenolic oxygen on residue Tyr-272 is a potential ligand to the Fe^{2+} in the catalytic site [14]. This region consists of 12 residues from F267 to N278 which connect β-sheets 12 and 13. Various structural and mutagenesis studies have shown that the β12-β13 loop of PP-1c interacts with microcystin-LR, okadaic acid, calyculin A, I-2, as well as other toxins and inhibitors [24, 41-44]. All of the crystal structures solved to date indicate that very few conformational changes to the loop occur upon binding of toxins and inhibitors. This was seen when three structures of PP-1c, bound to different ligands, were overlapped for comparison. An exception to this is evident in the crystal structure of PP-1c bound to microcystin-LR, where the loop has shifted due to a covalent bond between residue C273 of the enzyme and an N-methyldehydroalanine (Mdha) residue in the toxin (Figure 12).

F276 of PP-1c is an Important Residue in the β12-β13 Loop

Another important residue located in the β12-β13 loop, F276, has been shown by crystallographic studies to be critical in binding of okadaic acid (OA) [39]. OA has been shown to interact with the hydrophobic groove of PP-1c. OA is known to inhibit PP-2A two orders of magnitude more strongly than PP-1c [35] and a cysteine is located at the equivalent position in PP-2A. This suggests that the substitution of a cysteine at position 276 in PP-1c may lead to an increase in the sensitivity of PP-1c to OA. A study has indeed shown that mutation of phenylalanine to cysteine at position 276 increased the sensitivity of PP-1c to okadaic acid 40-fold [44]. The phenylalanine at position 276 in PP-1c has been hypothesized to block favorable hydrophobic interactions between OA and the PP-1c active site [45]. This may explain why PP-1c is two orders of magnitude less sensitive to OA than PP-2A. Thus, F276 has been proposed to be a key residue in the interactions between PP-1c and OA.
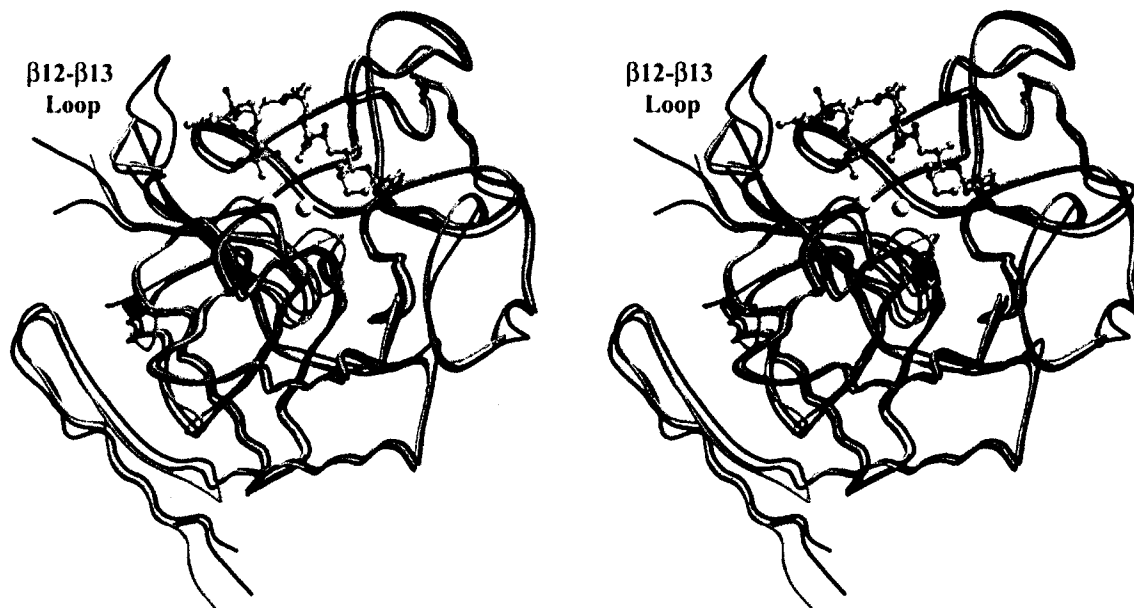
Figure 12: *Stereoview of Three Structures of PP-1c.*

Stereo representation of the backbone carbon alignment of tungstate-bound PP-1c (*green*), PP-1c:okadaic acid complex (*blue*), and PP-1c:microcystin-LR complex (PDB ID 1FJM) (*red*). Okadaic acid (OA) is shown in ball-and-stick representation with carbon atoms in *gray* and oxygen atoms in *red*. The metals are from the PP-1c:OA structure and are shown as yellow spheres. (Figure taken from [39].)

Comparison of the 3-D Structures of PP-1c and PP-2B

Backbone carbon alignment between 3-D structures of PP-1c bound to okadaic acid and PP-2B bound to phosphate were made to investigate differences in toxin sensitivity between PP-1c and PP-2B (Figure 13). The PP-1c backbone overlaps the PP-2B backbone except for the variable N and C terminal regions. Since the catalytic core of PP-2B shares 40% identity with the catalytic core of PP-1c, this is not surprising. One very important region to note on both structures is the $\beta12$-$\beta13$ loop, as the carbon backbone is very well aligned in this region. This is unexpected, since PP-2B is much less sensitive to toxins such as OA and MCLR which inhibit PP-1c by means of the $\beta12$-$\beta13$ loop. This suggests that it is not the backbone carbons, but amino acid side chains that mediate differences in toxin sensitivity between PP-1c and PP-2B.

The Y134 Residue of Protein Phosphatase-1

Residue Y134, located near the hydrophobic groove (Figure 14), is though to interact with p-Ser/Thr residues during dephosphorylation catalysis [14]. In a recent mutagenesis and molecular modeling study (Figure 15), Y134 was identified as a key residue in the binding of the marine sponge toxins calyculin A, and clavosines A and B (glycosylated members of the calyculin family) [36]. A separate study identified Y134 as key residue in the binding of the freshwater algae toxin microcystin-LR [24]. Mutagenesis analysis showed that a Y134F point mutation in PP-1c caused a decrease in sensitivity to calyculin A and okadaic acid [42].
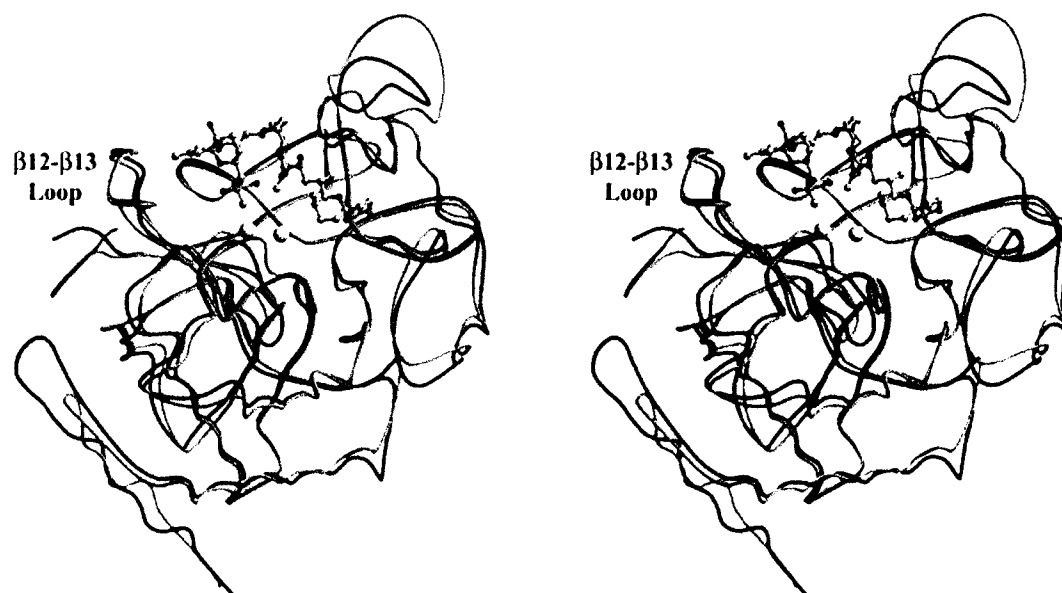
Figure 13: *Stereoview of the structural backbone of PP-1c and PP-2B.*

Stereo representation of the backbone carbon alignment of PP-1c:OA (*blue*) and the A subunit of PP2B (PDB ID 1TCO) (*green*). Note that the protein backbone of the catalytic core of PP-1c and PP-2B are very similar, especially in the β12-β13 loop region. (Figure taken from [39].)
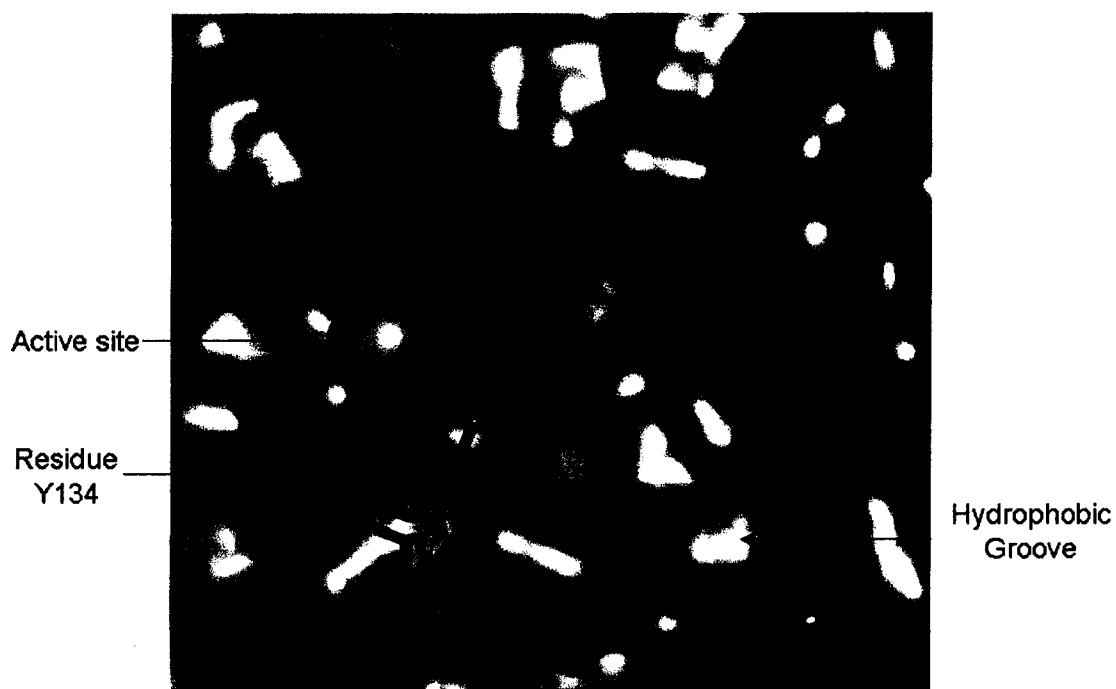
Figure 14 : *Location of Y134 Near the Hydrophobic Groove of PP-1c.*

A close up view of the surface of PP-1c. The two *orange* spheres represent the metal cations in the active site. Residue Y134 is visible in the catalytic site and the hydrophobic groove is also illustrated. (Figure taken from [40].)
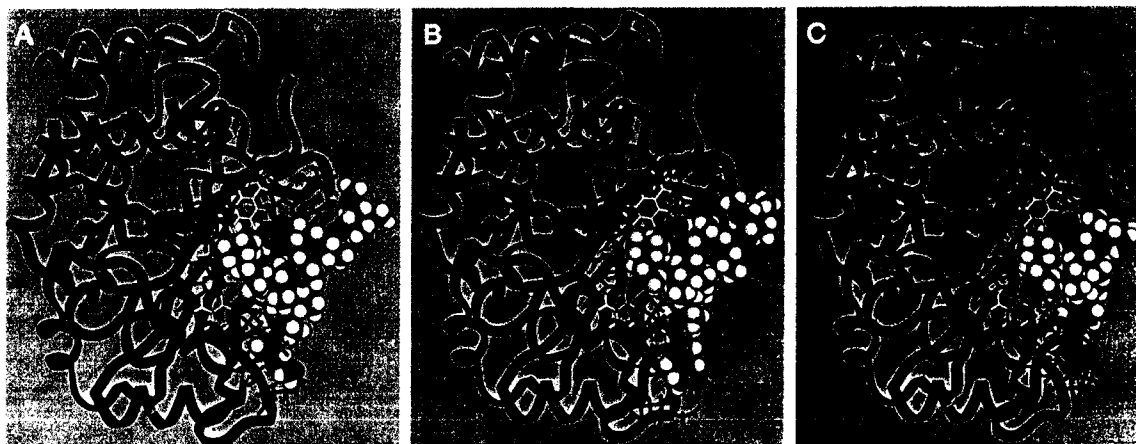
Figure 15: *Structure of PP-1c Bound to Clavosines A and B and Calyculin A.*

Molecular models of clavosine A, clavosine B, and calyculin A bound to PP-1c. Space-filling molecular models of (*a*) clavosine A, (*b*) clavosine B, and (*c*) calyculin A bound to a ribbon model of PP-1c are depicted. Metal cations (small *pink* balls) and amino acid side chains (*blue* sticks) in PP-1c residing within 4 Å of each inhibitor are shown. PP-1c residue Y134 *(top)* is highlighted in *yellow*. Atoms in the space-filling inhibitor models are colored as follows: carbon (*green*), oxygen (*red*), nitrogen (*blue*), phosphorus (*pink*), and hydrogen (*white*). (Figure taken from [36].)

The RVxF Binding Pocket of Protein Phosphatase-1

A structural feature involved in almost all interactions between PP-1c and its subunits is the RVxF binding pocket (where x is any amino acid), located opposite the catalytic site and flanked by negatively charged residues [46]. Subunits of PP-1c possessing a short, conserved amino acid sequence, Arg-Val-x(any amino acid)-Phe, interact with the RVxF binding pocket on PP-1c [15]. The G_M subunit of PP-1c, for example, has been shown to bind in this way. Residues F257 and C291 of PP-1c are involved in interactions between the enzyme and the G_M subunit (Figure 16). A crystallographic study using a peptide of G_M ($G_{M[63-75]}$) showed that C291 of PP-1c interacts hydrophobically with Val66' and Phe68' of $G_{M[63-75]}$, while there are polar interactions between nitrogens and oxygens of PP-1c C291 and $G_{M[63-75]}$ Ser67' and Ala69' (Figure 17). The same study showed that the side chain of PP-1c F257 interacts hydrophobically with Phe68' of $G_{M[63-75]}$.

A Model of the Interaction Between Protein Phosphatase-1 and Inhibitor-2

The most recent model of PP-1c and I-2 interactions has been proposed by the laboratory of Anna DePaoli-Roach [47]. Several experiments were done to find residues on I-2 which were important for these interactions. Evidence of interaction with PP-1c was obtained for five domains on I-2 [48]. However, the regions of PP-1c which interact with I-2 are still somewhat speculative.

According to the DePaoli-Roach model, the NH_2-terminal region of I-2, residues 1-35, contains a unique PP-1c binding sequence IKGI which is a key region for initial inhibition of PP-1c by I-2 and is proposed to bind to an I-2 specific site on PP-1c. Residues 64-114 form a masking region which is assumed to bind to the $\beta12$-$\beta13$ loop of PP-1c. This masking region contains Thr-72 (a target for protein phosphorylation) and may be involved in inactivation of the PP-1c:I-2 complex. Residues 135-151 contain a KLHY motif, which is suggested to be equivalent to the RVxF motif, and would thus bind to PP-1c in the RVxF binding pocket, distal from the catalytic site, and flanked by negatively charged residues. The COOH-terminal domain is alleged to bind to a distinct,
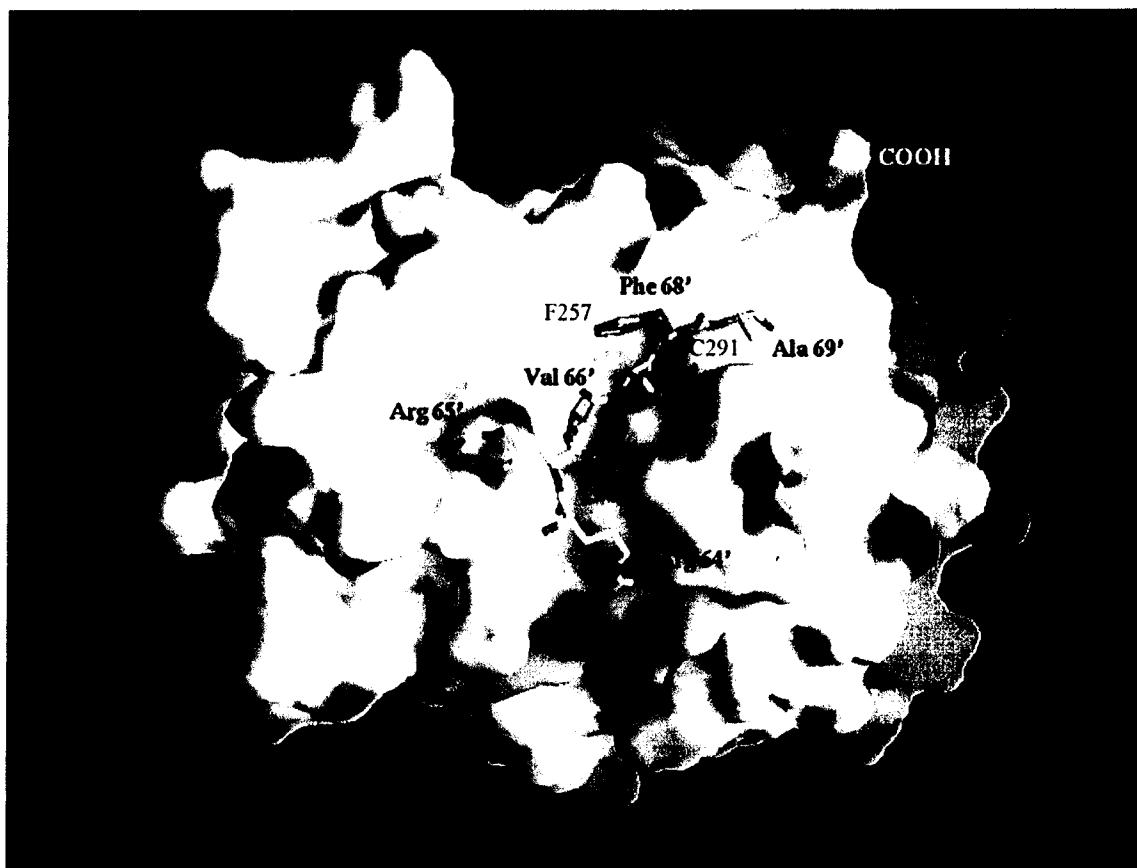
Figure 16: *Surface of the RVxF Binding Pocket of PP-1c.*

Solvent-accessible surface and surface electrostatic potential of the PP-1c:$G_{M[63-75]}$ peptide complex calculated with PP-1c coordinates alone and showing the peptide as a stick representation in the vicinity of the RVxF binding pocket. The protein surface is coloured according to electrostatic potential from *red* (most negative) to *blue* (most positive). The figure shows pronounced negative electrostatic potential in the region surrounding the N-terminus of the RVxF binding pocket that results from seven conserved acidic residues. The $G_{M[63-75]}$ residues which interact with the binding pocket are labeled, and the surface region where residues F257 and C291 of the PP-1c RVxF binding pocket are located can also be seen. (Figure taken from [46].)

Figure 17: *Ribbon Image of the RVxF Binding Pocket of PP-1c.*

Details of the structure of the peptide-binding site showing hydrophobic interactions between residues F257 and C291 of PP-1c with residues Val66' and Phe68' of the $G_{M[63-75]}$ peptide. (Figure taken from [46].)

yet ill-defined site on PP-1c. The 5th proposed I-2 binding site is a single residue, Trp-46, which is thought to interact with a region near the catalytic site of PP-1c (Figure 18) [47].

The NH$_2$-terminal region and the KLHY sequence of I-2 are proposed to act as anchors to position the masking region, residues 64-114 over the active site of PP-1c, thus blocking access to substrate. It has also been suggested that weakening of any of the five sites of interaction renders the masking region more mobile and allows access of substrate to the active site [47]. There is controversy about the importance of the KLHY region of I-2 and whether it does indeed function as an RVxF motif [47, 49]. The contested function of the KLHY sequence of I-2 is in direct contrast to the KIQF sequence of I-1, which as been shown to bind to the RVxF binding pocket of PP-1c [22]. Only one of the proposed I-2 interaction sites of PP-1c has been clearly identified to date. This confirmed I-2 binding site consists of residues E53, E55, K165, E166, K167 of PP-1c, and is located near the RVxF binding pocket. Mutagenesis studies have shown this region of PP-1c (region "A" in Figure 18) to bind the IKGI sequence of I-2 [50]. Thus, one of the five putative I-2 binding sites on PP-1c has been confirmed, but more work must be done to investigate the location of the remaining putative I-2 binding sites on PP-1c.

1.7 Purpose of the Current Study

PP-1c is an important enzyme which regulates many key metabolic pathways in eukaryotic cells. Therefore, it is important to understand PP-1c regulation. Eukaryotic cells may regulate PP-1c activity without altering the activity of other phosphatases through the use of specific endogenous inhibitors, such as I-2. Therefore, elucidation of the molecular mechanisms involved in protein-protein interactions between PP-1c and I-2 may lead to a greater understanding of PP-1c regulation. In addition, understanding molecular mechanisms involved in PP-1c:I-2 interactions may be the first step to rational design of specific inhibitors of PP-1c. This could then advance investigation of the role of PP-1c using a whole organism and eventually lead to the development of therapeutics for the treatment of diseases, such as type-2 diabetes [51]. This highlights the importance of the analysis of molecular mechanisms involved in PP-1c:I-2 interactions.
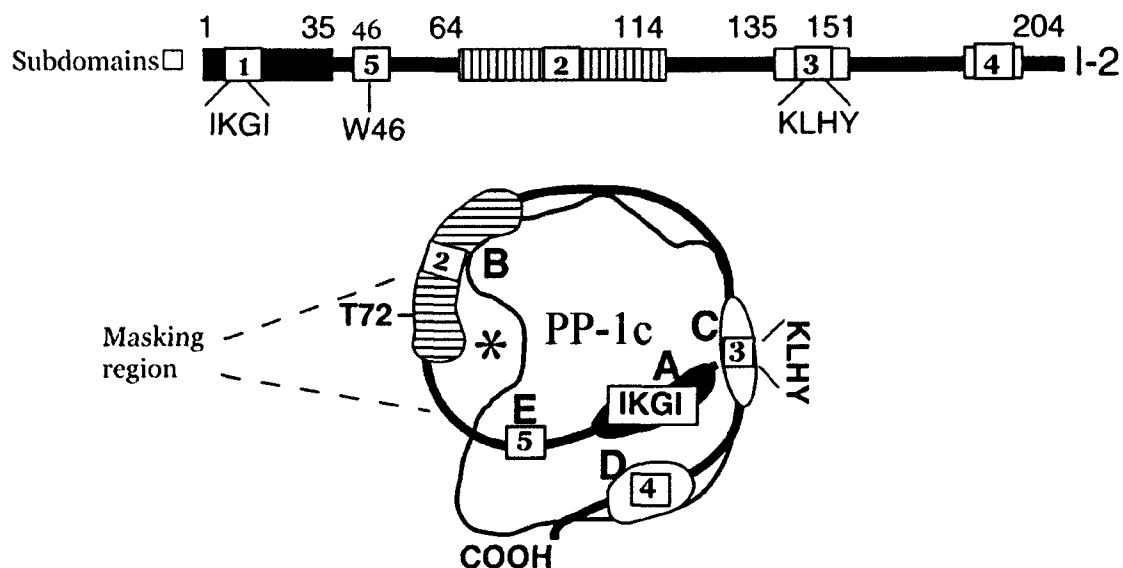
Figure 18: *DePaoli-Roach Model of PP-1c:I-2 Interaction.*

A schematic diagram of the regions of I-2 that interact with PP-1c is shown in the *upper part*. The IKGI and the KLHY motifs are indicated as subdomains 1 and 3, respectively. Subdomains 5, 2, and 4 denote, respectively, the region of I-2 comprising Trp^{46}, residues 64-114, and a site in the COOH terminus of I-2. The lower part shows a cartoon of I-2 (*thick line*) wrapped around the PP-1c. The interacting sites on PP-1c are indicated by capital letters *A, B, C, D*, and *E*. Interaction of I-2 with PP-1c positions the masking region in front of the active site (*), thus blocking the access of substrates. Sites A and C are located at the back of the active site and indicate the binding sites for IKGI and KLHY, respectively. Site B may correspond to the $\beta12$-$\beta13$ loop of PP-1c. Site D is a site that may interact with the COOH terminus of I-2, and site E indicates the Trp^{46} binding site. Weakening of any of the interactions renders the masking region more mobile, thus allowing access of substrates to the active site. See text for details. (Figure taken from [47].)

The purpose of this study was to identify key regions of PP-1c which are critical in the formation of the stable, inactive complex between PP-1c and I-2. Thus far, the majority of PP-1c:I-2 interaction studies have focused on regions of I-2 which interact with PP-1c and few studies have targeted regions of PP-1c involved in the PP-1c:I-2 interactions. Several possibilities have been deduced through analysis of the crystal structures of okadaic acid, microcystin-LR, and calyculin A bound to PP-1c. These sites include: the $\beta12$-$\beta13$ loop near the catalytic site which has been shown to interact with toxins, a residue near the hydrophobic groove that has been shown to interact with okadaic acid, microcystin-LR and calyculin A, and the RVxF binding pocket distal from the catalytic site which binds regulatory subunits (Figure 19).

A structure of the PP-1c:I-2 complex would be the most useful way to probe the molecular mechanism of their interaction. Although a complete crystal structure is possible, attempts to crystallize PP-1c:I-2 have not been fruitful. This may be due to the fact that I-2 possesses multiple PP-1c binding sites with different affinities and flexibilities.

In the present study, two distinct approaches have been undertaken to investigate interactions between PP-1c and I-2. The first approach was derived from an unexpected finding of the present study where the PP-1c:I-2 complex was found to have residual phosphatase activity. It had been previously suggested that a change in the residues involved in the positioning of I-2 near the active site would either destabilize or stabilize the PP-1c:I-2 interaction, allowing more or less substrate access to the active site [47]. The discovery of residual activity in the PP-1c:I-2 complex thus allowed this hypothesis to be explored. The second approach was to test the sensitivity of PP-1c to I-2 inhibition. A significant change in interactions between the two proteins would be expected to lead to a change in PP-1c sensitivity to I-2. In addition, recent advances in biochemical tools has enabled us to more accurately determine the ratio of PP-1 to I-2 in the PP-1c:I-2 complex.
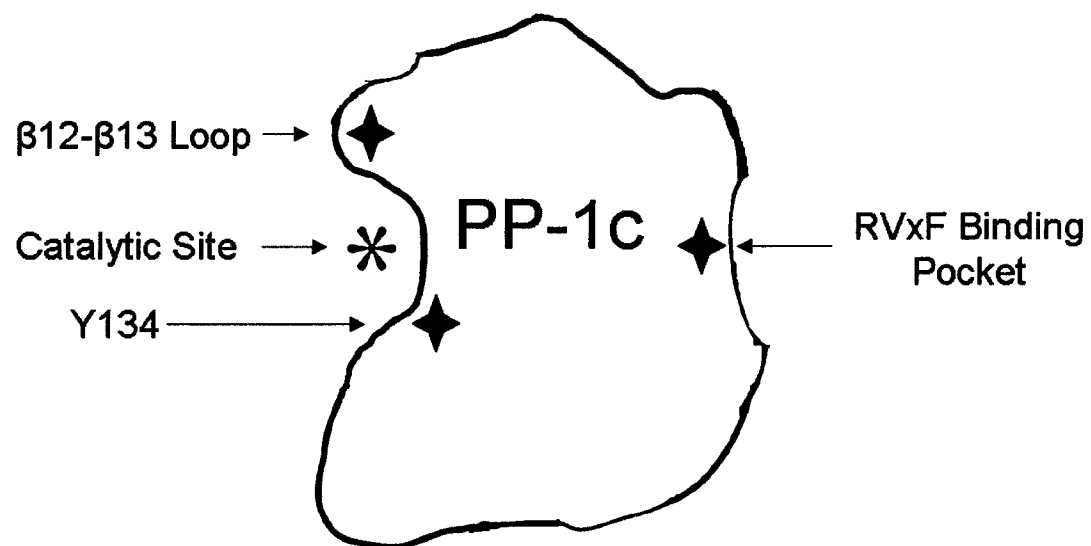
Figure 19: *Regions of PP-1c Investigated in this Study.*

The regions of PP-1c which are investigated in this study and which we hypothesized to interact with I-2 are shown here.

The β12-β13 Loop Mutant of PP-1c

Genetic and mutational analysis of PP-1c has implicated the β12-β13 loop (residues 267-278) in toxin and I-2 binding [52]. As PP-2B is known to be both insensitive towards inhibition by I-2 and to contain a different β12-β13 loop amino acid sequence, a β12-β13 loop mutant of PP-1c was created, containing a PP-1c [273]CGEFD[277] to PP-2B [312]LDVYN[316] substitution (Figure 20). Toxin sensitivity tests carried out in our lab using the β12-β13 loop mutant showed a significant decrease in sensitivity towards okadaic acid and microcystin-LR [53].

Crystal structures of PP-1c with okadaic acid and the β12-β13 loop mutant of PP-1c with okadaic acid have both been solved. The protein backbone in the loop region matched almost identically, only the side chains being in different orientations between the structures. This showed that the carbon backbone structure of the catalytic site of the PP-1c loop mutant had not been greatly altered by the substitution of PP-2B loop region residues (Figure 21). Thus, the observed decrease in PP-1c β12-β13 loop mutant sensitivity to okadaic acid may be due to the interaction of the PP-1c side chains with the toxin. Given these facts, we hypothesized that the I-2 insensitive β12-β13 loop region may lead to an increase in substrate accessibility to the active site, thus leading to an increase in the residual phosphatase activity of the β12-β13 loop mutant:I-2 complex.

F276Y Mutant of PP-1c

The F276 residue of PP-1c, located in the β12-β13 loop, has been shown to be important for binding okadaic acid [39]. The F276 residue forms hydrophobic interactions with the C-4 to C-16 region of okadaic acid through the action of its phenyl ring. It was suggested that the introduction of a polar hydroxyl group, through the mutation of phenylalanine 276 to tyrosine, may disrupt hydrophobic interactions between the toxin and PP-1c. However, recent work carried out in our lab showed that an F276Y point mutation displayed no change in okadaic acid sensitivity, suggesting that the phenyl ring of tyrosine was still able to form hydrophobic interactions [53]. The present study

PP1 263 L V T L F S A P N Y C G E F D N A G A M M
PP2B 302 L I TI F S A PN Y L D VY N N K A AV L

Figure 20: *Comparison of the Primary Structure of the β12-β13 Loop Region Between PP-1c and PP-2B.*

Boxed residues indicate amino acids of PP-1c which have been replaced with amino acids from PP-2B in the region of the β12-β13 loop.
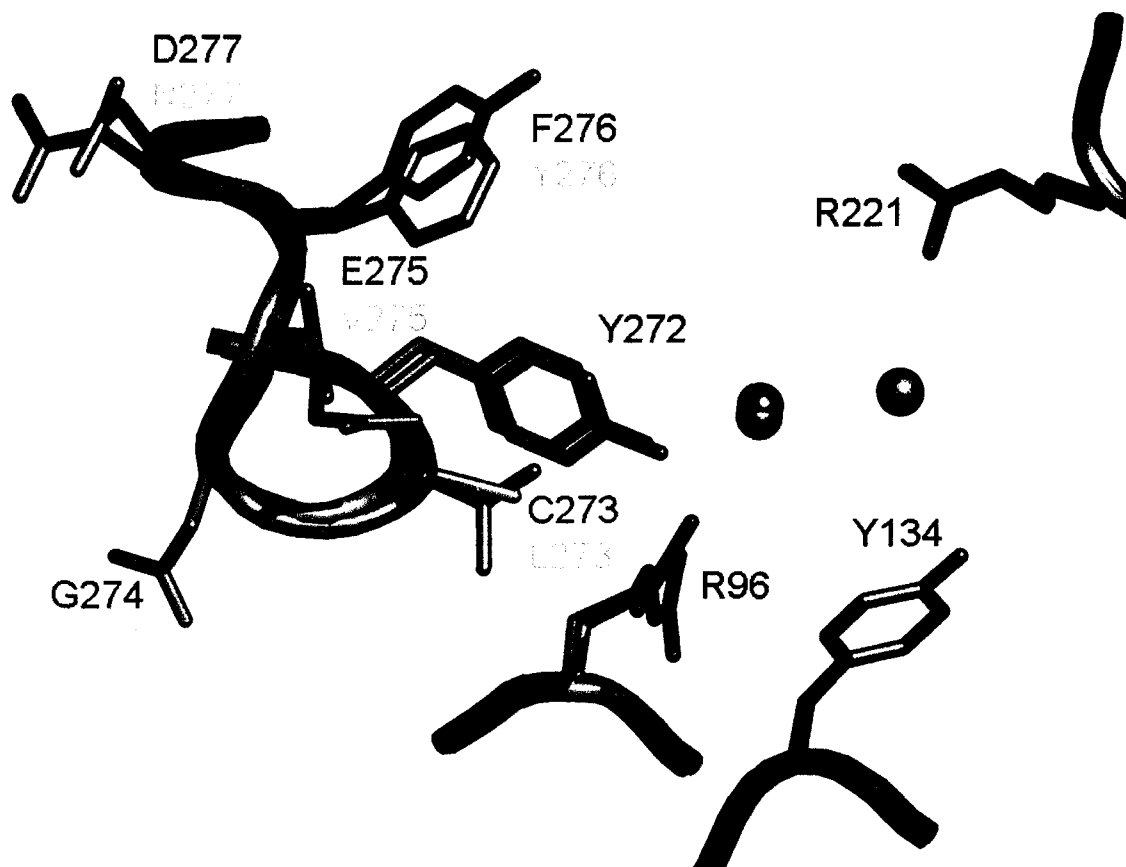
Figure 21: *Comparison Between Catalytic Sites of Wild Type PP-1c and the β12-β13 Loop Mutant.*

The wild type PP-1c structure is shown in *blue* while the loop mutant PP-1c structure is shown in *orange*. Okadaic acid was used as the ligand for both of these structure but has been removed for clarity. The divalent metal cations in the active site are shown as *blue* spheres for the wild type PP-1c and as *orange* spheres for the loop mutant PP-1c. Note that one of the cation spheres overlaps perfectly and so is all *orange*, while the other sphere does not and so is half *blue* and half *orange*. The colour scheme for the residues are carbon (*gray*), nitrogen (*blue*), oxygen (*red*), and sulphur (*yellow*). Notice how the backbone of the protein is relatively unchanged in the catalytic site between the wild type and loop mutant structures. Thus, there are very few differences between the two structures at the catalytic site. (Figure taken from [40].)

anticipated a similar hydrophobic interaction between PP-1c and I-2, and tested it using the F276Y mutant of the phosphatase. While the substitution of a Tyr for a Phe may disrupt I-2 interactions with PP-1c, we also hypothesized that the F276Y substitution would allow PP-1c to make a hydrogen bond with I-2 through the action of tyrosine's hydroxyl group. If PP-1c:I-2 interactions were stronger for the mutant, substrate accessibility should be reduced, evidenced by a decrease in the residual phosphatase activity of the PP-1c:I-2 complex.

Y134A Mutant of PP-1c

Previous studies have shown that the Y134 residue of PP-1c is involved in the binding of microcystin-LR, clavosines A and B, and calyculin A [24, 36]. Y134 forms a hydrogen bond with the carboxylate group of the methyl aspartic acid (Masp) side chain of microcystin-LR [24] and forms van der Waals interactions with calyculin A and the clavosines [36, 54]. The present study investigated the PP-1c:I-2 interactions using a Y134A mutant, thinking that removal of the phenol group might remove the potential for hydrogen bonding with I-2. We hypothesized that this mutation may allow more access of substrate into the catalytic site, thus leading to an increase in the residual activity of the PP-1c:I-2 complex.

RVxF Binding Pocket

The RVxF binding pocket of PP-1c is a common regulatory subunit binding site located distal from the catalytic site. Previous studies have focused primarily on the I-2 regions involved in the interaction with PP-1c [47, 49]. Residues in the RVxF binding pocket have not yet been analyzed with regard to I-2 binding and inhibition.

The present study used two mutations, F257A and the C291A, located in the RVxF binding pocket of PP-1c, to determine if the pocket is involved in I-2 inhibition of PP-1c. Since both mutants are expected to abolish interaction at those residues, any change in inhibitory activity of I-2 would suggest that the RVxF binding pocket is a

source of interaction, while no change might indicate that the pocket is not involved in I-2 mediated inhibition.

1.8 Hypotheses Tested in this Study

The following hypotheses were addressed in the present study:

1. The $\beta12$-$\beta13$ loop region of PP-1c is a key region involved in the positioning of I-2 over the catalytic site of PP-1c.

2. Y134, near the hydrophobic groove, is an important residue involved in the positioning of I-2 over the catalytic site of PP-1c.

3. The RVxF binding pocket, distal from the catalytic site, is an important region for the mediation of PP-1c:I-2 interactions.

Chapter 2: Experimental Procedures

2.1 Materials

Yeast Casein Kinase-2 (CK-2) was obtained from Dr. Michael Schultz in the Department of Biochemistry at the University of Alberta. Other materials were obtained from Sigma Chemicals unless otherwise stated.

The $\beta12$-$\beta13$ loop mutant clone, which involved a substitution of residues $^{273}CGEFD^{277}$ of PP-1c for residues $^{312}LDVYN^{316}$ from PP-2B, as well as the F276Y point mutant clone were both provided by Kathleen Perreault. The Y134A point mutant clone as well as the I-2 clone were both provided by Hue Ahn Luu. The F257A and C291A point mutant clones were provided by Andrea Fong. These researchers were in the laboratory of Dr. Charles Holmes in the Department of Biochemistry at the University of Alberta.

Media

- *Luria Broth ampicillin liquid media:* Luria Broth (Difco^{TM}), 0.2mg/ml ampicillin, 0.001% (w/v) Vitamin B$_1$, and 1mM MnCl$_2$

Buffers

- *Buffer A:* 50mM Imidazole pH 7.3, 0.5mM EDTA, 0.5mM EGTA, 100mM NaCl, 2.0mM MnCl$_2$, 3.0mM DTT, 2.0mM Benzamidine, 0.5mM PMSF, 10% (v/v) Glycerol.
- *Buffer B:* 50mM Imidazole pH 7.3, 0.5mM EDTA, 0.5mM EGTA, 3.0mM MnCl$_2$, 3.0mM DTT, 2.0mM Benzamidine, 0.5mM PMSF, 10% (v/v) Glycerol.
- *Buffer C:* 50mM Imidazole pH 7.3, 0.5mM EDTA, 0.5mM EGTA, 300mM NaCl, 2.0mM Benzamidine, 2.0 mM MnCl$_2$, 3.0mM DTT, and 10% (v/v) Glycerol.

- *Buffer D:* 50mM Tris-HCl pH 7.5, 2mM EDTA, 2mM EGTA, 1% Triton X-100, 1mM PMSF, 1mM Benzamidine, 0.1% (v/v) β-mercaptoethanol.

- *Buffer E:* 20mM Ammonium Acetate pH 5.0, 0.1mM EGTA, 1mM DTT.

- *Extraction buffer:* 50mM Tris-HCl pH7.5 2mM EDTA, 2mM EGTA, 1% (v/v) Triton X-100, Leupeptin 0.01 mg/ml, Pepstatin 0.01 mg/ml, Aprotinin A 0.01 mg/ml, Chymostatin 0.005 mg/ml, PMSF 1.0mM, Benzamidine 10mM, and Lysozyme 200mg/ml.

- *Glycogen phosphorylase dialysis buffer:* 50mM Tris pH 7.0, 1mM EDTA, 25mM NaF, and 0.1% (v/v) β-mercaptoethanol.

Solutions

- *Solution A:* 50mM Tris-HCl, pH 7.0, 0.1mM EDTA, 1mg/ml BSA, 0.2% (v/v) β-mercaptoethanol, 0.8mM $MnCl_2$.

- *pNPP assay solution:* 50mM Tris, pH 8.3, 0.1mM EDTA, 17mM $MgCl_2$, 0.1% (w/v) BSA, 0.5mM $MnCl_2$, 0.2% (v/v) β-mercaptoethanol.

<u>2.2 Methods</u>

Protein determination

Protein concentrations of PP-1c and I-2 were estimated using the Bio-Rad Protein Assay (BIORAD).

para-nitrophenolphosphate (pNPP) phosphatase assay

The pNPP assay is a kinetic endpoint screening test designed to detect the presence of PP-1c phosphatase activity. Recombinant PP-1c can remove the phosphate group from pNPP. This changes the colour of the pNPP in solution from colourless to yellow. The yellow colour can be detected at 405 nm. The intensity of absorbance at 405 nm corresponds to the amount of phosphatase activity in the solution. (This protocol was taken from [55].)

A sample of solution (10μl) thought to contain PP-1c was added to 40μl of pNPP assay buffer. Reactions were initiated by adding pNPP to the reaction mixture to a final concentration of 5mM. Reactions were incubated at 37°C for 1hr and the absorbance at 405 nm was read using a Vmax kinetic microplate reader from Molecular Devices. A colour change from colourless to yellow indicated the presence of PP-1c.

The pNPP assay was also used to screen for the presence of I-2. The assay was carried out as above with the following modifications. A known quantity of PP-1c (10μl) was added to 36μl of pNPP assay buffer and 4μl of sample thought to contain I-2. The solution was incubated at 25°C for 10min prior to the addition of the pNPP. The presence of I-2 was detected by comparing the absorbance at 405 nm of the sample wells to a control well containing only PP-1c. A lower absorbance at 405 nm compared to the PP-1c control indicated the presence of I-2 in the sample.

Sodium dodecyl sulfate polyacrylamide gel electrophoresis (SDS PAGE)

Gels used for all protocols were made with a 4% stacking gel and a 12% running gel. SDS PAGE Molecular Weight Standards, Low Range (BIORAD), were used to estimate the sizes of bands on gels. The proteins standards are: Glycogen Phosphorylase *b* 97.4 kDa, Serum Albumin 66.2 kDa, Ovalbumin 45 kDa, Carbonic Anhydrase 31 kDa, Trypsin Inhibitor 21.5 kDa, and Lysozyme 14.4 kDa. Gels were operated at 200V for 55min in a solution of 25mM Tris, 200mM Glycine, and 0.1% SDS. Gels were stained in a 0.25%(w/v) solution of coomassie blue in a 40% methanol/10% acetic acid solution, then destained in a 40% methanol/10% acetic acid solution. Gels were dried on Fisherbrand chromatography paper using a Model 583 BIORAD gel dryer.

Preparation of recombinant DH5α *E.coli* culture for PP-1c$_{\gamma 1}$

Glycerol stocks of recombinant DH5α *E. Coli* (Invitrogen) were streaked on LB Amp plates to isolate single colonies. For each liter of LB Amp, a single colony was picked and grown in 100ml of LB Amp media at 37°C for 16hr in a Series 25 Incubator Shaker from New Brunswick Scientific Co., Inc. The culture was added to 900ml of LB Amp and incubated under the same conditions until the OD$_{600}$ of the culture was between

0.6 and 1. Expression of PP-1c was induced by adding IPTG to a final concentration of 1mM and incubating at 37°C for 15-17hr. The culture was then centrifuged at 3500xg for 45min at 4°C using a swinging bucket rotor (Beckman J6B centrifuge). The supernatant was discarded and the pellets were frozen at -70°C until purification of PP-1c. (This protocol was taken from [56].)

Purification of human PP-1c from recombinant DH5α *E. coli*

Frozen cell pellets were resuspended in 80ml of Buffer A and sonicated six times using a Branson Sonifier 450 at constant cycle, level eight duty, for 40sec with 2min cooling between each pulse in an ethanol/ice bath. The lysate was centrifuged at 17000xg for 1hr at 4°C using an F0630 rotor in a Beckman GS-15R centrifuge. The supernatant was decanted and loaded onto an 80ml Heparin Sepharose column (Pharmacia). The unbound protein was washed off with buffer A at a flow rate of 5ml per min. PP-1c was eluted using buffer A at a flow rate of 5ml per min and a salt gradient of 100mM to 600mM NaCl in 80min. Fractions (5ml) were collected and assayed for phosphatase activity using a pNPP assay.

Active fractions were pooled together and diluted one part in four with buffer B and loaded onto a MonoQ 10/10 (10mm in diameter and 10 cm in length) column (Pharmacia) at 2ml per min. Unbound protein was washed off at a flow rate of 2ml per min using buffer B and the PP-1c was eluted with buffer B using a flow rate of 2ml per min and a salt gradient of 50mM to 400mM NaCl in 80min. Fractions (2ml) were collected and assayed for phosphatase activity using a pNPP assay. Active fractions were analyzed by 12% SDS PAGE and the most active and most pure fractions were pooled and concentrated to less than 2ml using an Amicon Ultra-15 centrifugal filter device with a 10,000 molecular weight cut-off (Millipore). The filter device was centrifuged at 4000xg for 10min at 4°C using a swinging bucket rotor (Beckman J6B centrifuge) until the volume of sample was less than 2ml.

The sample was loaded into a 2ml injection loop connected to a Superdex 75 26/60 (26mm in diameter and 60cm in length) column (Pharmacia) and the PP-1c was

eluted with buffer C at a flow rate of 0.2 ml per min, for 1871min. Ninety-five 600μl fractions, corresponding to the PP-1c absorbance peak at 280 nm, were collected after 124.2ml (621min) had elapsed. Fractions were assayed for phosphatase activity using a pNPP assay and the active fractions were analyzed by 12% SDS PAGE. The most active and most pure fractions were pooled and concentrated to less than 2ml using an Amicon Ultra-15 centrifugal filter device with a 10,000 kDa molecular mass cut-off (Millipore). The filter device was centrifuged at 4000xg for 10min at 4°C using a swinging bucket rotor (Beckman J6B centrifuge) until the volume of the sample was less than 2ml. Glycerol was added to the sample to a final concentration of 50% (v/v) and the sample was stored at -20°C. A sample of PP-1c was analyzed on a Superdex 75 column (Pharmacia) (Figure 22). In a separate experiment, PP-1c was analyzed by gel filtration and fractions which eluted off the column were examined by 12% SDS PAGE (Figure 23). (This protocol was taken from [56].)

The specific activity of wild type PP-1c and PP-1c mutants

The specific activity of PP-1c was expressed in units per milligram of protein (U/mg), where 1U is the amount of enzyme which released one μmole of phosphate per minute. The specific activity of the wild type PP-1c (wtPP-1c) was 4.4U/mg. The specific activity of the mutants were: β12-β13 loop (3.6U/mg), F276Y (7.7U/mg), Y134A (1.1U/mg), F257A (0.0024U/mg), and C291A (1.0U/mg).

Preparation of recombinant BL21DE3 *E.coli* culture for I-2

Glycerol stocks of recombinant BL21DE3 *E. Coli* (Stratagene) were streaked on LB Amp plates to isolate single colonies. For each liter of NZCYM Amp, a single colony was picked and grown in 100ml of LB Amp media at 37°C for 16hr in a Series 25 Incubator Shaker from New Brunswick Scientific Co., Inc. The culture was added to 900ml of LB Amp and incubated under the same conditions until the OD_{600} of the culture was between 0.6 and 1. Expression of I-2 was induced by adding IPTG to a final concentration of 1mM and incubating at 37°C for 5hr. The culture was then centrifuged at 3500xg for 45min at 4°C using a swinging bucket rotor (Beckman J6B centrifuge). The supernatant was discarded and the pellet was resuspended using 2.5ml of extraction
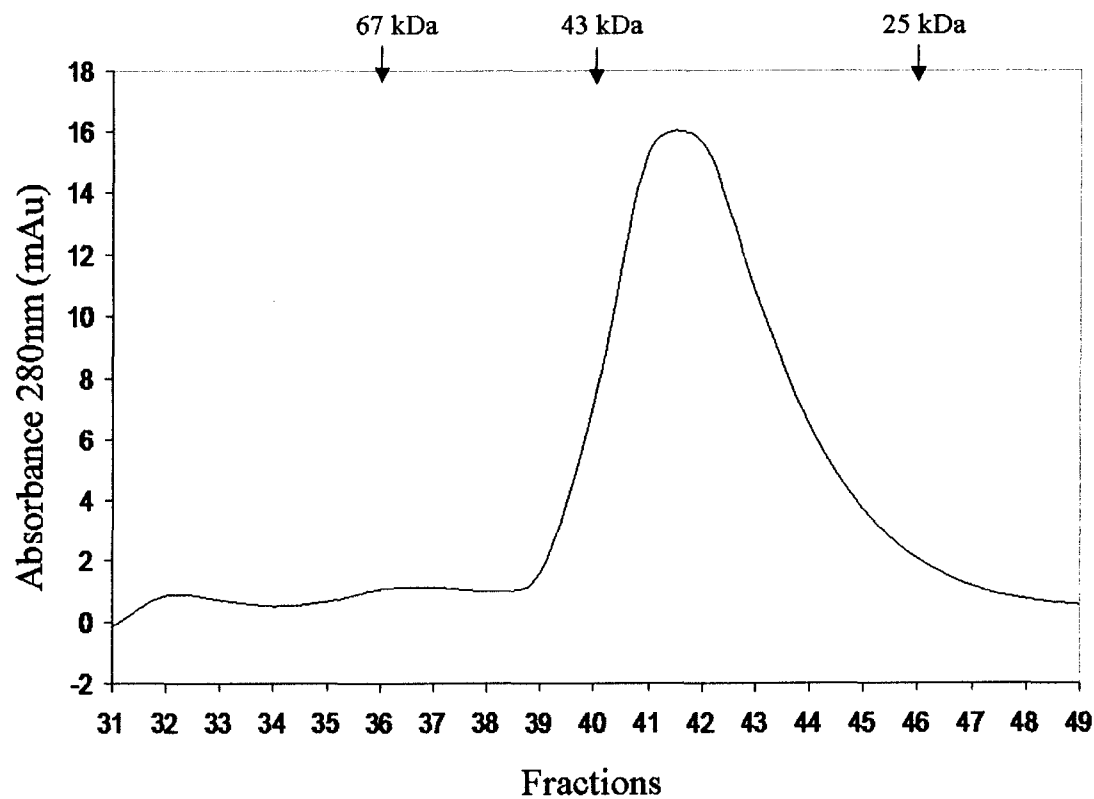
Figure 22: *Analysis of Free Protein Phosphatase-1 Catalytic Subunit using Gel Filtration.*

PP-1c (50μg) was analyzed on a Superdex 75 gel filtration column (Pharmacia) at a flow rate of 0.5ml/min, collecting 250μl fractions using the Pharmacia AKTA P-920 pump and visualized using the UPC-900 detector at 280 nm and the UNICORN 4.0 software (Pharmacia).
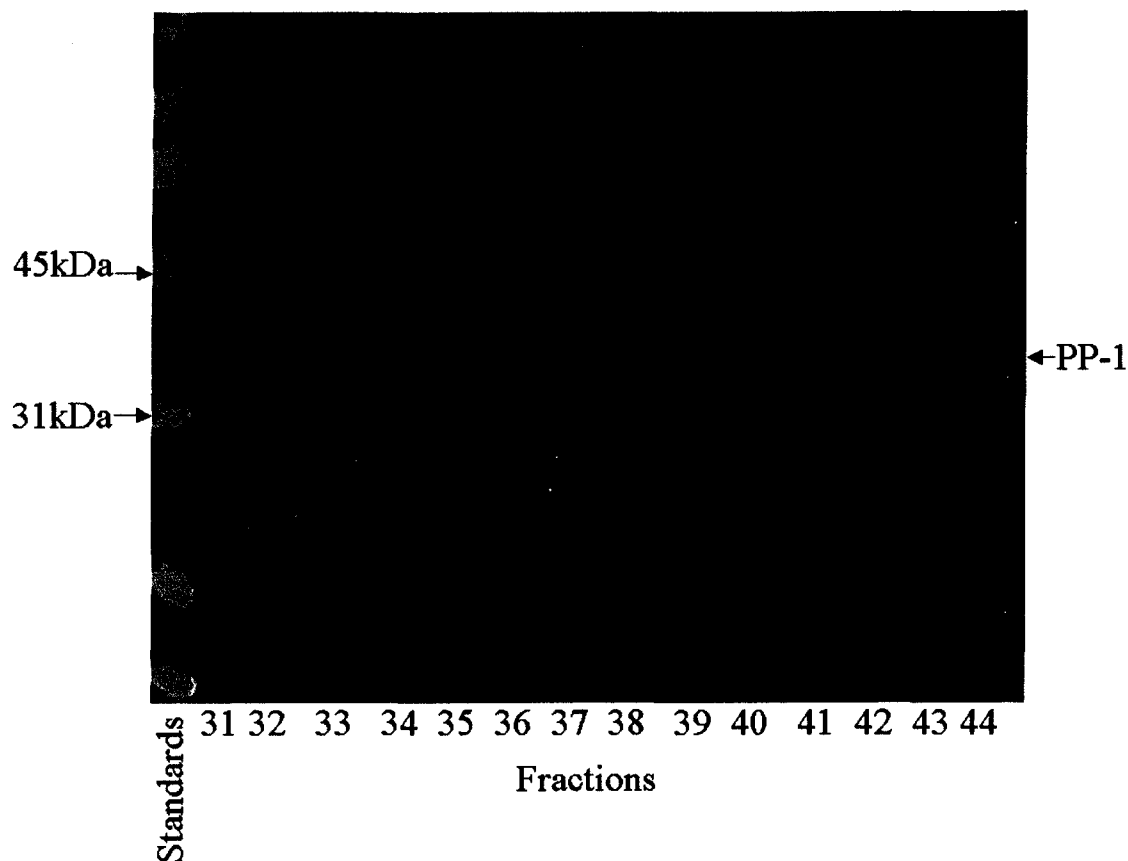
Figure 23: *SDS PAGE Analysis of Free Protein Phosphatase-1 Catalytic Subunit after Elution off a Gel Filtration Column.*

PP-1c (50μg) was analyzed on a Superdex 75 gel filtration column (Pharmacia) at a flow rate of 0.5ml/min using the Pharmacia LKB P-500 pump and LCC-501Plus controller. Fractions (250μl) were collected and samples from fractions 31 to 44 were analyzed by 12% SDS PAGE, stained and visualized using the Odyssey system as described in Experimental Procedures. Note that there is some non-specific binding of coomassie blue stain and a small amount of higher molecular weight impurities in the upper part of the gel.

buffer for each gram of wet weight pellet. The resuspended pellet was frozen at -70°C until purification of I-2. (This protocol was taken from [57]).

Purification of human I-2 from recombinant BL21DE3 *E. coli*

Frozen cell pellets were thawed using 2.5ml of extraction buffer for each gram of wet weight pellet. The resuspended cells were sonicated 3 times using a Branson Sonifier 450 at constant cycle and level 6 duty for 20sec each with 2min cooling on ice between pulses. The sample was boiled in a water bath for 20min, cooled on ice for 1hr and then centrifuged at 17000xg for 45min at 4°C using an F0630 rotor in a Beckman GS-15R centrifuge. The supernatant was loaded onto a Q-Sepharose 16/10 column (Pharmacia) and unbound protein was washed off the column with buffer D. The protein was eluted with buffer D at a flow rate of 3ml per min and a salt gradient of 0-500mM NaCl in 140min. Fractions (3ml) were collected and assayed for I-2 inhibition using a pNPP assay and the active fractions were analyzed by 12% SDS PAGE to determine purity.

The most active and most pure fractions were dialyzed against buffer E and loaded onto a Mono-Q 10/10 column at 2ml per min using buffer E. Unbound protein was washed off using buffer E and the I-2 was eluted using buffer E at a flow rate of 2ml per min and a salt gradient of 0-400mM NaCl in 85min. Fractions (2ml) were collected and assayed for I-2 inhibition using pNPP assay and the active fractions were analyzed by 12% SDS PAGE to determine purity. Pure samples of I-2 were concentrated to less than 2ml using an Amicon Ultra-15 Centrifugal Filter Device with a 10,000 kDa molecular mass cut-off (Millipore). The filter device was centrifuged at 4000xg for 10min at 4°C using a swinging bucket rotor (Beckman J6B centrifuge) until the volume of sample was less than 2ml. The I-2 was stored at -20°C. A sample of I-2 was analyzed on a Superdex 75 column (Pharmacia) (Figure 24). In a separate experiment, I-2 was analyzed by gel filtration and fractions which eluted off the column were examined by 12% SDS PAGE (Figure 25). (This protocol was taken from [57]).
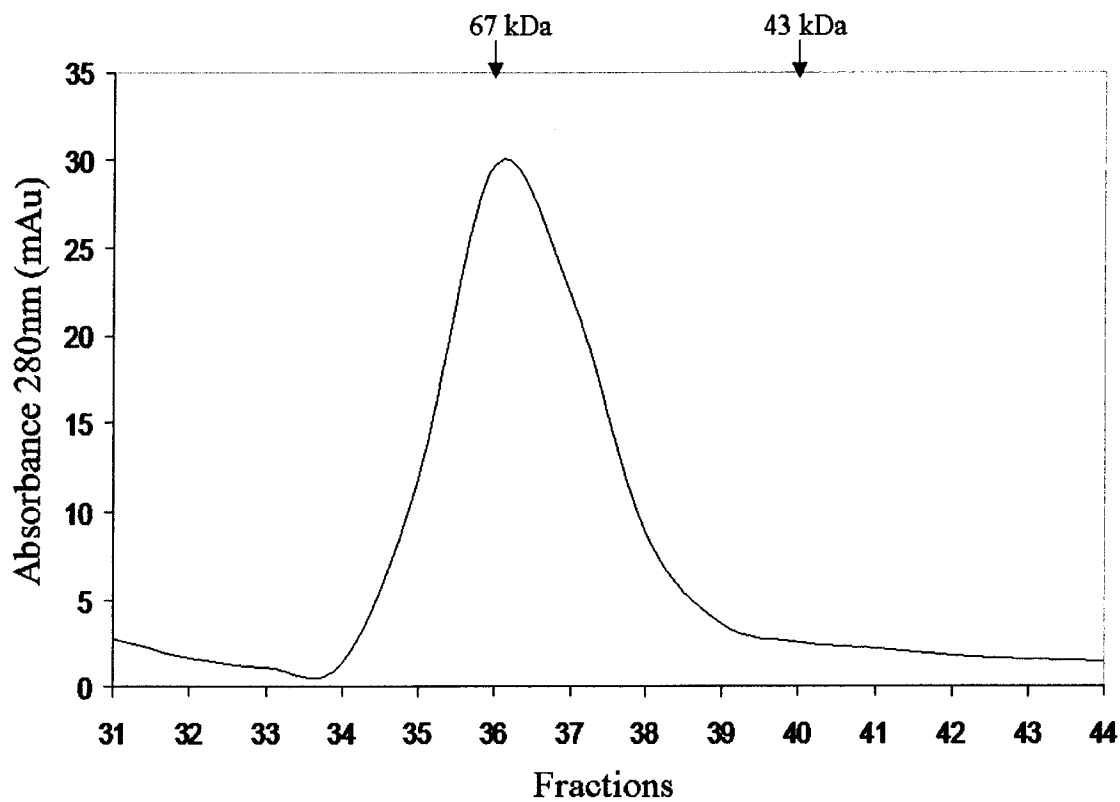
Figure 24: *Analysis of Free Inhibitor-2 using Gel Filtration.*

I-2 (100μg) was analyzed on a Superdex 75 gel filtration column (Pharmacia) at a flow rate of 0.5ml/min, collecting 250μl fractions using the Pharmacia AKTA P-920 pump and visualized using the UPC-900 detector at 280 nm and the UNICORN 4.0 software (Pharmacia).
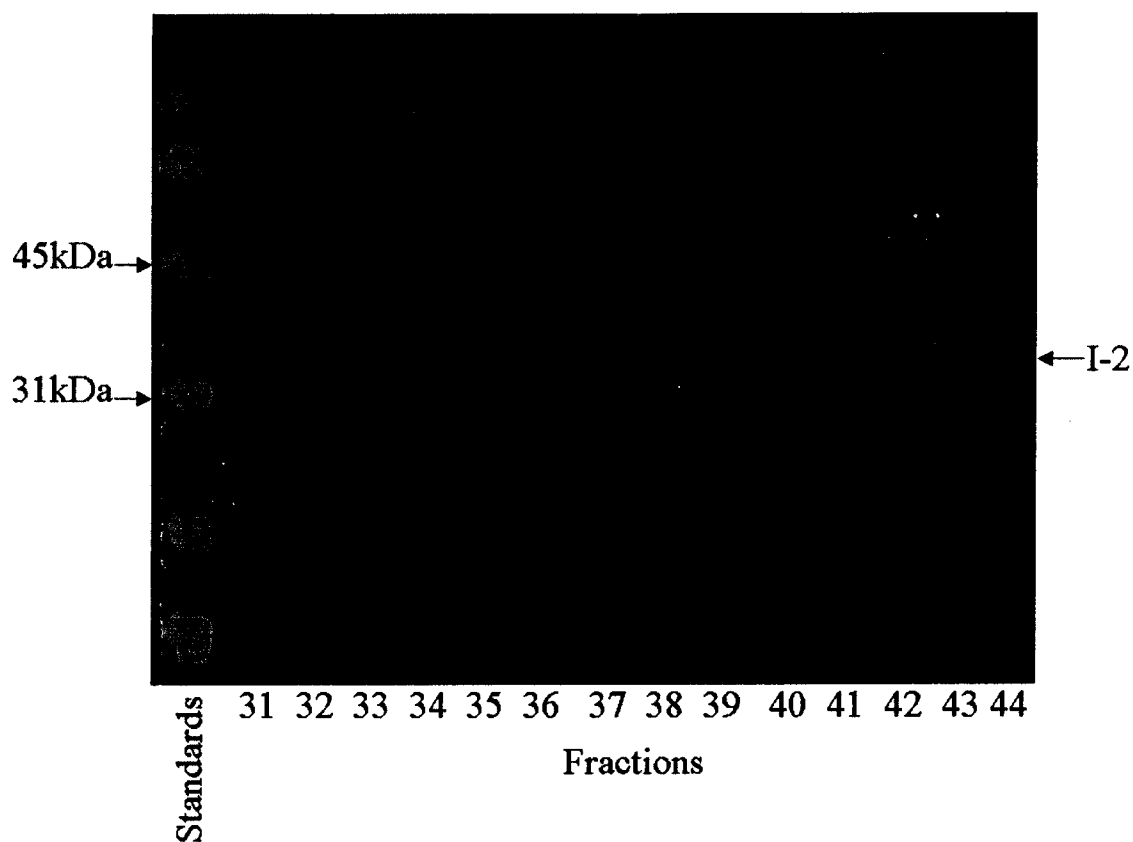
Figure 25: *SDS PAGE Analysis of Free Inhibitor-2 after Elution off a Gel Filtration Column.*

I-2 (100µg) was analyzed on a Superdex 75 gel filtration column (Pharmacia) at a flow rate of 0.5ml/min using the Pharmacia LKB P-500 pump and LCC-501Plus controller. Fractions (250µl) were collected and samples from fractions 31 to 44 were analyzed by 12% SDS PAGE, stained and visualized using the Odyssey system as described in Experimental Procedures.

Glycogen phosphorylase *a* preparation

Conversion of glycogen phosphorylase *b* (the unphosphorylated form of glycogen phosphorylase) to glycogen phosphorylase *a* (the phosphorylated form of glycogen phosphorylase) followed the protocol previously described, except that a larger amount of glycogen phosphorylase *a* was prepared and the crystallization step was omitted. One thousand units of glycogen phosphorylase kinase (Sigma) and 75 mg of glycogen phosphorylase *b* were dissolved in 600µl and 800µl of deionized water respectively (the enzymes from Sigma contained dried buffer constituents). These protein solutions were each dialyzed in tubing (Fisherbrand) with a 3500 kDa molecular mass cut off against 2L of glycogen phosphorylase dialysis buffer for 16 hrs at 4°C. The glycogen phosphorylase *b* crystallized during dialysis and so was re-dissolved by leaving it at room temp in dialysis buffer. The glycogen phosphorylase *b* was then concentrated to 600µl using a Centricon YM-30 Centrifugal Filter Device with a 30,000 kDa molecular mass cut-off (Millipore). The filter device was centrifuged at 3000xg at 15°C using a swinging bucket rotor (Beckman J6B centrifuge) until the volume of sample was reduced to 600µl. The glycogen phosphorylase kinase did not need to be concentrated after dialysis.

Glycogen phosphorylase *b* and the glycogen phosphorylase kinase were incubated at 30°C for 1hr in a solution containing 7.2mM Tris, pH 8.6, 23mM Magnesium Acetate, 0.29mM $CaCl_2$, 7.2mM Sodium Glycerophosphate, 57µCi [γ-^{32}P]ATP, and 0.57mM ATP. The reaction was then transferred to a clean centrifuge tube and 1500µl of saturated $(NH_4)_2SO_4$ solution was added to induce precipitation of the two proteins. The reaction was cooled on ice for 15 min and centrifuged at 17000xg for 10min at 4°C using an F0630 rotor in a Beckman GS-15R centrifuge. The pellet was resuspended in 2ml of glycogen phosphorylase dialysis buffer and dialyzed against 4L of glycogen phosphorylase dialysis buffer, both without NaF, at 4°C to remove unincorporated [γ-^{32}P]ATP. The buffer was changed seven times and each dialysis lasted 3hr. Following dialysis, aliquots of 1.2mg of radioactive glycogen phosphorylase *a* were placed in eppendorf tubes and stored at 4°C. (This protocol was taken from [58].)

Glycogen phosphorylase *a* assay

Activity of PP-1c was determined using the glycogen phosphorylase *a* substrate, prepared as previously described. Glycogen phosphorylase *a* was resuspended to a concentration of 3mg per ml in solution A without $MnCl_2$, then caffeine was added to a final concentration of 11.25mM. PP-1c (10µl) sample was added to 10µl of Solution A and incubated at 30°C for 10min then added to 10µl of resuspended glycogen phosphorylase *a* and the reaction was incubated at 30°C for 10min. The reaction was stopped with 200µl 20% (w/v) TCA, cooled on ice for 2min and centrifuged at room temp for 3min at 16,000xg in an Eppendorf Centrifuge 5415C. The supernatant (200µl) was added to 1ml of Aqueous Counting Scintillant (Amersham Bioscience) and counted in a Wallac 1209 RackBeta Liquid Scintillation counter (Pharmacia). (This protocol was taken from [58].)

Glycogen phosphorylase *a* assay calculations

The amount of enzyme activity is related to the amount of ^{32}P released from the ^{32}P labeled glycogen phosphorylase *a* during the reaction relative to the total amount of ^{32}P labeled glycogen phosphorylase *a* in the reation. The equation to calculate % ^{32}P released from glycogen phosphorylase *a* is:

$$\% \text{ release} = \frac{(\text{sample-blank}) \times 1.15}{(\text{total-blank})} \times 100$$

where sample is the amount of PP-1c activity (in cpm) resulting from adding 10µl of free PP-1c or 10µl of PP-1c:I-2 complex to the phosphatase reaction, blank is the cpm resulting from free ^{32}P-phosphate and/or ^{32}P-ATP present in the assay in the absence of any additional phosphatase activity, total is cpm obtained from the counting of 10µl of ^{32}P labeled glycogen phosphorylase *a* added directly to scintillation fluid, and 1.15 is a dilution factor derived from the volume of the reaction counted (200µl) divided by the total reaction volume (230µl). The linear range of the assay is below 30% release[59].

Thus, dilutions of the samples had to be made until the % release from the assay fell within the linear range.

The activity of PP-1c is expressed in Units (U); 1U is equal to 1 μmole of phosphate released per minute. Calculation for Units of PP-1c activity is based upon the fact that 30% release of ^{32}P-phosphate in the assay is equal to 10μU of PP-1c activity vs. glycogen phosphorylase a [59].

$$U = \frac{(\% \text{ release}/30) \times (10 \times 10^{-6} \text{ U})}{(V) \times (D)}$$

where % release is the calculated % release of the sample using the previous equation, 10 x 10^{-6} U is the amount of PP-1c activity corresponding to 30% release of ^{32}P-phosphate released from ^{32}P-labeled glycogen phosphorylase a, V is the volume of enzyme used in the assay expressed in ml, and D is the dilution of the enzyme used to get 30% release or lower.

PP-1c:I-2 complex formation for fast protein liquid chromatography (FPLC) profiles

PP-1c and I-2 were mixed together in a molar ratio of 3:1 PP-1c:I-2 in buffer C and incubated at 30°C for 45min to form the PP-1c:I-2 complex. (This protocol was taken from [60].)

Separation of PP-1c, I-2, andf the PP-1c:I-2 complex

PP-1c, I-2, and the PP-1c:I-2 complex were loaded separately onto Superdex 75 10/30 gel filtration columns (Pharmacia) using 200μl injection loops. The complex was eluted from the column at a flow rate of 0.5ml per min and ninety-five fractions of 250μl each were collected. A gel filtration calibration kit (Pharmacia) was used to calibrate the column using the proteins: Ribonuclease A (13.7 kDa), Chymotrypsinogen A (25 kDa),

Ovalbumin (43 kDa), Bovine Serum Albumin (67 kDa), and Blue Dextran 2000 (2000 kDa). (This protocol was taken from [60].)

Total phosphatase activity calculations

The total phosphatase activity of the free PP-1c and the PP-1c:I-2 complex gel filtration profiles was calculated by summing the phosphatase activity of the five most active fractions in each profile.

Amino acid analysis

Amino acid analysis was carried out by Michael Carpenter and Jack Moore in the Department of Biochemistry at the University of Alberta. Samples of protein were hydrolyzed for 1 hr at 160°C with 100μl of 5.7M HCl and 0.1% phenol in sealed, evacuated ampoules. Hydrolysis acid was removed after hydrolysis under vacuum using a speedvac. Hydrolyzed samples were injected onto a Beckman 6300 analyzer using cation exchange chromatography at a flow rate of 14ml per hr with 0.2M sodium citrate buffer at pH 3.20, 4.50, and 6.45 and temperature steps of 24°C, 66°C, and 78°C respectively. Ninhydrin was used for post-column detection at a flow rate of 7ml per hr.

Crosslinking PP-1c and I-2

Disuccinimidyl suberate (DSS), purchased from PIERCE, was used as the crosslinking reagent following the protocol from PIERCE. PP-1c (50μg) was added to 15.5μg of I-2 (at a molar ratio of 2:1 PP-1c:I-2) in a solution containing 20mM H_2NaPO_4 pH 7.5, 150mM NaCl, and 5mM DSS. The reaction was incubated at 30°C for 30min and quenched by adding 1M Tris-HCl, pH 7.5.

Activity of the PP-1c:I-2 complex

For consistency, whenever the complex was incubated for 45min at 30°C, free PP-1c was also incubated under the same conditions so that the activity of free PP-1c and the complex, using glycogen phosphorylase a as the substrate, could be accurately compared with one another.

Technical considerations regarding potent inhibitors of PP-1c

Endogenous I-2 is a tight binding inhibitor of PP-1c which displays an IC_{50} in the low nanomolar range [47]. The use of Michaelis-Menten kinetic equations to calculate the dissociation constant (K_i) do not apply to analysis with tight binding inhibitors such as I-2 [61]. Calculation of the dissociation constant of I-2 would assume that the amount of inhibitor bound to PP-1c is very low compared to the concentration of free I-2 in solution. However, both the concentration of PP-1c in the inhibition assay and the IC_{50} of I-2 are in the low nanomolar range. Therefore, the concentration of I-2 in solution is very low while the amount of I-2 bound to PP-1c is very high. This is opposite to the assumptions made in traditional kinetic analysis. Measurement of the IC_{50}, for I-2 as an inhibitor is much more informative [61]. Additionally, the majority of the literature uses the IC_{50} to compare the effects of PP-1c mutations with I-2 and other tight binding inhibitors [13, 35]. This makes it also practical to use the IC_{50} instead of the dissociation constant.

Determination of the concentration of I-2 which inhibits PP-1c to 50% of its original activity (IC_{50})

The protocol for establishing the IC_{50} of the F257A and C291A PP-1c mutants used the standard glycogen phosphorylase a assay as described above except for the following modifications. The glycogen phosphorylase a assay for the positive control of PP-1c activity was identical to the assay described above, except that inhibition activity was determined by using 9μl instead of 10μl of buffer along with 1μl of diluted I-2. The different concentrations of I-2 which were used in the assay were created by diluting a sample of an I-2 stock into deionized water. The final concentrations of I-2 in the assay ranged from 4.9 to 246 nM. The activity of the samples containing I-2 was compared with the control sample to determine the concentration of I-2 which resulted in a 50% loss of PP-1c activity.

IC_{50} calculations

The IC_{50} of wild type PP-1c and the PP-1c mutants were calculated as follows.

$$\text{Phosphatase Activity (\% of Control)} = \frac{\text{Activity of PP-1c exposed to I-2}}{\text{Control activity of PP-1c}} \times 100\%$$

The phosphatase activity of PP-1c which has been exposed to I-2 was divided by the activity of PP-1c which has not been exposed to I-2. The number was multiplied by one hundred and expressed as a percentage. The % release of the control for the different concentrations of I-2 was plotted on a logarithmic scale and the concentration of I-2 which inhibited phosphatase activity by 50% (IC_{50}) was extrapolated using the "Forecast" equation from the Microsoft Excel program.

The Odyssey infrared imaging system

The Odyssey infrared imaging system and software (LI-COR), provided by Dr. David Brindley in the Department of Biochemistry at the University of Alberta, were used to scan and analyze dried SDS PAGE gels stained with Coomassie blue at 800 nm. The absolute integrated intensity (II) which takes into account background fluorescence was calculated using the following formula:

$$\text{Absolute II} = S\text{-}B$$

where (S) is the integrated intensity of the protein band, and (B) is the integrated intensity of an area without protein. The absolute II of bands were used in calculations of PP-1c and I-2 purity and the calculation of the ratio of the PP-1c to I-2 in the PP-1c:I-2 complex.

Calculation of molecular mass of bands from SDS PAGE

The apparent molecular mass of the PP-1c and I-2 bands was calculated using the BIORAD protein ladder and the Odyssey software from LI-COR Biosciences.

Phosphorylation of I-2 by casein kinase-2

I-2 was phosphorylated by casein kinase-2 (CK-2) as described by Alessi et al[60] with the following modifications. I-2 (5.1mg) was incubated with CK-2 for 60min at 30°C in a solution containing 50mM Tris/HCl, pH 7.5, 0.1mM EGTA, 0.1% (v/v) β-mercaptoethanol, 100mM KCl, 10mM Magnesium acetate, 1μM ATP, and 10μCi of [γ-^{32}P]ATP. The phosphorylated I-2 was stored at -20°C. (This protocol was taken from [60].)

GSK-3β phosphorylation of I-2 and the PP-1c:I-2 complex

GSK-3β (Sigma) was reconstituted in a solution containing 20mM Tris, pH 7.5, 50mM NaCl, 1mM Na$_2$EDTA, 2mM DTT, and 50% glycerol. I-2 and the PP-1c:I-2 complex were phosphorylated separately as previously described with the following modifications: PP-1c (50μg) was added to 15.5μg of I-2 in a solution containing 50mM Tris/HCl pH 7.5, 3mM MgCl$_2$, 0.1% (v/v) β-mercaptoethanol, and 0.3mM ATP. The PP-1c and I-2 were incubated at 30°C for 45min to form the complex. Next, 0.4U GSK-3β was added to the reaction which was incubated at 30°C for 1hr. One unit of GSK-3β transfers one pmol of phosphate from ATP to I-2 per min. For the radioactive GSK-3β phosphorylation autoradiograph experiments, the cold ATP was substituted with 10μCi of [γ-^{32}P]ATP. (This protocol was taken from [60].)

Calculation of the stoichiometry of I-2 phosphorylation by GSK-3

The stoichiometry of phosphorylation by GSK-3 of the I-2 in the PP-1c:I-2 complex was calculated as follows.

Stoichiometry of phosphorylation (mol/mol) = $\dfrac{\text{Moles of I-2 labeled by } [\gamma\text{-}^{32}\text{P}]\text{ATP}}{\text{Total moles of I-2 in reaction}}$

Where *Moles of I-2 labeled by [γ-^{32}P]ATP* is the moles of I-2 in the PP-1c:I-2 complex which had been labeled with [γ-^{32}P]ATP by GSK-3 in the phosphorylation reaction. *Total*

moles of I-2 in reaction is the total amount of I-2 in the PP-1c:I-2 complex in the GSK-3 phosphorylation reaction.

Chapter 3: Results

3.1 Research Goals

Eukaryotic PP-1c is a Ser/Thr protein phosphatase inhibited by endogenous I-2. The inhibitor binds PP-1c to form an inactive complex. The purpose of these experiments was to identify regions of PP-1c which interact with I-2. The experimental approach utilized was to analyze potential residues of PP-1c which might mediate the interaction between PP-1c and I-2.

Three regions of PP-1c were hypothesized to be important in PP-1c:I-2 interactions: the $\beta12$-$\beta13$ loop region, residue Y134, and the RVxF binding pocket. Five mutants of PP-1c were used to investigate these regions: the $\beta12$-$\beta13$ loop, F276Y, and Y134A mutants (active site mutants), and the F257A and C291A mutants (RVxF mutants).

One important finding of this study was the discovery that the PP-1c:I-2 complex was not inactive as previously thought, but instead possessed a small amount of residual phosphatase activity. This discovery led to the development of a novel protocol. The new procedure made possible an investigation of PP-1c residues which, during interaction with I-2, may block substrate access to the active site.

3.2 Formation of the PP-1c:I-2 Complex

Purification of PP-1c and I-2

Human PP-1c and human I-2 were purified from recombinant *E. coli* by Fast Protein Liquid Chromatography (FPLC) using a series of ion exchange and gel filtration columns. Purified proteins were analyzed by SDS PAGE and the relative intensities of the protein bands of PP-1c and I-2 were compared to the protein bands of impurities. It was determined that PP-1c and I-2 had been purified to 95% and 91% respectively

(Figure 26). Both proteins showed single peaks of absorbance when analyzed using gel filtration chromatography.

The PP-1c:I-2 Complex Eluted Close to Free I-2 on Gel Filtration

Separation of the PP-1c:I-2 complex from free I-2 was technically challenging because they eluted from the gel filtration column close to each other. The molecular masses of PP-1c, I-2, and the PP-1c:I-2 complex were calculated from the amino acid sequence, by SDS PAGE analysis, and by gel filtration chromatography. The amino acid sequence indicated the molecular masses of PP-1c and I-2 to be 37 kDa and 23 kDa respectively while the 1:1 PP-1c:I-2 complex was the sum of the two proteins at 60 kDa. SDS PAGE indicated an apparent molecular mass of 38.4 kDa for PP1-c and 30.4 kDa for I-2. The large discrepancy between I-2's true and apparent molecular masses can be explained by the anomalous binding of SDS by I-2 [62, 63].

PP-1c, I-2, and the PP-1c:I-2 complex were analyzed separately on a Superdex 75 gel filtration column to determine apparent molecular masses. By comparing the elution rate of the protein peaks to the elution rate of known protein standards on gel filtration, apparent molecular masses of PP-1c, I-2, and the PP-1c:I-2 complex were shown to be 39 kDa, 66 kDa, and 83 kDa respectively (Figure 27). Again, the discrepancy between I-2's true molecular mass and its apparent molecular mass on gel filtration was due to the asymmetric structure of the protein [10, 12].

Both tyrosine and tryptophan residues absorb at 280 nm but tryptophan residues absorb more strongly at 280 nm. PP-1c contains 66% more Tyr residues and 53% more Trp residues than I-2 and thus absorbs light at a higher intensity than I-2. This explains the observation depicted in Figure 27, where three fold the amount of I-2 (in moles) compared to PP-1c showed an absorbance peak at 280 nm of only twice (instead of three fold) that of PP-1c.

Previous studies have shown that free I-2 migrates at an apparent molecular mass of 65 kDa on a sephadex G-75 gel filtration column [62] and that the PP-1c:I-2 complex migrates with an apparent molecular mass between 77 kDa and 87 kDa on Sephacryl S300
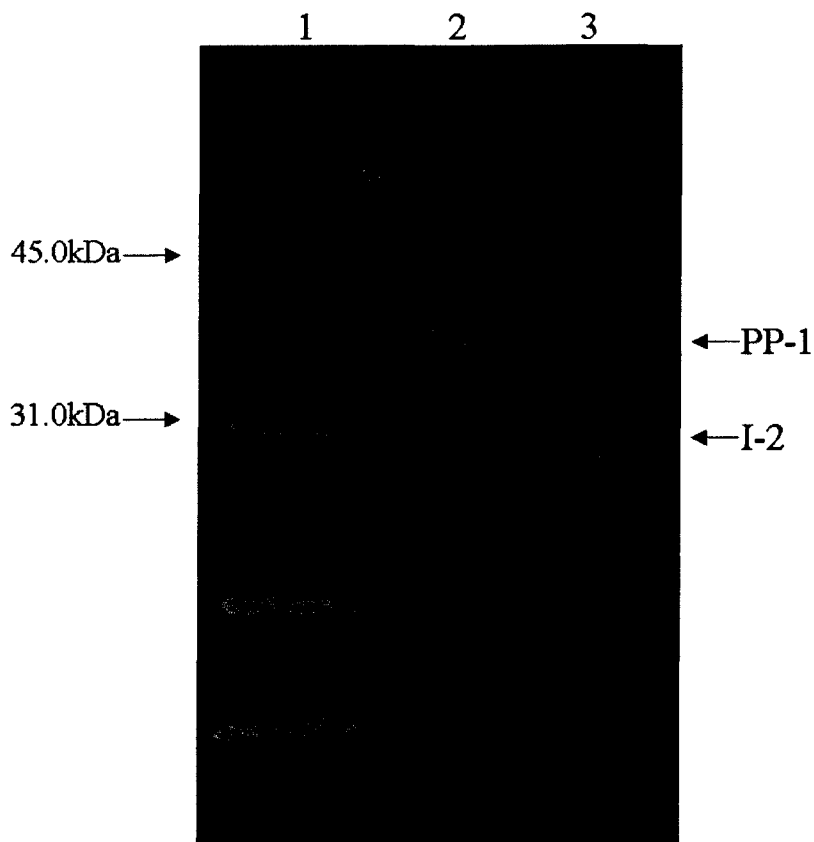
Figure 26: *Purity of Protein Phosphatase-1 and Inhibitor-2.*

PP-1c and I-2 were analyzed by 12% SDS PAGE along with a protein standard ladder (BIORAD) as described in experimental procedures. (Lane 1) Standard BIORAD protein ladder, (Lane 2) PP-1c, (Lane 3) I-2. After staining, destaining, and drying, the gel was scanned using the Odyssey system and the computer software was used to calculate the integrated intensity (II) as described in experimental procedures. For PP-1c, the II of four contaminating bands were compared with the II of the PP-1c band. For I-2, the II of five contaminating bands were compared with the II of the I-2 band. Purity was calculated by dividing the absolute II of the protein band over the sum of the absolute II of all bands in the lane, see experimental procedures.
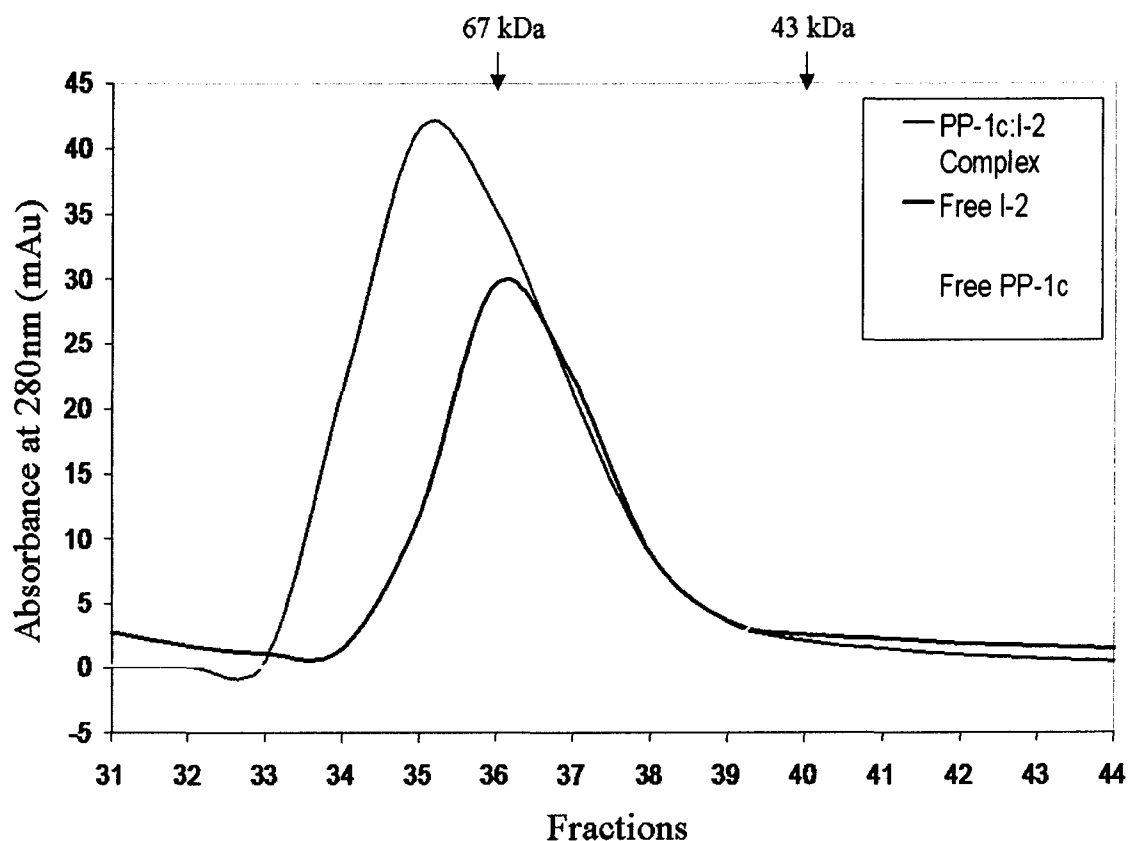
Figure 27: *Analysis of PP-1c, I-2, and the PP-1c:I-2 Complex Using Size Exclusion Chromatography.*

Free PP-1c, free I-2, and the PP-1c:I-2 complex were analyzed separately on a gel filtration column (Superdex 75) as described in Experimental Procedures. The amount of protein for each analysis was as follows: The free PP-1c is shown in *aqua* (50μg of PP-1c), the free I-2 is shown in *black* (100μg of I-2), and the PP-1c:I-2 complex is shown in *red* (50μg of PP-1c with 100μg of I-2). The standards at 67 kDa and 43 kDa are shown as small *blue* dots. The absorbance at 280 nm of fractions 31 to 44 for each analysis were plotted and superimposed on the same chart for comparison. The PP-1c:I-2 complex eluted at fraction 34, before the free I-2 which eluted at fraction 35. The free PP-1c eluted at fraction 40.

[32] and on Sephadex G-100 [30]. This is consistent with the findings presented here and illustrates the technical difficulty of separating the PP-1c:I-2 complex from free I-2.

The Molar Ratio of the PP-1c:I-2 Complex is 1:1

Determination of the molar ratio of PP-1c to I-2 in the PP-1c:I-2 complex facilitated the examination of the interaction between PP-1c and I-2. In order to determine the ratio of PP-1c to I-2 in the PP-1c:I-2 complex, protein standards of PP-1c and I-2 were analyzed. Known amounts of PP-1c and I-2 were loaded separately onto SDS PAGE and the amount of protein versus the intensity of the protein bands was charted using the Odyssey software (Figure 28).

The PP-1c:I-2 complex was loaded onto a Superdex 75 gel filtration column and eluted in discrete fractions. Samples of these fractions were analyzed by SDS PAGE and the intensity of the PP-1c band was compared to the intensity of the I-2 band for each fraction (Figure 29). Note that the height of the peak on the chromatogram (Figure 29, panel A) was disproportionate to the amount of protein visible on the gel in fractions 34 and 35 (Figure 29, panel B). This was due to the fact that PP-1c displays a higher absorbance at 280 nm than I-2 and that I-2 elutes close to the PP-1c:I-2 complex (see Figure 27 for a comparison of the elution rates of free PP-1c, I-2, and the PP-1c:I-2 complex).

By calculating the ratio of PP-1c and I-2 in the first two fractions, it was determined that the PP-1c:I-2 complex eluted off the gel filtration column as a 1:1 complex (Table 2). The absolute integrated intensity (fluorescence) of both the PP-1c and I-2 bands was calculated by comparing the integrated intensity of each band to a blank (a section of the gel containing no protein, see Experimental Procedures). Note that the protein ratios from fraction 35 were greater than 1:1 when compared with the ratios from fraction 34. This was due to the fact that fraction 35 contained excess I-2, as I-2 eluted off the gel filtration column very close to the PP-1c:I-2 complex (see Figure 27). This result was consistent with results published by other laboratories in which the molar ratio of the PP-1c and I-2 in the PP-1c:I-2 complex was shown to be 1:1 [30].
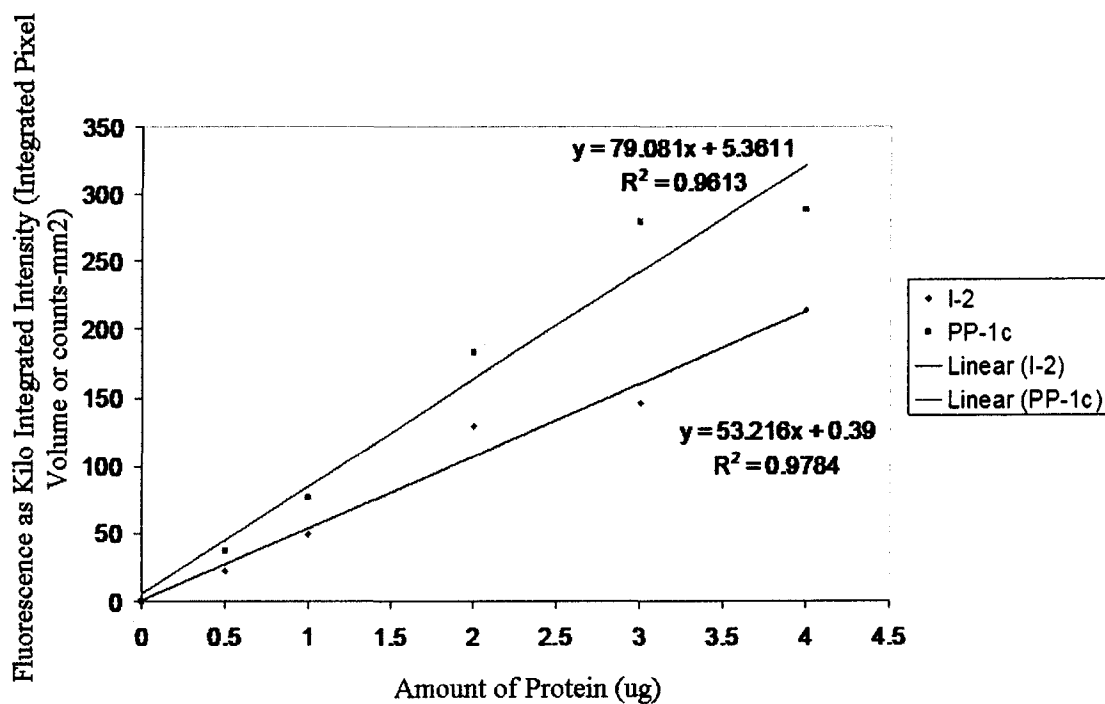
Figure 28: *Standard Curve for Protein vs. Fluorescence of PP-1c and I-2 Using the Odyssey System.*

After carrying out amino acid analysis on PP-1c and I-2, discrete amounts of each proteins was separated by 12% SDS PAGE (0.5μg, 1μg, 2μg, 3μg, and 4μg). The PP-1c and I-2 bands on the gel were analyzed using the Odyssey system as described in experimental procedures. The amount of protein vs. fluorescence (kilo integrated intensity) was plotted and a line of best fit was calculated using Microsoft Excel. PP-1c is shown in *violet* while I-2 is shown in *red*.
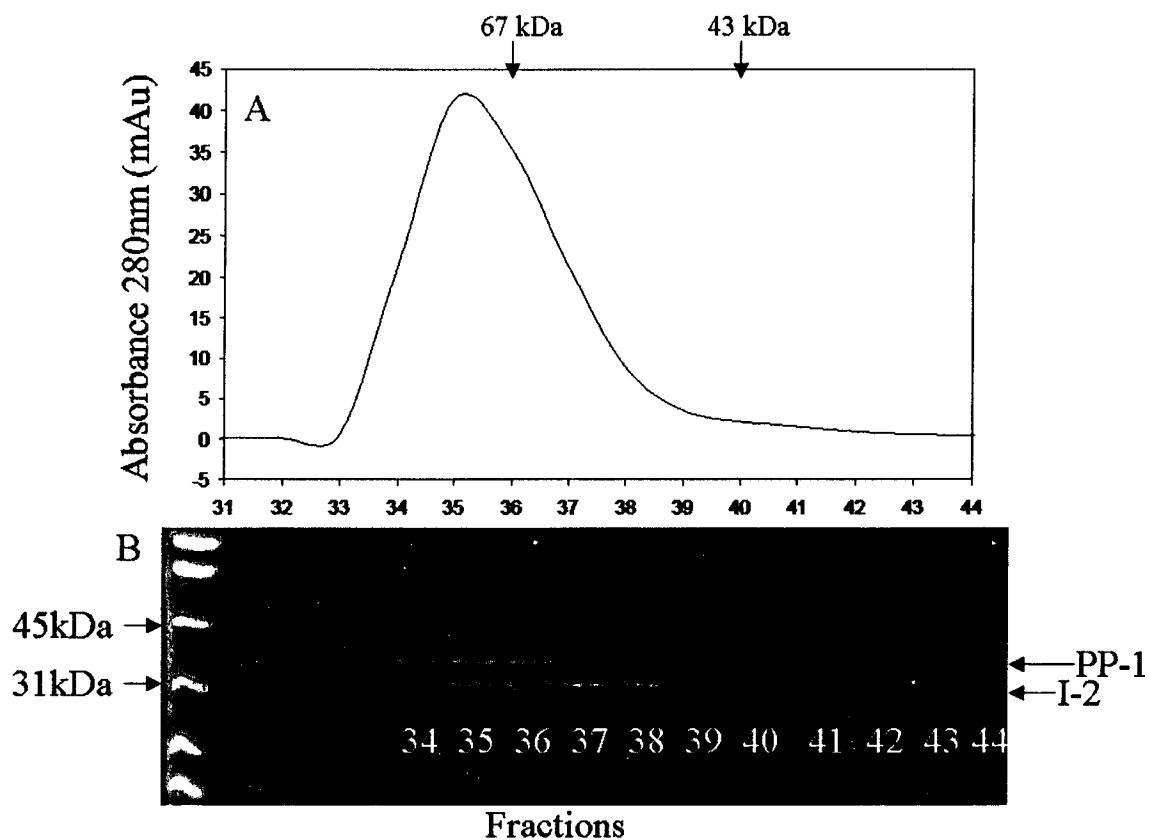
Figure 29: *Analysis of The Protein Phosphatase-1:Inhibitor-2 Complex.*

(A) The PP-1c:I-2 complex was analyzed on a gel filtration column (Superdex 75) as described in Experimental Procedures. Standards at 67 kDa and 43 kDa are shown as *blue* dots and marked with arrows. (B) Samples of fractions 31 to 44 were analyzed by 12% SDS PAGE and visualized using the Odyssey system as described in Experimental Procedures. Lanes 34-39 correspond to the equivalent points on the chromatograph and show the location of PP-1c and I-2 in the PP-1c:I-2 complex.

Fraction	I-2 (nmol)	PP-1c (nmol)	Ratio I-2:PP-1c	Ratio PP-1c:I-2
34	15	15	1 : 1	1 : 1
35	60	48	1.3 : 1	0.8 : 1

Table 2: *The Ratio of PP-1c to I-2 in the Isolated PP-1c:I-2 Complex.*

The Integrated Intensity of the bands in fractions 34 and 35 from Figure 29 was analyzed using the Odyssey system. The standard curve from Figure 28 was used to calculate the amounts of protein (µg) and in turn, the number of moles of PP-1c and I-2. The mol/mol ratios of PP-1c to I-2 showed that fractions 34 and 35 from Figure 29 contained an isolated 1:1 complex of PP-1c and I-2.

Previous studies which analyzed the PP-1c:I-2 complex using gel filtration chromatography used ratios of PP-1c to I-2 similar to those used in the present study [60, 64]. Therefore, in the earlier investigations the PP-1c:I-2 complex was formed in the presence of excess I-2. Additionally, when previous studies separated PP-1c from the PP-1c:I-2 complex by gel filtration, chromatographs showing the protein peaks were never displayed. This was a limitation of previous studies, such that only the phosphatase activity profiles of fractions eluted from gel filtration columns were published. The present study used a large amount of protein, which allowed the protein peaks to be seen on the gel filtration chromatograph.

The present study also showed that it was impossible to completely separate excess I-2 from the PP-1c:I-2 complex. It was primarily the lead fraction of the PP-1c:I-2 complex which contained low amounts of excess I-2. Earlier investigations did not address this issue [60, 64]. The present study has shown that the ratio of PP-1c to I-2 in the PP-1c:I-2 complex is 1:1. Therefore, excess I-2 would not be expected to interfere with either the formation of the PP-1c:I-2 complex or the phosphatase activity profile (see section 3.3), as only one molecule of I-2 can bind to each molecule of PP-1c. Excess PP-1c would have made the phosphatase activity profiles difficult to interpret, therefore the PP-1c:I-2 complex was prepared in the absence of excess PP-1c. In fact, PP-1c:I-2 complex formation was carried out in the presence of excess I-2.

Crosslinking of the PP-1c:I-2 Complex

PP-1c and I-2 were crosslinked to further confirm that they formed a 1:1 complex. After the crosslinking reaction was carried out, the crosslinked PP-1c:I-2 complex was analyzed by SDS PAGE along with controls of PP-1c, I-2, and the non-crosslinked PP-1c:I-2 complex (Figure 30). The unusual migrational behavior of I-2 and the PP-1c:I-2 complex was seen with the formation of the crosslinked PP-1c:I-2. The crosslinked PP-1c:I-2 complex would be expected to display a molecular mass of 60 kDa (37 kDa PP-1c plus 23 kDa I-2), however, it displayed an apparent molecular mass of 74 kDa on SDS PAGE gels. This was consistent with previous work in which the apparent molecular
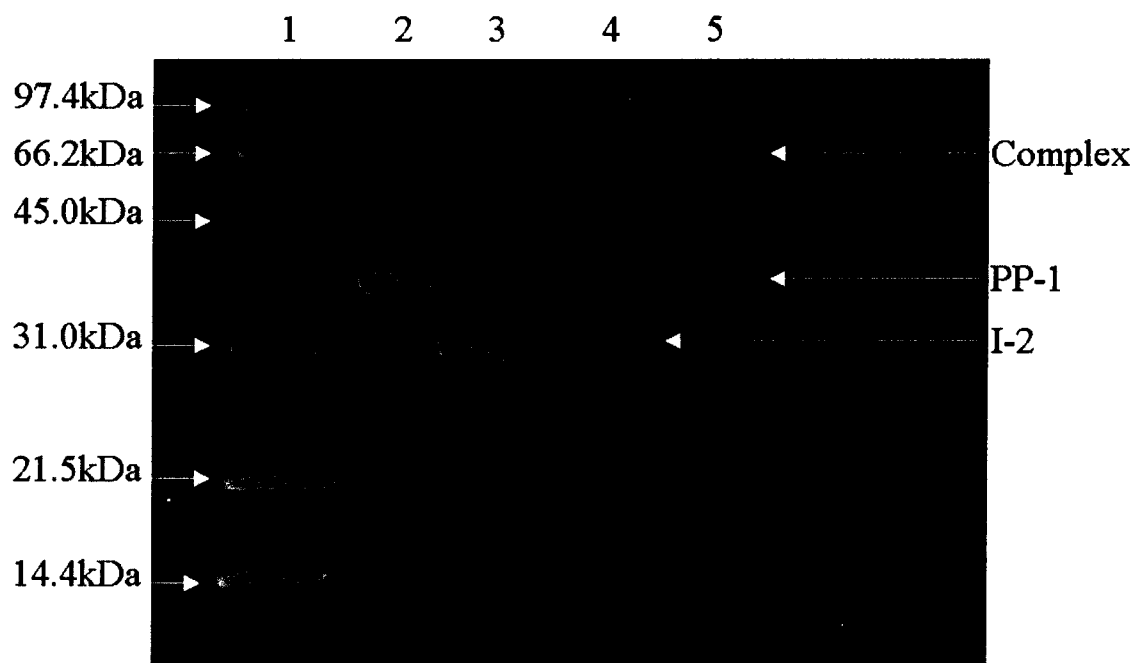
Figure 30: Crosslinking *of Protein Phosphatase-1 and Inhibitor-2*.

PP-1c and I-2 were incubated together with an excess of PP-1c using DSS as the crosslinking reagent (see Experimental Procedures). The gel conditions, staining, drying, and visualization using the Odyssey system are described in Experimental Procedures. (Lane 1) The standard BIORAD protein ladder, (Lane 2) free PP-1c, (Lane 3) free I-2, (Lane 4) the PP-1c:I-2 complex, formed in the presence of excess PP-1c, which separated into PP-1c and I-2 on SDS PAGE, (Lane 5) the crosslinked PP-1c:I-2 complex, formed in the presence of excess PP-1c, which did not separate on SDS PAGE.

mass of the crosslinked PP-1c:I-2 complex was shown to be 70 kDa [30]. The unusual migration behavior of the crosslinked PP-1c:I-2 complex was probably due to the anomalous SDS binding properties of I-2.

3.3 Active Site Mutants of PP-1c Limited or Increased Substrate Access to the PP-1c Catalytic Site

To investigate the importance of the $\beta 12$-$\beta 13$ loop, and residues F276 and Y134 in the positioning of I-2 near the active site, residual phosphatase activity of the PP-1c:I-2 complex was compared to activities of free PP-1c, wild type and active site mutants. In order to accurately compare activities of mutant PP-1c:I-2 complexes with the wtPP-1c:I-2 complex, the ratio of phosphatase activities of free mutant PP-1c to the mutant PP-1c:I-2 complex was used (i.e. free Y134A phosphatase activity compared to Y134A:I-2 complex phosphatase activity).

PP-1c:I-2 Complex Had Residual Phosphatase Activity

wtPP-1c and the wtPP-1c:I-2 complex were analyzed separately by Superdex 75 gel filtration and eluted off the column into discrete fractions. Fractions were then tested for phosphatase activity. The phosphatase activity profiles of free wtPP-1c and the wtPP-1c:I-2 complex were assayed using glycogen phosphorylase a as substrate (glycogen phosphorylase a assay) (Figure 31). The wtPP-1c:I-2 complex possessed residual phosphatase activity 19 fold less that the activity of free wtPP-1c (Figure 32). Previous studies in the literature did not comment on residual phosphatase activity in the wtPP-1c:I-2 complex [12, 60, 64].

Figure 31: *Phosphatase Activity Profiles of PP-1c and the PP-1c:I-2 Complex After Analysis on a Gel Filtration Column.*

Free PP-1c and the PP-1c:I-2 complex were analyzed separately using gel filtration (see Experimental Procedures). Fractions 30-48 for the free PP-1c and fractions 30-48 for the PP-1c:I-2 complex were diluted and assayed separately for PP-1c activity using the glycogen phosphorylase *a* assay described in Experimental Procedures. This analysis was carried out three times. The points on the chart (curve) represent the mean values from the three analyses, whereas the error bars represent the standard deviation from the mean. (A) Free PP-1c is shown as *open circles on a solid line.* Fractions 40-44 were used to calculate the total phosphatase activity of the free PP-1c. (B) The PP-1c:I-2 complex is shown as *closed circles on a dotted line.* Fractions 33-37 were used to calculate the total residual phosphatase activity of the PP-1c:I-2 complex.
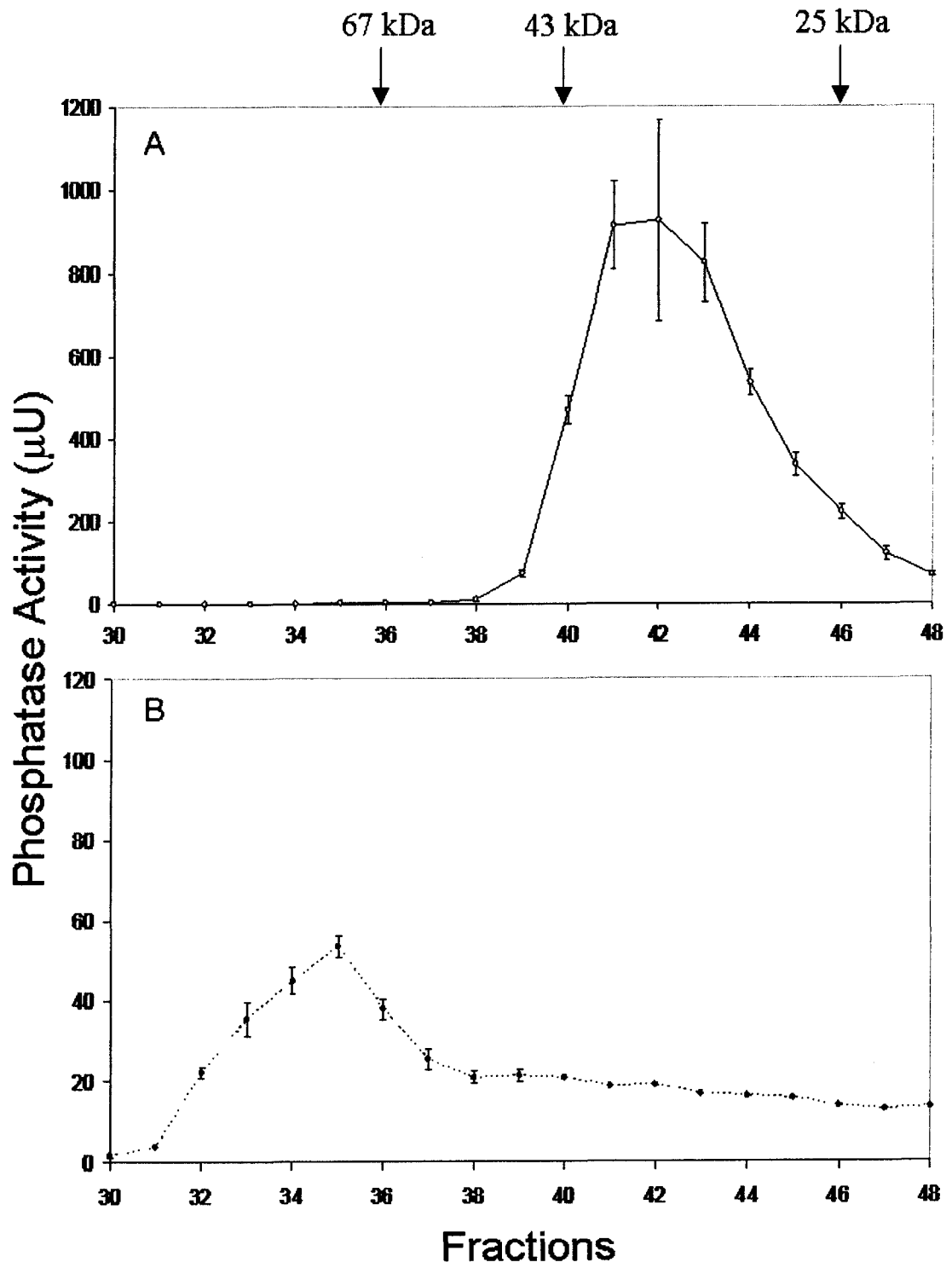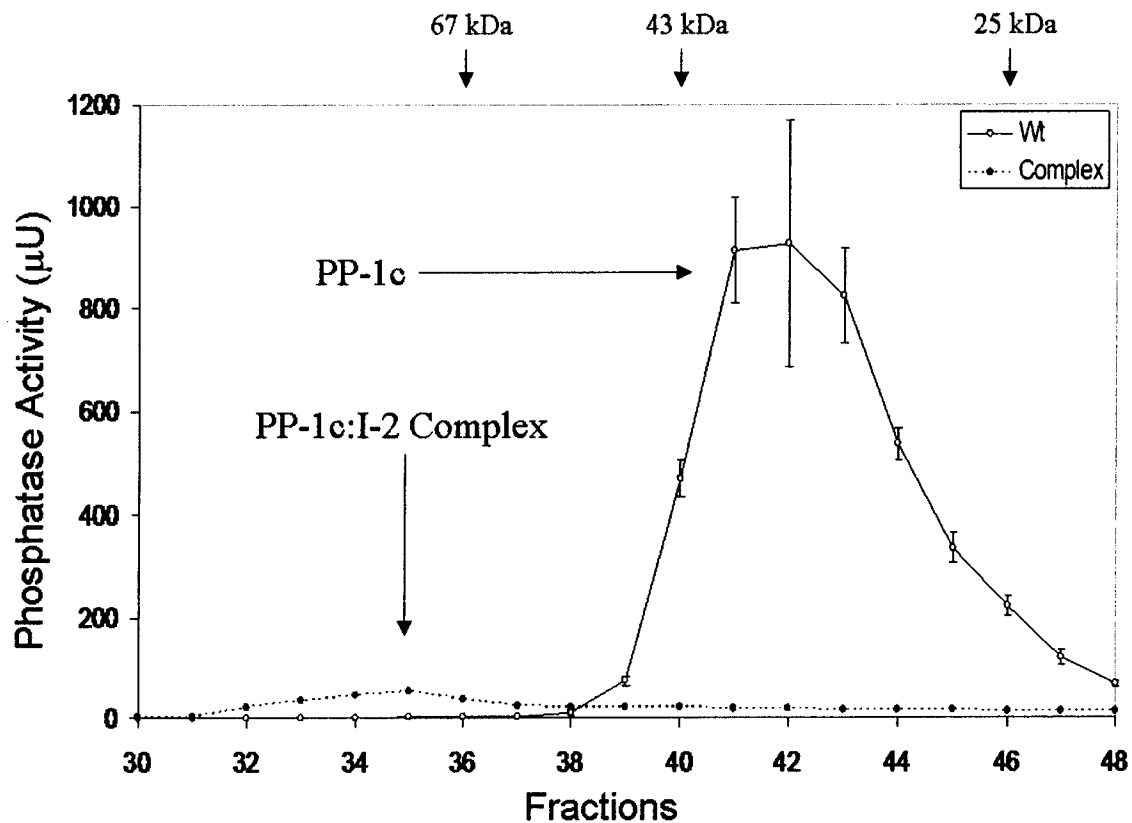
Figure 32: *Superimposition of the Activity Profiles of PP-1c and the PP-1c:I-2 Complex After Analysis on a Gel Filtration Column.*

The activity profiles from Figure 31 were superimposed on the same chart to show relative PP-1c activity. Note the residual activity of the PP-1c:I-2 complex.

The β12-β13 Loop Mutant:I-2 Complex Possessed More Phosphatase Activity than the Wild Type PP-1c:I-2 Complex

The β12-β13 loop mutant used in the present study, involved a substitution of residues ^{273}CGEFD^{277} of PP-1c for residues ^{312}LDVYN^{316} from PP-2B. Both the β12-β13 loop mutant PP-1c and the β12-β13 loop mutant:I-2 complex were analyzed separately by Superdex 75 gel filtration and eluted off the column into discrete fractions. Fractions were then tested for phosphatase activity (Figure 33). The β12-β13 loop mutant:I-2 complex possessed reduced phosphatase activity (6.0 fold) compared to free β12-β13 loop mutant PP-1c. In addition, the β12-β13 loop mutant PP-1c:I-2 complex was 3.1 fold more active relative to the wtPP-1c:I-2 complex. These results suggested that the switching of the residues in the β12-β13 loop of PP-1c for β12-β13 loop residues from PP-2B may have disrupted the mechanism by which I-2 blocks substrate access to the active site.

F276Y:I-2 Complex Possessed Less Phosphatase Activity than Wild Type

Both the F276Y mutant PP-1c and F276Y:I-2 complex were analyzed separately by Superdex 75 gel filtration and eluted off the column into discrete fractions. Fractions were then tested for phosphatase activity (Figure 34). The F276Y:I-2 complex possessed reduced phosphatase activity (31 fold) compared to free F276Y mutant PP-1c. In addition, the F276Y:I-2 complex was 1.7 fold less active relative to the wtPP-1c:I-2 complex. These results suggested that the introduction of a tyrosine at residue 276 may have reinforced the mechanism by which I-2 blocks substrate access to the active site.

Y134A:I-2 Complex Possessed More Phosphatase Activity than Wild Type

Both the Y134A mutant PP-1c and the Y134A:I-2 complex were analyzed separately by Superdex 75 gel filtration and eluted off the column into discrete fractions. Fractions were then tested for phosphatase activity (Figure 35). The Y134A:I-2 complex possessed reduced phosphatase activity (13 fold) compared to free Y134A mutant PP-1c.
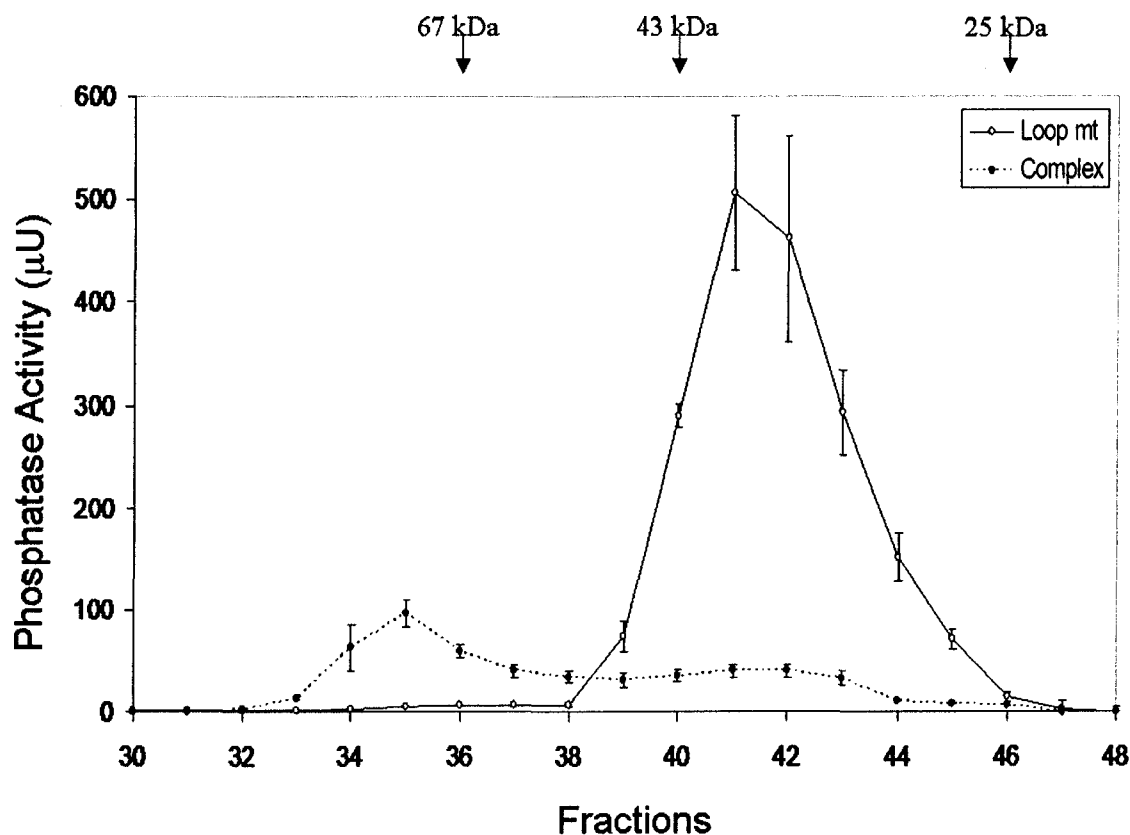
Figure 33: *Superimposition of the Phosphatase Activity Profiles of the β12-β13 Loop Mutant PP-1c and the β12-β13 Loop Mutant:1-2 Complex After Analysis on a Gel Filtration Column.*

Free β12-β13 loop mutant PP-1c and the PP-1c:I-2 complex (formed with β12-β13 loop mutant PP-1c) were analyzed separately on gel filtration, see Experimental Procedures. Fractions eluted off the column were diluted and assayed separately for PP-1c activity using the glycogen phosphorylase *a* assay described in Experimental Procedures. This analysis was carried out three times. The points on the chart (curve) represent the mean values from the three analyses, whereas the error bars represent the standard deviation from the mean. The free β12-β13 loop mutant PP-1c is shown as *open circles on a solid line*. Fractions 39-43 were used to calculate the activity of the free PP-1c. The β12-β13 loop mutant:I-2 complex is shown as *closed circles on a dotted line*. Fractions 33-37 were used to calculate the activity of the PP-1c:I-2 complex. The phosphatase activity profiles for free PP-1c and the PP-1c:I-2 complex were superimposed on the same chart for comparison.
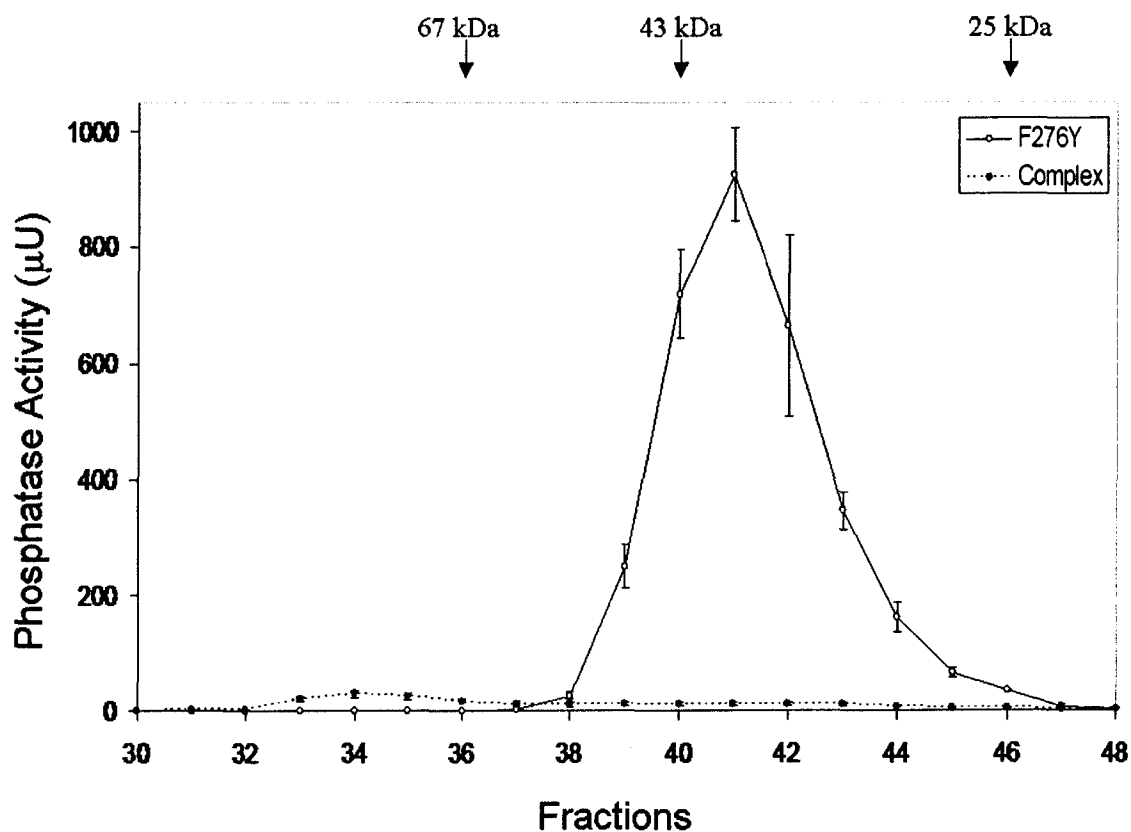
Figure 34: *Superimposition of the Phosphatase Activity Profiles of the F276Y Mutant PP-1c and the F276Y:I-2 Complex After Analysis on a Gel Filtration Column.*

Free F276Y mutant PP-1c and the PP-1c:I-2 complex (formed with F276Y mutant PP-1c) were analyzed separately on gel filtration, see Experimental Procedures. Fractions eluted off the column were diluted and assayed separately for PP-1c activity using the glycogen phosphorylase *a* assay described in Experimental Procedures. This analysis was carried out three times. The points on the chart (curve) represent the mean values from the three analyses, whereas the error bars represent the standard deviation from the mean. The free F276Y mutant PP-1c is shown as *open circles on a solid line*. Fractions 39-43 were used to calculate the activity of the free PP-1c. The F276Y:I-2 complex is shown as *closed circles on a dotted line*. Fractions 32-36 were used to calculate the activity of the PP-1c:I-2 complex. The phosphatase activity profiles for free PP-1c and the PP-1c:I-2 complex were superimposed on the same chart for comparison.
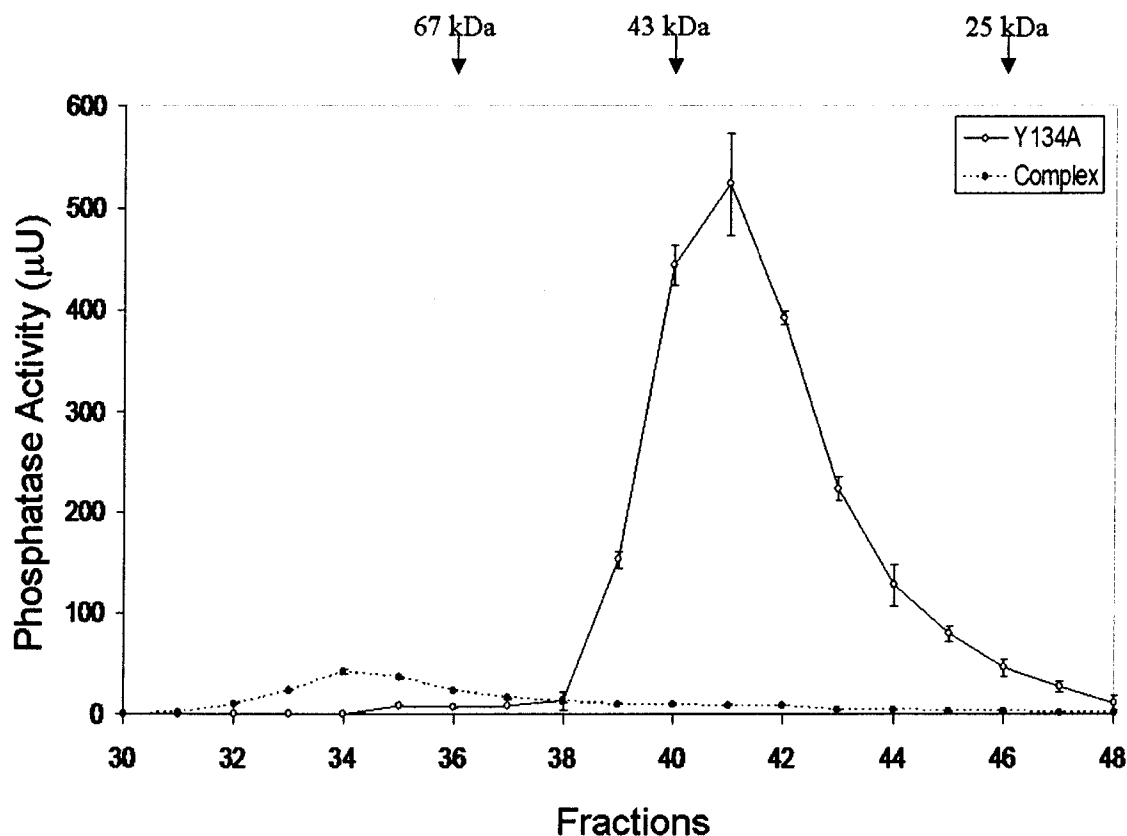
Figure 35: *Superimposition of the Phosphatase Activity Profiles of the Y134A Mutant PP-1c and the Y134A:I-2 Complex After Analysis on a Gel Filtration Column.*

Free Y134A mutant PP-1c and the PP-1c:I-2 complex (formed with Y134A mutant PP-1c) were analyzed separately on gel filtration, see Experimental Procedures. Fractions eluted off the column were diluted and assayed separately for PP-1c activity using the glycogen phosphorylase *a* assay described in Experimental Procedures. This analysis was carried out three times. The points on the chart (curve) represent the mean values from the three analyses, whereas the error bars represent both the highest and lowest values obtained for each point. The free Y134A mutant PP-1c is shown as *open circles on a solid line*. Fractions 39-43 were used to calculate the activity of the free PP-1c. The Y134A mutant PP-1c:I-2 complex is shown as *closed circles on a dotted line*. Fractions 32-36 were used to calculate the activity of the PP-1c:I-2 complex. The phosphatase activity profiles for free PP-1c and the PP-1c:I-2 complex were superimposed on the same chart for comparison.

In addition, the Y134A:I-2 complex was 1.4 fold more active relative to the wtPP-1c:I-2 complex (Table 3). These results suggested that the removal of a tyrosine at residue 134 may have disrupted the mechanism by which I-2 blocks substrate access to the active site.

3.4 Mutants of PP-1c Showed Variation in I-2 Sensitivity

The RVxF Mutants Were Not Used in the Residual Activity Experiments

In order to address the controversy surrounding I-2 interactions with the RVxF binding pocket of PP-1c, the present study analyzed two residues in the pocket (F257 and C291) with respect to inhibition by I-2. As it is far from the active site, the RVxF binding pocket was presumed not to be a key region involved in positioning I-2 near the active site. Therefore, the residual phosphatase activity of the PP-1c:I-2 complexes formed with the F257A and C291A PP-1c mutants was not tested. Only the interaction with the pocket, as measured by PP-1c sensitivity to I-2, was analyzed (IC_{50}). I-2 IC_{50} assays were carried out using wtPP-1c as well as the F257A and C291A PP-1c mutants. Different dilutions of I-2 were added to the assays to create the I-2 sensitivity profiles used to calculate the IC_{50}s.

I-2 Interacted with Residue F257 of the RVxF Binding Pocket

The IC_{50} of the F257A mutant of PP-1c was calculated using the Forecast equation from Microsoft Excel to be 17.7 nM, compared to the wtPP-1c IC_{50} of 7.3 nM. The IC_{50} of F257A was 2.4 fold greater than wtPP-1c. Additionally, the F257A displayed a complex I-2 sensitivity profile, such that the concentration of I-2 required to inhibit F257A to near completion was twenty-six fold greater than for wtPP-1c (Figure 36). This result suggested that F257A may be a key residue for I-2 interactions in the RVxF binding pocket.

	Activity of Free PP-1c (μU)	Activity of PP-1c:I-2 Complex (μU)	Fold Inactivation of PP-1c:I-2 Complex	Fold Residual Activity of PP-1c:I-2 Complex Compared to WT
Wt	3700 ± 500	200 ± 15	19 ± 1.1	-
Loop	1600 ± 240	270 ± 50	6.0 ± 0.5	+3.1 ± 0.3
F276Y	2900 ± 380	100 ± 20	31 ± 5.5	-1.7 ± 0.3
Y134A	1700 ± 90	130 ± 5	13 ± 0.2	+1.4 ± 0.1

Table 3: *Comparison of the Activity of Free Protein Phosphatase-1 vs. the Activity of the PP-1c:I-2 Complex for Wild Type and Mutants.*

Phosphatase activities of the free PP-1c and the PP-1:I-2 complexes for wtPP-1c and each of the mutants were calculated as described in Experimental Procedures. The calculations of the phosphatase activity of the free PP-1c and the corresponding PP-1c:I-2 complex were based on the average of three experiments. The sum of the five most active fractions of each peak (mean of three experiments) is displayed along with the standard deviation (± symbol).
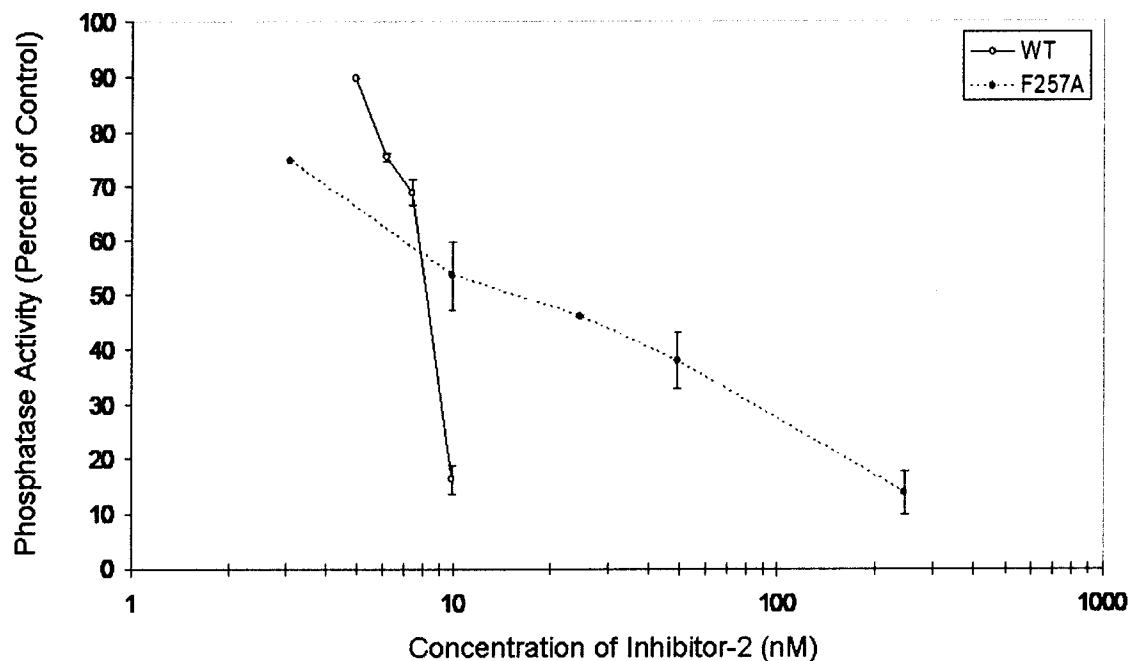
Figure 36: *Inhibition of F257A PP-1c Mutant by Inhibitor-2.*

IC_{50} values for I-2 inhibition of wtPP-1c (*blue*) and the F257A PP-1c mutant (*green*) were determined. The X-axis shows the concentration of I-2 found in the assay, expressed in nM. The Y-axis shows the phosphatase activity as a percentage of the control. This analysis was carried out three times. The points on the chart (curve) represent the mean values from the three analyses, whereas the error bars represent the standard deviation from the mean. The IC_{50} of F257A and wtPP-1c were calculated using the Forecast equation from Microsoft Excel and were based on the average of three assays.

I-2 Did Not Interact with Residue C291 of the RVxF Binding Pocket

The IC_{50} of C291A mutant of PP-1c was calculated to be 7.7 nM, compared with the wtPP-1c IC_{50} of 5.9 nM. The IC_{50} for C291A was only 1.3 fold greater than wtPP-1c (Figure 37). This suggested that this residue may not be critical for the interaction of I-2 with the RVxF binding pocket.

3.5 Phosphorylation of the PP-1c:I-2 Complex

Phosphorylation of Thr-72 on I-2 in the PP-1c:I-2 complex has previously been shown to fully restore phosphatase activity [60, 64]. The present study has shown that the $\beta 12$-$\beta 13$ loop, residue F276 (located in the $\beta 12$-$\beta 13$ loop), and residue Y134 are all important regions for mediation of the interaction with I-2 which blocks substrate access to the catalytic site. Therefore, the present study proposed to test the effects of amino acid residue substitutions in the PP-1c mutants on GSK-3 mediated reactivation of the PP-1c:I-2 complex. To facilitate Thr-72 phosphorylation of I-2, the wtPP-1c:I-2 complex was first phosphorylated by CK-2 on Ser-86. Phosphorylation was confirmed by SDS PAGE and autoradiography (Figure 38). Following the phosphorylation of I-2 by CK-2, and using a similar procedure, the wtPP-1c:I-2 complex was phosphorylated on Thr-72 with GSK-3. Phosphorylation was confirmed as previously described (Figure 39).

Stoichiometry of phosphorylation of the PP-1c:I-2 complex by GSK-3 was calculated to be 0.008 mol/mol. The calculation was carried out by comparing the moles of I-2 phosphorylated by GSK-3 to the total moles of I-2 in the reaction (see Experimental Procedures). This value is low, but consistent with values in the literature: 0.07 mol/mol [34], 0.015-0.03 mol/mol [65], and 0.04 mol/mol [66]. The phosphatase activity of the GSK-3 phosphorylated PP-1c:I-2 complex was tested using the glycogen phosphorylase a assay. Contrary to previous experimental findings [30, 33], no significant difference in activity was seen between the GSK-3 phosphorylated and non-phosphorylated PP-1c:I-2 complexes. Therefore, the effects of the PP-1c mutants upon reactivation of the PP-1c:I-2 complex could not be investigated.
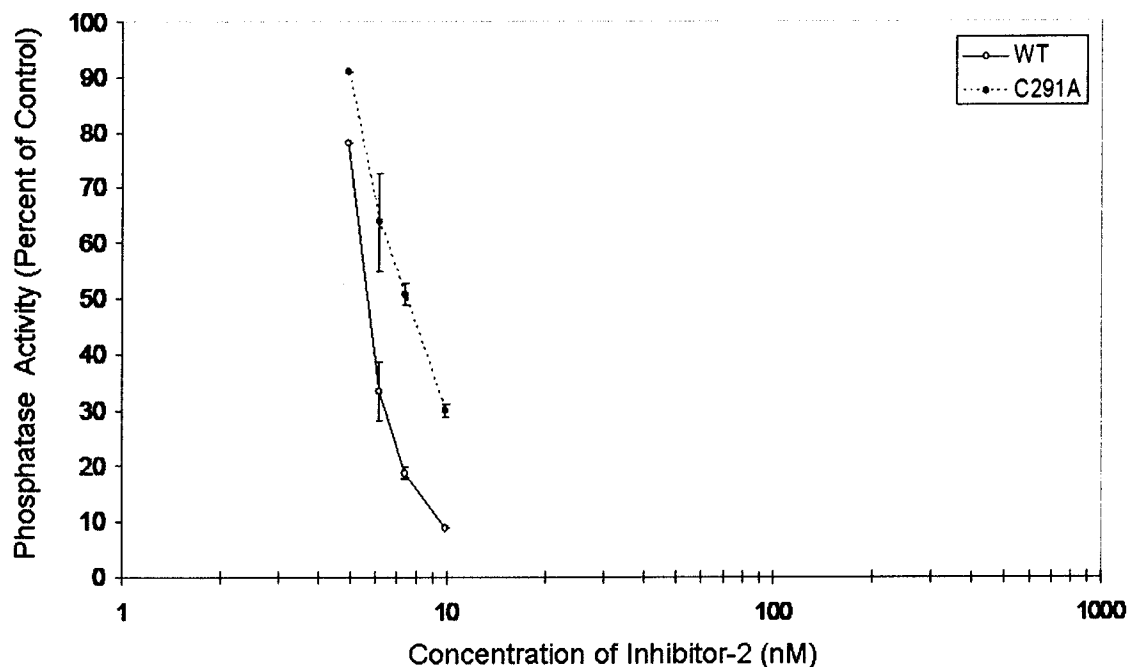
Figure 37: *Inhibition of C291A PP-1c Mutant by Inhibitor-2.*

IC$_{50}$ values for I-2 inhibition of wtPP-1c (*blue*) and the C291A PP-1c mutant (*red*) were determined. The X-axis shows the concentration of I-2 found in the assay, expressed in nM. The Y-axis shows the phosphatase activity as a percentage of the control. This analysis was carried out four times. The points on the chart (curve) represent the mean values from two of the analyses, and the error bars represent the standard deviation from the mean. The IC$_{50}$ of C291A and wtPP-1c were calculated using the Forecast equation from Microsoft Excel and were based on the average of four assays.
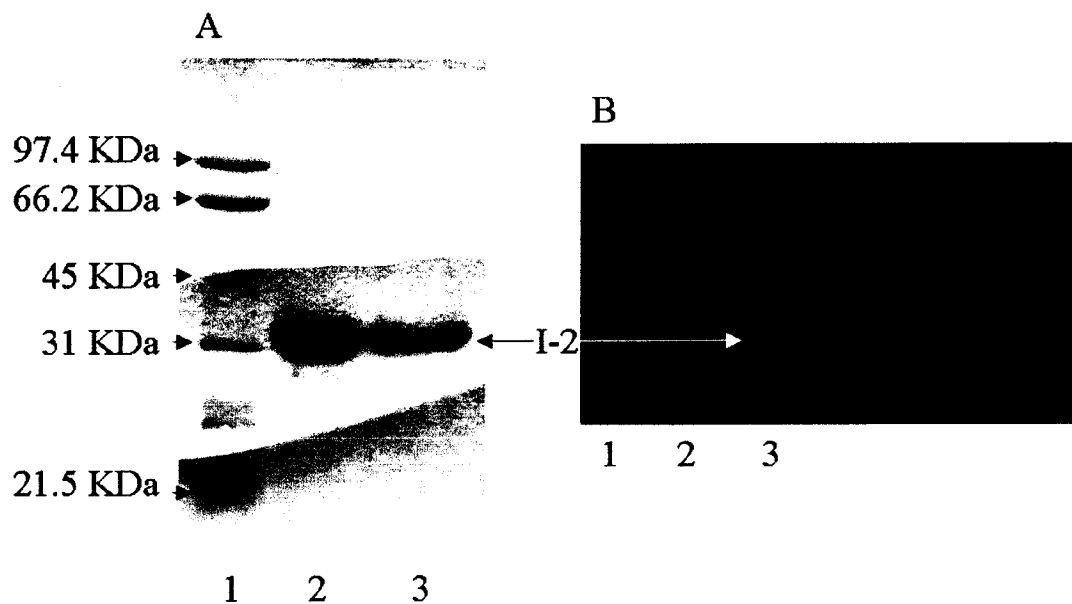
Figure 38: *Phosphorylation of Inhibitor-2 by Casein Kinase-2.*

(A) 12% SDS PAGE. (Lane 1) protein standards (BIORAD), (lane 2) free I-2, (lane 3) free I-2 phosphorylated by CK-2 as described in Experimental Procedures. (B) autoradiograph of the gel in panel A.
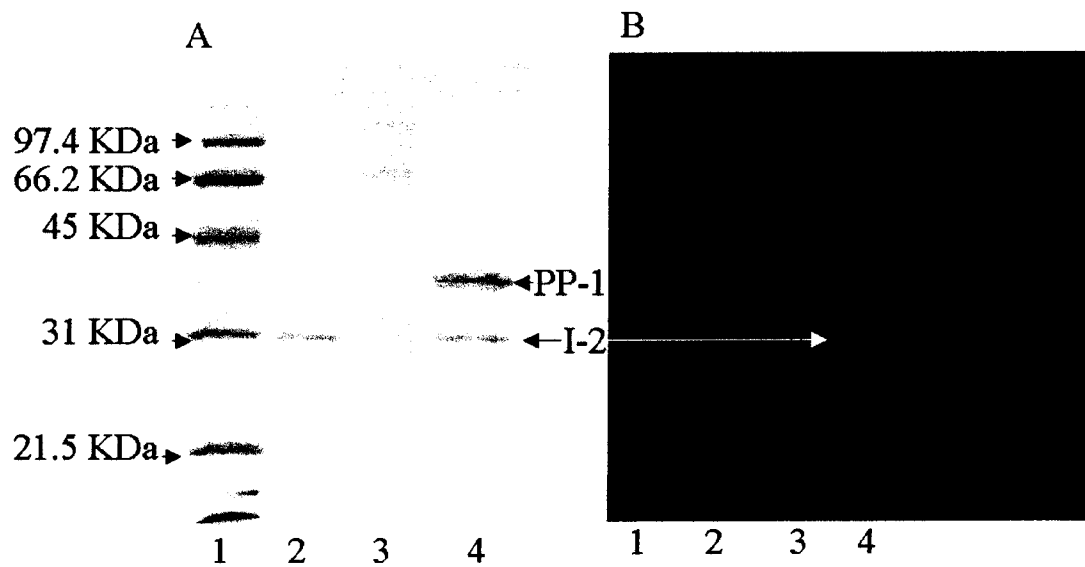
Figure 39: *Phosphorylation of the Protein Phosphatase-1:Inhibitor-2 Complex by Glycogen Synthase Kinase-3.*

(A) 12% SDS PAGE. (Lane 1) protein standard (BIORAD), (lane 2) free I-2, (lane 3) the crosslinked PP-1c:I-2 complex, (lane 4) the PP-1c:I-2 complex phosphorylated by GSK-3 as described in Experimental Procedures. (B) autoradiograph of the gel in panel B.

Chapter 4: Discussion

4.1 Properties of the PP-1c:I-2 Complex

PP-1c and I-2 form a complex with a 1:1 molar ratio upon prolonged incubation [32]. Previous studies have stated that the PP-1c:I-2 complex possessed no phosphatase activity using glycogen phosphorylase a as a substrate [12, 60, 64].

The Residual Phosphatase Activity of the PP-1c:I-2 Complex Led to New Findings

The phosphatase activity of the PP-1c:I-2 complex has not been comprehensively investigated to date as several studies have stated that the PP-1c:I-2 complex possesses no activity [30, 32, 34, 60, 67]. The present study, however, indicates that the PP-1c:I-2 complex does indeed possess residual phosphatase activity (Figure 31).

It has been previously proposed that in the PP-1c:I-2 complex, I-2 is positioned over the catalytic site and blocks substrate access [47]. It has also been suggested that a destabilization of PP-1c:I-2 interactions near the catalytic site may dislodge the I-2, making it easier for substrate to access the catalytic site [47]. The present study therefore proposes that the observed residual phosphatase activity is due to a small amount of destabilization of PP-1c:I-2 interactions which normally occurs in the PP-1c:I-2 complex. This destabilization allows the region of I-2, which blocks the PP-1c active site, to "wiggle around" (Figure 18). This partial movement of I-2 away from the PP-1c active site may allow a small amount of glycogen phosphorylase a substrate to gain access to the PP-1c active site.

The residual activity was detected using very high concentrations of the PP-1c:I-2 complex. The concentration of the PP-1c:I-2 complex used for the glycogen phosphorylase a assay in previous studies may have been too low to detect the residual phosphatase activity. This finding made it possible to investigate the mechanism of I-2 inactivation of PP-1c using different PP-1c mutants in the formation of the PP-1c:I-2 complex.

Alternate Interpretations of the Residual Activity of the PP-1c:I-2 Complex

An alternate interpretation for the residual activity of the PP-1c:I-2 complex is that it is due to the dissociation of the I-2 from PP-1c over time. In this case the residual activity seen is caused by free PP-1c, which has been freed from I-2 and is no longer bound in the PP-1c:I-2 complex. However, studies have shown that dilution of the inactive PP-1c:I-2 complex, or proteolytic cleavage of I-2 [30], does not lead to an increase in PP-1c phosphatase activity [68]. Studies have also shown that only phosphorylation of I-2 while complexed to PP-1c can lead to an increase in PP-1c phosphatase activity [30, 34, 60, 64] of the inactive PP-1c:I-2 complex. However, detailed studies of the stability of the PP-1c:I-2 complex over time have not yet been carried out.

An experiment which could be done in the future to test the stability of the PP-1c:I-2 complex over time is as follows. The PP-1c:I-2 complex is formed and its residual activity is tested at regular intervals. An increase in residual activity would indicate that that the PP-1c:I-2 complex is not stable over time, while no change or a decrease in residual activity would indicate that the complex is stable over time. In addition, samples of the PP-1c:I-2 complex could be subjected to gel filtration chromatography at regular time intervals. Appearance of a peak corresponding to free PP-1c (37 kDa) would indicate that I-2 is dissociating from PP-1c. Combined with the activity data, gel filtration could be used to test the stability of the PP-1c:I-2 complex over time and may indicate whether the residual activity is caused by I-2 dissociating from PP-1c.

Residual Activity of the RVxF Binding Pocket Mutants

Even though the RVxF binding pocket is far from the PP-1c catalytic site, analyzing the residual activity of the RVxF binding pocket mutants may give insights into the importance of this region in mediating interactions with I-2 which block substrate access to the PP-1c active site. In particular, there may be a difference between the residual activity of the F257A:I-2 complex and the wild type PP-1c:I-2 complex. The specific activity of the F257A mutants is three orders of magnitude lower than wild type.

This implies that, while residue F257 is far from the PP-1c active site, it has an indirect effect on PP-1c activity. Forming a complex between the F257A PP-1c mutant and I-2 and measuring the residual activity may provide insight into the importance of this residue in both PP-1c phosphatase activity and in mediating interactions with I-2 which block substrate access to the active site. Likewise, analyzing the residual activity of the C291A mutant:I-2 complex may also provide insight into the importance of this residue in mediating interactions with I-2 which block substrate access to the active site. However, it must be noted that the specific activity of the C291A mutant does not differ greatly from the specific activity of the wild type PP-1c. Therefore, the measurement of the residual activity of the C291A:I-2 complex may not provide as much insight as the F257A:I-2 complex into the importance of the RVxF binding pocket in mediating interactions with I-2 which block substrate access to the active site.

4.2 Interactions Between PP-1c and I-2

The DePaoli-Roach model of PP-1c:I-2 interactions proposed that I-2 wraps around PP-1c and binds to several regions [47] (Figure 18). The present study has confirmed three regions of PP-1c which interact with I-2. They are the β12- β13 loop, a residue near the hydrophobic groove (Y134), and the RVxF binding pocket.

The β12-β13 Loop Region of PP-1c

The β12-β13 loop of PP-1c is located near the active site and is believed to participate in catalysis [14]. Substitution of the PP-1c loop residues with PP-2B loop residues was expected to reduce PP-1c interactions with I-2, as PP-2B is known to be insensitive to I-2 inhibition [10]. The results of the present study supported this hypothesis. Compared to wtPP-1c:I-2 complex, the β12-β13 loop mutant:I-2 complex showed an increase in the residual phosphatase activity. This may suggest that I-2, when complexed with the β12-β13 loop mutant, did not fully block the PP-1c active site (Table 3). In addition, this indicates a possible weakening of the interaction between I-2 and the β12-β13 loop region of the β12-β13 loop mutant of PP-1c and suggests that the β12-β13

loop of PP-1c may play a role in mediating interactions with I-2 which block substrate access to the active site. In addition, recent work carried out in our lab has shown that the β12-β13 loop mutant PP-1c had an IC_{50} 1.9 fold higher than wtPP-1c, which suggests that the β12-β13 loop may be an important region for I-2 inhibition of PP-1c [53].

Rational analysis offers potential residues of the β12-β13 loop which may be important for PP-1c interactions with I-2. In the wild type β12-β13 loop, C273 may form a disulphide bridge with an I-2 residue while E275 and D277 could form salt bridges with I-2 residues. However, without a crystal structure the exact interactions between PP-1c and I-2 cannot be determined with certainty.

In the β12-β13 loop mutant:I-2 complex, any potential disulphide bond from C273 is lost, and the two potential salt bridges of E275 and D277 are also lost. In addition, the mutated residues F276Y and D277N could form hydrogen bonds with one another. These changes might prevent residues on the loop from interacting with I-2 which would lead to a destabilization of the bound inhibitor, thus allowing more substrate access to the PP-1c active site (Figure 21, Figure 40).

The F276Y Mutant of PP-1c

The F276 residue is located in the β12-β13 loop of PP-1c. F276 has been implicated in the binding and inhibition of PP-1c by several toxins [36, 39, 52]. In one study, it was proposed that the mutation of phenylalanine to tyrosine would disrupt hydrophobic interactions between PP-1c and okadaic acid [39]. The present study hypothesized that the point mutant may allow less substrate to access the catalytic site. The hypothesis was confirmed when the present study showed that the F276Y:I-2 complex possesses less residual phosphatase activity compared to the wtPP-1c:I-2 complex (Table 3). This suggested that the introduced tyrosine at residue 276 might have created a stronger interaction between PP-1c and I-2, possibly by forming a hydrogen bond with I-2 using its hydroxyl group. This stronger interaction could stabilize the positioning of I-2 near the catalytic site which would have reduced substrate access. Conversely, recent work carried out in our lab showed very little effect on the IC_{50} of the

GLMKIDE[70]   PSTPYHSMMG[80]   DDEDACSDTE[90]

ATEAMAPDIL[100]   ARKLAAAEGL[110]   EPKY[114]

Figure 40: *Sequence of the Masking Region of I-2.*

Residues 64-114 of I-2 form the masking region which interacts with the β12-β13 loop of PP-1c. Highlighted is a cysteine residue (*blue*) which may form a disulphide bridge with residue C273 of PP-1c. Also highlighted are positively charged residues (*red*) which may form salt bridges with E275 and D277 of PP-1c. These interactions may be disrupted in the β12-β13 loop mutant:I-2 complex, as C273 is mutated to Lys, disrupting the putative disulphide bond. Also, E275 is mutated to Val and D277 is mutated to N, disrupting putative salt bridges. Lastly, Y276 and N277 of the PP-1c loop mutant may form hydrogen bonds with each other instead of with the I-2, thus further disrupting PP-1c:I-2 interactions in the β12-β13 loop region (see Figure 21 for the catalytic site of the β12-β13 loop region).

F276Y PP-1c mutant, suggesting that residue F276 may not be important residue in mediating the inhibition of PP-1c by I-2 [53].

The Y134A Mutant of PP-1c

Residue Y134 resides in the active site, near the hydrophobic groove of PP-1c. This residue is thought to stabilize substrate during dephosphorylation by interacting with p-Ser/Thr residues on the substrate [14]. Mutation of Tyr to Ala at position 134 removes the potential for a hydrogen bonding interaction with I-2. Thus, the present study hypothesized that this change may allow more access of substrate into the PP-1c catalytic site. The results of the present study show that the residual phosphatase activity of the Y134A:I-2 complex is higher than wtPP-1c:I-2 complex (Table 3). This confirms the hypothesis and suggests that residue Y134 may help to position I-2 near the active site of PP-1c, and that the mutation to alanine destabilized this interaction, allowing more access to substrate. The loss of tyrosine on residue 134 removes the potential for hydrogen bonding between the hydroxyl group on Y134 and I-2, and this could account for the observed destabilization. Additionally, recent work carried out in our lab has shown that the IC_{50} of the Y134A mutant was 3.5 fold greater than wtPP-1c [53]. This finding supports the hypothesis that residue Y134 of PP-1c may form a hydrogen bond with I-2.

The F257A Mutant of PP-1c.

The involvement of the RVxF binding pocket of PP-1c in I-2 interactions is controversial [47, 49]. However, experiments conducted in the present study using the F257A PP-1c mutant may have settled that controversy. Mutation of Phe to Ala at position 257 induced a 2.4 fold increase in the IC_{50} for I-2, although the greatest change was seen in the high concentration of I-2 required to inhibit the F257A mutant of PP-1c to near completion (Figure 36).

This result indicates that F257 may be a key residue in mediating PP-1c:I-2 interactions in the RVxF binding pocket and is also consistent with the hypothesis of

multiple I-2 binding sites on PP-1c. The nature of the interaction between residue F257 of PP-1c and I-2 may be strongly hydrophobic, mediated by the phenyl group of F257.

These finding suggests that I-2 may indeed interact with the RVxF binding pocket as previously suggested [47]. However, the residues of I-2 involved in binding the RVxF binding pocket are still not well defined and it is uncertain if it is the KLHY motif of I-2 which binds the RVxF binding pocket or some other I-2 amino acid sequence [49].

The C291A Mutant of PP-1c

The C291 residue is located in the RVxF binding pocket on PP-1c, distal from the catalytic site. The IC_{50} of I-2 for the C291A PP-1c mutant was similar to that of wtPP-1c (Figure 37). Therefore, residue C291 is not a key residue involved in the I-2 mediated inhibition of PP-1c. The nature of the interaction between C291 on PP-1c and I-2 could be weak, such as a Van der Waals or a hydrophobic interaction.

4.3 Summary Model of PP-1c:I-2 Complex

Previous reports have concluded that the inhibition of PP-1c by I-2 is a complex process by which the initial binding of I-2 to PP-1c inhibits phosphatase activity and prolonged incubation leads to conformational changes in the enzyme [12, 31, 32]. This study has confirmed the hypothesis that the $\beta12$-$\beta13$ loop region serves as a key region which positions I-2 near the PP-1c catalytic site [47]. One residue of the loop in particular, residue F276 might be a key residue involved in mediating the interaction with I-2 which blocks substrate access to the active site. Residue F276 may function to prevent I-2 from becoming too tightly bound to PP-1c during PP-1c:I-2 complex formation and may play a role in the reversible binding of I-2.

Compared with the wtPP-1c:I-2 complex, the $\beta12$-$\beta13$ loop mutant:I-2 complex allowed more substrate to access the active site, and the F276Y mutant complex allowed less substrate to access the active site. A novel $\beta12$-$\beta13$ loop mutant in which the Phe at position 276 is not replaced by Tyr may show an even greater increase in substrate accessibility while bound in the I-2 complex.

The Y134A:I-2 complex shows only a small difference in residual phosphatase activity compared to the wtPP-1c:I-2 complex. This indicates that the involvement of Y134 in mediating the interaction with I-2 which blocks substrate access to the active site may be small. On the other hand, the high IC_{50} of I-2 for the Y134A PP-1c mutant, carried out in our lab, shows that a tyrosine residue at position 134 is important for I-2 inhibition [53].

Residue F257, located in the RVxF binding pocket, has been shown to be a key residue in mediating PP-1c:I-2 interactions. The IC_{50} for I-2 inhibition of the F257A PP-1c mutant was two fold higher than that of wtPP-1c. This I-2 sensitivity profile supports the hypothesis of multiple I-2 binding sites on PP-1c and suggests that I-2 might bind the RVxF binding pocket. Residue C291 shows only a slight increase in the IC_{50}. This indicates that C291 might not be involved in I-2 inhibition of PP-1c.

The current model of PP-1c:I-2 interactions agrees with the previous model in that I-2 makes multiple contacts with PP-1c (Figure 18). In the present study, several of the PP-1c residues which have been proposed to make contact with I-2 have been investigated. The $\beta12$-$\beta13$ loop region, especially residue F276, Y134 near the hydrophobic groove, and F257 in the RVxF binding pocket could all be involved in formation of the PP-1c:I-2 complex (Figure 41). Residues of the $\beta12$-$\beta13$ loop may create disulphide and salt bridges, Y134 might establish a hydrogen bond, and hydrophobic interactions could be mediated by F257. However, more studies must be carried out to clarify the structure of the PP-1c:I-2 complex.

4.4 Questions Proposed by the Present Study

A Possible Reason Why Previous Crystallographic Studies of the PP-1c:I-2 Complex Were Unsuccessful.

It is known that I-2 binds multiple sites on PP-1c [47]. In addition, the present study has shown that the PP-1c:I-2 complex possesses residual phosphatase activity. This suggests that I-2 displays flexibility while bound to PP-1c, allowing a small
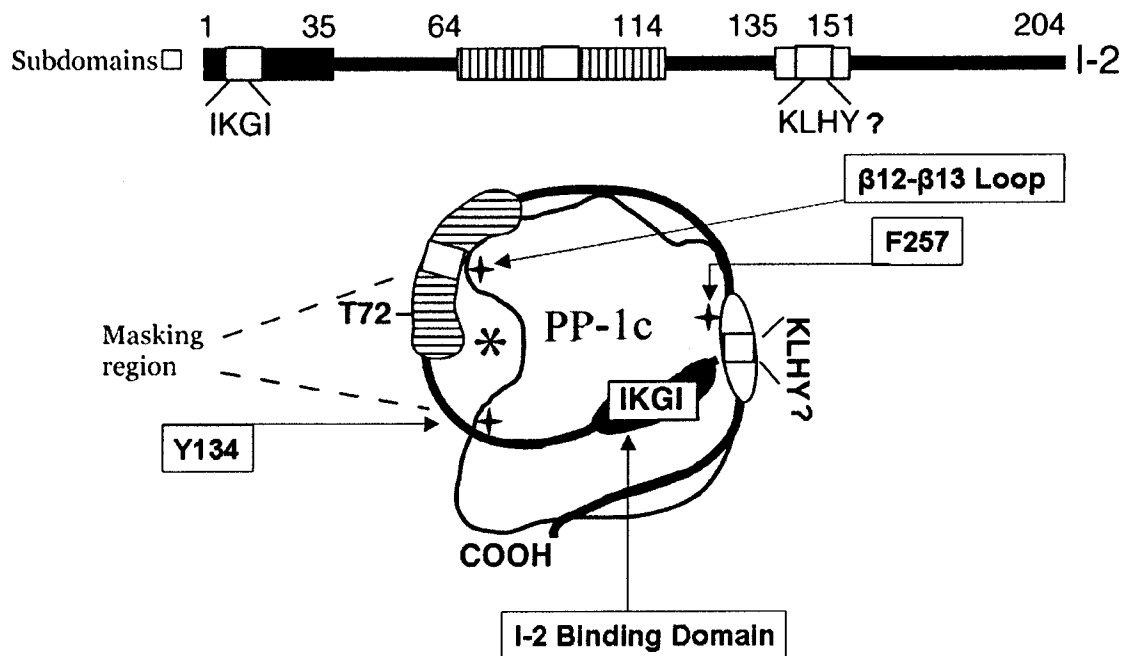
Figure 41: *Current Model of PP-1c:I-2 Interactions.*

This figure is a modification of the DePaoli-Roach model (Figure 18). The IKGI sequence of I-2, binding to the I-2 binding domain has been kept from the previous model. The KLHY sequence of I-2 binding to the RVxF binding pocket of PP-1c has also been kept, although whether it is indeed KLHY or some other sequence of I-2 which binds the pocket remains unknown at this time. The present study has shown that residues C291 and especially F257, in the RVxF binding pocket, interact with I-2. The present study has also shown that the masking region of I-2 binds the β12-β13 loop (including residue F276) as well as residue Y134.

amount of substrate to access the catalytic site. Flexible components of a protein make it difficult to form the crystals necessary for crystallographic studies. This may be why crystals of the PP-1c:I-2 complex have not yet been obtained.

A promising alternative to crystallography is nuclear magnetic resonance spectroscopy (NMR). NMR spectroscopy analyzes the relaxation rates of nitrogen,carbon, and hydrogen atoms in proteins after exposing them to a magnetic field [69]. Thus, the flexible regions of I-2 would not prevent the gathering of structural information using NMR spectroscopy. Even though there is a limit to the size of the protein which can be analyzed with NMR spectroscopy, recent advances place the size limit at close to 100 kDa [69]. This makes NMR spectroscopy a promising method to aquire structural data on the 60 kDa PP-1c:I-2 complex.

The Phosphorylation and Reactivation of the PP-1c:I-2 Complex

Previous studies have shown that the PP-1c:I-2 complex can be reactivated through phosphorylation of I-2 by glycogen synthase kinase-3 (GSK-3) [60]. I-2 is phosphorylated on Ser 86, 120, and 121 by casein kinase-2 (CK-2) and on Thr-72 by GSK-3. Phosphorylation on Ser-86 has no noticeable effect other than to enhance the rate of phosphorylation on Thr-72 by GSK-3 [33, 70].

In this study, phosphorylation of the complex was accomplished but reactivation was not seen. The cause for the inability to reactivate the PP-1c:I-2 complex is not clear. In this study, the crosslinked complex was not phosphorylated by GSK-3 (Figure 39). This is consistent with reports in the literature, as it is known that crosslinking prevents phosphorylation by GSK-3 [30].

The Stoichiometry of I-2 Phosphorylation

It is noted that in the present study, as with previous studies [34, 65, 66], the stoichiometry of I-2 phosphorylation using GSK-3 is low. The predominant explanation is that once the I-2 in the PP-1c:I-2 complex is phosphorylated, it reactivates the previously inactive phosphatase. The active PP-1c, still bound to I-2, then

dephosphorylates the I-2. This autodephosphorylation has been suggested as the cause for the low stoichiometry of phosphorylation of the PP-1c:I-2 complex. Conversely, the stoichiometry of thiophosphorylation of the PP-1c:I-2 complex using GSK-3 can approach 1mol/mol, however thiophosphate cannot mimic phosphate in the reactivation of the PP-1c phosphatase activity in the PP-1c:I-2 complex [34].

The Phosphorylation of PP-1c:I-2 Complex by Cyclin Dependent Kinases

It is unknown why phosphorylation by GSK-3 failed to reactivate the PP-1c:I-2 complex. Investigation of the reactivation of the PP-1c:I-2 complexes formed by PP-1c mutants presented in this study, might have provided insights into the mechanism by which phosphorylation of I-2 reactivates the PP-1c:I-2 complex. An alternative to GSK-3 mediated phosphorylation of I-2 was proposed in a recent study. It has been shown that GSK-3 is not a major I-2 kinase during mitosis in mammalian cells [25]. This study suggested that cyclin dependent kinases (CDKs) carried out the majority of I-2 phosphorylation on Thr-72 during mitosis. Therefore, the use of CDKs may prove to be more successful than GSK-3 in the phosphorylation and reactivation of the PP-1c:I-2 complex.

4.5 Insights Gained From the Present Study

The Importance of the RVxF Binding Pocket in Mediating Interactions with I-2

It has previously been established that the RVxF binding pocket, located distal to the catalytic site of PP-1c, is an important structural feature of PP-1c which is involved in mediating interactions with various regulatory subunits [46]. It has also been shown that many PP-1c regulatory subunits possess a short, conserved sequence of amino acids, Arg-Val-x(any amino acid)-Phe which interacts with the RVxF binding pocket on PP-1c [15]. The present study establishes that I-2 also interacts with the RVxF binding pocket of PP-1c, although it is not known if it is the KLHY sequence or some other I-2 sequence that

mediates this interaction (see page 26 and Figure 18 for discussion of a model of this interaction).

Two PP-1c residues (F257 and C291) were analyzed in the present study in order to assess their role in interacting with I-2. These residues have previously been shown to be important in interacting with the G_M subunit [46]. A key finding of this thesis was that, whilst residue C291 of PP-1c appears to be more important than residue F257 in mediating interactions with G_M, residue F257 is more important than C291 in mediating interactions with I-2 (see page 26, Figure 36, and Figure 37 for a model describing G_M interactions with PP-1c). These results suggest that the RVxF binding pocket of PP-1c interacts differently with I-2 than with the G_M subunit. Further mutagenesis studies of other residues in the PP-1c RVxF binding pocket (e.g. residues I169, L243, L289, and F293) may provide additional insight into the differences between the interactions of both the G_M and I-2 subunits and the PP-1c RVxF binding pocket.

The Similarities and Differences Between I-1 and I-2 Interactions With PP-1c

I-1 is similar to I-2 in that it is an unstructured heat and acid stable endogenous inhibitor of PP-1c. Like I-2, I-1 inhibits native PP-1c activity in the nanomolar range [12]. Unlike I-2, I-1 requires covalent modification to be an active inhibitor of PP-1c, that is, phosphorylation on Thr-35 by cAMP-dependent protein kinase (PKA) [12]. While I-2 possesses multiple domains which bind PP-1c, I-1 is thought to make only two contacts with PP-1c. I-1 has a KIQF sequence to bind the RVxF binding pocket on PP-1c and, when phosphorylated, it binds to the PP-1c catalytic site [22]. A study using mutations in the β12- β13 loop of PP-1c showed it to be a key region in I-1 binding and inhibition [71], similar to its importance for I-2 inhibition.

Recent work from our lab has confirmed that I-1 binds the PP-1c RVxF binding pocket through its KIQF sequence motif [72]. The F257A PP-1c mutant showed an increase in the IC_{50} for I-1 inhibition of more than one hundred fold. This confirmed F257 as a key residue which mediates binding of both I-1 and I-2. In comparison to wtPP-1c, a small increase in IC_{50} for I-1 inhibition of the C291A PP-1c mutant was

observed. This behavior is similar to that of I-2 with this mutant and suggests that C291 might not be a key residue for either I-1 or I-2 binding.

4.6 Conclusion

The present study has investigated three regions of PP-1c proposed to interact with I-2. The study confirmed that the $\beta 12$-$\beta 13$ loop region of PP-1c is a key region for mediating the interaction between PP-1c and I-2. In addition, residue Y134, located near the hydrophobic groove, is also a key region. Lastly, it has been shown that residue F257, located in the PP-1c RVxF binding pocket, interacts with I-2. The results of the present study has therefore increased the understanding of interactions between PP-1c and I-2.

References

1.   Sweatt, J.D., *Memory mechanisms: the yin and yang of protein phosphorylation.* Curr Biol, 2001. **11**(10): p. R391-4.

2.   Bollen, M., S. Keppens, and W. Stalmans, *Specific features of glycogen metabolism in the liver.* Biochem J, 1998. **336 (Pt 1)**: p. 19-31.

3.   Berndt, N., *Protein dephosphorylation and the intracellular control of the cell number.* Front Biosci, 1999. **4**: p. D22-42.

4.   Klumpp, S. and J. Krieglstein, *Serine/threonine protein phosphatases in apoptosis.* Curr Opin Pharmacol, 2002. **2**(4): p. 458-62.

5.   Tamir, I., J.M. Dal Porto, and J.C. Cambier, *Cytoplasmic protein tyrosine phosphatases SHP-1 and SHP-2: regulators of B cell signal transduction.* Curr Opin Immunol, 2000. **12**(3): p. 307-15.

6.   Neumann, J., *Altered phosphatase activity in heart failure, influence on Ca2+ movement.* Basic Res Cardiol, 2002. **97 Suppl 1**: p. I91-5.

7.   Barford, D., *Molecular mechanisms of the protein serine/threonine phosphatases.* Trends Biochem Sci, 1996. **21**(11): p. 407-12.

8.   Fauman, E.B. and M.A. Saper, *Structure and function of the protein tyrosine phosphatases.* Trends Biochem Sci, 1996. **21**(11): p. 413-7.

9.   Honkanen, R.E. and T. Golden, *Regulators of serine/threonine protein phosphatases at the dawn of a clinical era?* Curr Med Chem, 2002. **9**(22): p. 2055-75.

10.   Cohen, P., *The structure and regulation of protein phosphatases.* Annu Rev Biochem, 1989. **58**: p. 453-508.

11.   Shenolikar, S. and A.C. Nairn, *Protein phosphatases: recent progress.* Adv Second Messenger Phosphoprotein Res, 1991. **23**: p. 1-121.

12.   Bollen, M. and W. Stalmans, *The structure, role, and regulation of type 1 protein phosphatases.* Crit Rev Biochem Mol Biol, 1992. **27**(3): p. 227-81.

13.   Oliver, C.J. and S. Shenolikar, *Physiologic importance of protein phosphatase inhibitors.* Front Biosci, 1998. **3**: p. D961-72.

14.   Egloff, M.P., P.T. Cohen, P. Reinemer, and D. Barford, *Crystal structure of the catalytic subunit of human protein phosphatase 1 and its complex with tungstate.* J Mol Biol, 1995. **254**(5): p. 942-59.

15.   Cohen, P.T., *Protein phosphatase 1--targeted in many directions.* J Cell Sci, 2002. **115**(Pt 2): p. 241-56.

16.   Faux, M.C. and J.D. Scott, *More on target with protein phosphorylation: conferring specificity by location.* Trends Biochem Sci, 1996. **8**: p. 312-315.

17.   Bollen, M., *Combinatorial control of protein phosphatase-1.* Trends Biochem Sci, 2001. **26**(7): p. 426-31.

18.   Ceulemans, H., W. Stalmans, and M. Bollen, *Regulator-driven functional diversification of protein phosphatase-1 in eukaryotic evolution.* Bioessays, 2002. **24**(4): p. 371-81.

19.   McCready, T.L., *Inhibition of protein phosphatase-1 by endogenous inhibitor proteins and natural product toxins.* Thesis, 1999.

20.   Dohadwala, M., E.F. da Cruz e Silva, F.L. Hall, R.T. Williams, D.A. Carbonaro-Hall, A.C. Nairn, P. Greengard, and N. Berndt, *Phosphorylation and inactivation of protein phosphatase 1 by cyclin-dependent kinases.* Proc Natl Acad Sci U S A, 1994. **91**(14): p. 6408-12.

21.   Liu, C.W., R.H. Wang, M. Dohadwala, A.H. Schonthal, E. Villa-Moruzzi, and N. Berndt, *Inhibitory phosphorylation of PP1alpha catalytic subunit during the G(1)/S transition.* J Biol Chem, 1999. **274**(41): p. 29470-5.

22.   Barford, D., A.K. Das, and M.P. Egloff, *The structure and mechanism of protein phosphatases: insights into catalysis and regulation.* Annu Rev Biophys Biomol Struct, 1998. **27**: p. 133-64.

23.   Aramburu, J., A. Rao, and C.B. Klee, *Calcineurin: from structure to function.* Curr Top Cell Regul, 2000. **36**: p. 237-95.

24.   Goldberg, J., H.B. Huang, Y.G. Kwon, P. Greengard, A.C. Nairn, and J. Kuriyan, *Three-dimensional structure of the catalytic subunit of protein serine/threonine phosphatase-1.* Nature, 1995. **376**(6543): p. 745-53.

25. Leach, C., S. Shenolikar, and D.L. Brautigan, *Phosphorylation of phosphatase inhibitor-2 at centrosomes during mitosis.* J Biol Chem, 2003. **278**(28): p. 26015-20.

26. Tung, H.Y., W. Wang, and C.S. Chan, *Regulation of chromosome segregation by Glc8p, a structural homolog of mammalian inhibitor 2 that functions as both an activator and an inhibitor of yeast protein phosphatase 1.* Mol Cell Biol, 1995. **15**(11): p. 6064-74.

27. Eto, M., E. Elliott, T.D. Prickett, and D.L. Brautigan, *Inhibitor-2 regulates protein phosphatase-1 complexed with NimA-related kinase to induce centrosome separation.* J Biol Chem, 2002. **277**(46): p. 44013-20.

28. Terry-Lorenzo, R.T., E. Elliot, D.C. Weiser, T.D. Prickett, D.L. Brautigan, and S. Shenolikar, *Neurabins recruit protein phosphatase-1 and inhibitor-2 to the actin cytoskeleton.* J Biol Chem, 2002. **277**(48): p. 46535-43.

29. Vijayaraghavan, S., D.T. Stephens, K. Trautman, G.D. Smith, B. Khatra, E.F. da Cruz e Silva, and P. Greengard, *Sperm motility development in the epididymis is associated with decreased glycogen synthase kinase-3 and protein phosphatase 1 activity.* Biol Reprod, 1996. **54**(3): p. 709-18.

30. Resink, T.J., B.A. Hemmings, H.Y. Tung, and P. Cohen, *Characterisation of a reconstituted Mg-ATP-dependent protein phosphatase.* Eur J Biochem, 1983. **133**(2): p. 455-61.

31. Picking, W.D., W. Kudlicki, G. Kramer, B. Hardesty, J.R. Vandenheede, W. Merlevede, I.K. Park, and A. DePaoli-Roach, *Fluorescence studies on the interaction of inhibitor 2 and okadaic acid with the catalytic subunit of type 1 phosphoprotein phosphatases.* Biochemistry, 1991. **30**(42): p. 10280-7.

32. Tung, H.Y. and P. Cohen, *The protein phosphatases involved in cellular regulation. Comparison of native and reconstituted Mg-ATP-dependent protein phosphatases from rabbit skeletal muscle.* Eur J Biochem, 1984. **145**(1): p. 57-64.

33. DePaoli-Roach, A.A., *Synergistic phosphorylation and activation of ATP-Mg-dependent phosphoprotein phosphatase by F A/GSK-3 and casein kinase II (PC0.7).* J Biol Chem, 1984. **259**(19): p. 12144-52.

34. Hemmings, B.A., T.J. Resink, and P. Cohen, *Reconstitution of a Mg-ATP-dependent protein phosphatase and its activation through a phosphorylation mechanism.* FEBS Lett, 1982. **150**(2): p. 319-24.

35. Dawson, J.F. and C.F. Holmes, *Molecular mechanisms underlying inhibition of protein phosphatases by marine toxins.* Front Biosci, 1999. **4**: p. D646-58.

36. McCready, T.L., B.F. Islam, F.J. Schmitz, H.A. Luu, J.F. Dawson, and C.F. Holmes, *Inhibition of protein phosphatase-1 by clavosines A and B. Novel members of the calyculin family of toxins.* J Biol Chem, 2000. **275**(6): p. 4192-8.

37. Bagu, J.R., B.D. Sykes, M.M. Craig, and C.F. Holmes, *A molecular basis for different interactions of marine toxins with protein phosphatase-1. Molecular models for bound motuporin, microcystins, okadaic acid, and calyculin A.* J Biol Chem, 1997. **272**(8): p. 5087-97.

38. Senogles-Derham, P.J., A. Seawright, G. Shaw, W. Wickramisingh, and M. Shahin, *Toxicological aspects of treatment to remove cyanobacterial toxins from drinking water determined using the heterozygous P53 transgenic mouse model.* Toxicon, 2003. **41**(8): p. 979-88.

39. Maynes, J.T., K.S. Bateman, M.M. Cherney, A.K. Das, H.A. Luu, C.F. Holmes, and M.N. James, *Crystal structure of the tumor-promoter okadaic acid bound to protein phosphatase-1.* J Biol Chem, 2001. **276**(47): p. 44078-82.

40. Maynes, J.T., *Unpublished.*

41. Connor, J.H., T. Kleeman, S. Barik, R.E. Honkanen, and S. Shenolikar, *Importance of the beta12-beta13 loop in protein phosphatase-1 catalytic subunit for inhibition by toxins and mammalian protein inhibitors.* J Biol Chem, 1999. **274**(32): p. 22366-72.

42. Huang, H.B., A. Horiuchi, J. Goldberg, P. Greengard, and A.C. Nairn, *Site-directed mutagenesis of amino acid residues of protein phosphatase 1 involved in catalysis and inhibitor binding.* Proc Natl Acad Sci U S A, 1997. **94**(8): p. 3530-5.

43. Zhang, J., Z. Zhang, K. Brew, and E.Y. Lee, *Mutational analysis of the catalytic subunit of muscle protein phosphatase-1.* Biochemistry, 1996. **35**(20): p. 6276-82.

44.   Zhang, L., Z. Zhang, F. Long, and E.Y. Lee, *Tyrosine-272 is involved in the inhibition of protein phosphatase-1 by multiple toxins.* Biochemistry, 1996. **35**(5): p. 1606-11.

45.   Holmes, C.F., J.T. Maynes, K.R. Perreault, J.F. Dawson, and M.N. James, *Molecular enzymology underlying regulation of protein phosphatase-1 by natural toxins.* Curr Med Chem, 2002. **9**(22): p. 1981-9.

46.   Egloff, M.P., D.F. Johnson, G. Moorhead, P.T. Cohen, P. Cohen, and D. Barford, *Structural basis for the recognition of regulatory subunits by the catalytic subunit of protein phosphatase 1.* Embo J, 1997. **16**(8): p. 1876-87.

47.   Yang, J., T.D. Hurley, and A.A. DePaoli-Roach, *Interaction of inhibitor-2 with the catalytic subunit of type 1 protein phosphatase. Identification of a sequence analogous to the consensus type 1 protein phosphatase-binding motif.* J Biol Chem, 2000. **275**(30): p. 22635-44.

48.   Park, I.K. and A.A. DePaoli-Roach, *Domains of phosphatase inhibitor-2 involved in the control of the ATP-Mg-dependent protein phosphatase.* J Biol Chem, 1994. **269**(46): p. 28919-28.

49.   Wakula, P., M. Beullens, H. Ceulemans, W. Stalmans, and M. Bollen, *Degeneracy and function of the ubiquitous RVXF motif that mediates binding to protein phosphatase-1.* J Biol Chem, 2003. **278**(21): p. 18817-23.

50.   Connor, J.H., D. Frederick, H. Huang, J. Yang, N.R. Helps, P.T. Cohen, A.C. Nairn, A. DePaoli-Roach, K. Tatchell, and S. Shenolikar, *Cellular mechanisms regulating protein phosphatase-1. A key functional interaction between inhibitor-2 and the type 1 protein phosphatase catalytic subunit.* J Biol Chem, 2000. **275**(25): p. 18670-5.

51.   Newgard, C.B., M.J. Brady, R.M. O'Doherty, and A.R. Saltiel, *Organizing glucose disposal: emerging roles of the glycogen targeting subunits of protein phosphatase-1.* Diabetes, 2000. **49**(12): p. 1967-77.

52.   Zhang, Z., S. Zhao, F. Long, L. Zhang, G. Bai, H. Shima, M. Nagao, and E.Y. Lee, *A mutant of protein phosphatase-1 that exhibits altered toxin sensitivity.* J Biol Chem, 1994. **269**(25): p. 16997-7000.

53. Perreault, K.R., J.T. Maynes, J.F. Dawson, M.M. Cherney, M.N. James, and C.F. Holmes, *Unpublished.*

54. Kita, A., S. Matsunaga, A. Takai, H. Kataiwa, T. Wakimoto, N. Fusetani, M. Isobe, and K. Miki, *Crystal structure of the complex between calyculin A and the catalytic subunit of protein phosphatase 1.* Structure (Camb), 2002. **10**(5): p. 715-24.

55. MacKintosh, C., *Assay and Purification of Protein (Serine/Threonine) Phosphatases.* Protein Phosphorylation: A Practical Approach, 1993: p. 197-230.

56. Zhang, A.J., G. Bai, S. Deans-Zirattu, M.F. Browner, and E.Y. Lee, *Expression of the catalytic subunit of phosphorylase phosphatase (protein phosphatase-1) in Escherichia coli.* J Biol Chem, 1992. **267**(3): p. 1484-90.

57. Zhang, Z., S. Zhao, S.D. Zirattu, G. Bai, and E.Y. Lee, *Expression of recombinant inhibitor-2 in E. coli and its utilization for the affinity chromatography of protein phosphatase-1.* Arch Biochem Biophys, 1994. **308**(1): p. 37-41.

58. Cohen, P., S. Alemany, B.A. Hemmings, T.J. Resink, P. Stralfors, and H.Y. Tung, *Protein phosphatase-1 and protein phosphatase-2A from rabbit skeletal muscle.* Methods Enzymol, 1988. **159**: p. 390-408.

59. Holmes, C.F., *Liquid chromatography-linked protein phosphatase bioassay; a highly sensitive marine bioscreen for okadaic acid and related diarrhetic shellfish toxins.* Toxicon, 1991. **29**(4-5): p. 469-77.

60. Alessi, D.R., A.J. Street, P. Cohen, and P.T. Cohen, *Inhibitor-2 functions like a chaperone to fold three expressed isoforms of mammalian protein phosphatase-1 into a conformation with the specificity and regulatory properties of the native enzyme.* Eur J Biochem, 1993. **213**(3): p. 1055-66.

61. Takai, A., K. Sasaki, H. Nagai, G. Mieskes, M. Isobe, K. Isono, and T. Yasumoto, *Inhibition of specific binding of okadaic acid to protein phosphatase 2A by microcystin-LR, calyculin-A and tautomycin: method of analysis of interactions of tight-binding ligands with target protein.* Biochem J, 1995. **306** (Pt 3): p. 657-65.

62. Cohen, P., G.A. Nimmo, and J.F. Antoniw, *Specificity of a protein phosphatase inhibitor from rabbit skeletal muscle.* Biochem J, 1977. **162**(2): p. 435-44.

63. Chisholm, A.A. and P. Cohen, *Molecular mass of inhibitor-2 from rabbit liver.* Biochim Biophys Acta, 1985. **847**(1): p. 155-8.

64. Bennett, D., B. Szoor, and L. Alphey, *The chaperone-like properties of mammalian inhibitor-2 are conserved in a Drosophila homologue.* Biochemistry, 1999. **38**(49): p. 16276-82.

65. Price, D.J. and H.C. Li, *Activation of bovine heart ATP-MG2+-dependent phosphoprotein phosphatase: isolation of a phosphoenzyme intermediate and its conversion to the active form via a Mg2+-dependent autodephosphorylation reaction.* Biochem Biophys Res Commun, 1985. **128**(3): p. 1203-10.

66. Vandenheede, J.R., C. Vanden Abeele, and W. Merlevede, *On the dephosphorylation of the ATP,Mg-dependent protein phosphatase modulator.* FEBS Lett, 1987. **216**(2): p. 291-4.

67. Villa-Moruzzi, E., *Purification and inactivation-reactivation of phosphorylase phosphatase from the protein-glycogen complex.* Arch Biochem Biophys, 1986. **247**(1): p. 155-64.

68. Vandenheede, J.R., J. Goris, S.D. Yang, T. Camps, and W. Merlevede, *Conversion of active protein phosphatase to the ATP-Mg-dependent enzyme form by inhibitor-2.* FEBS Lett, 1981. **127**(1): p. 1-3.

69. Yu, H., *Extending the size limit of protein nuclear magnetic resonance.* Proc Natl Acad Sci U S A, 1999. **96**(2): p. 332-4.

70. Holmes, C.F., N.K. Tonks, H. Major, and P. Cohen, *Analysis of the in vivo phosphorylation state of protein phosphatase inhibitor-2 from rabbit skeletal muscle by fast-atom bombardment mass spectrometry.* Biochim Biophys Acta, 1987. **929**(2): p. 208-19.

71. Connor, J.H., H.N. Quan, N.T. Ramaswamy, L. Zhang, S. Barik, J. Zheng, J.F. Cannon, E.Y. Lee, and S. Shenolikar, *Inhibitor-1 interaction domain that mediates the inhibition of protein phosphatase-1.* J Biol Chem, 1998. **273**(42): p. 27716-24.

72. Fong, A., *Unpublished.*